ANALYZING TEA REPLANTATION PATTERN BY WAVELET AND GEOSPATIAL TECHNIQUE

Alka Singh

January, 2009

ANALYZING TEA REPLANTATION PATTERN BY WAVELET AND GEOSPATIAL TECHNIQUE

by
Alka Singh

Thesis submitted to Indian Institute of Remote Sensing (IIRS) and International Institute for Geo-information Science and Earth Observation (ITC) in partial fulfilment of the requirements for the Joint Master in Geoinformatics.

Thesis Assessment Board:

Chairperson	**:**	Prof.Dr.Ir.A.(Alfred)Stein , (ITC)
External Examiner	**:**	Dr. R.D.Garg
IIRS Member	**:**	Dr. Anil Kumar, IIRS, Mr. P. L. N. Raju, IIRS, Dr. Sameer Saran, IIRS

Supervisors:

IIRS Supervisors
Anil Kumar
ITC Supervisors
Prof.Dr.Ir.A.(Alfred)Stein
Rishiraj Dutta (Advisor)

INTERNATIONAL INSTITUTE FOR GEO-INFORMATION SCIENCE AND EARTH OBSERVATION ENSCHEDE, THE NETHERLANDS

&

INDIAN INSTITUTE OF REMOTE SENSING, NATIONAL REMOTE SENSING CENTRE (NRSC), DEPARTMENT OF SPACE, DEHRADUN, INDIA

I certify that although I may have conferred with others in preparing for this assignment, and drawn upon a range of sources cited in this work, the content of this thesis report is my original work.

Signed …….
(Alka Singh)

Disclaimer

This document describes work undertaken as part of a programme of study at the International Institute for Geo-information Science and Earth Observation. All views and opinions expressed therein remain the sole responsibility of the author, and do not necessarily represent those of the institute.

Dedicated to respected Buaji, Maa and my ever supportive Husband

ACKNOWLEDGEMENTS

A journey is easier when you travel together. Interdependence is certainly more valuable than independence. This thesis is the result of six month of work whereby I have been accompanied and supported by many people. It is a pleasant aspect that I have now the opportunity to express my gratitude for all of them.

First of all, I wish to express my deep sense of appreciation and gratitude to my ITC guide Prof. Dr. Alfred Stein, who suggested me the interesting area of wavelet analysis and gave many valuable suggestions and technical assistance regarding this work which has enabled me to complete the work in the present form. He tried to make me more and more independent and taught me how to work towards the goal. I am also obliged to my ITC advisor Mr Rishiraj Dutta, who has been a source of enthusiasm and encouragement. Without the secondary data provided by him, the current level of work was not possible. His constructive comments were very important to give shape and correct the text of my present thesis.I would like to thank my IIRS guide Dr. Anil Kumar who kept an eye on the progress of my work and always was available when I needed his advice.

My appreciation is incomplete, if I do not mention the support and help extended by Dr. V.K. Dadhwal, Dean, IIRS, by means of valuable suggestions, integral view on research and encouragements. The technical and emotional support of Dr. Sameer Saran, course coordinator IIRS-ITC Joint Study Program IIRS, Dehradun, has been very much appreciable during this research work. It gave me the strength to move forward. Here I also want to thank to Dr Nicholos Hamm, course coordinator ITC, whose continuous concern cannot be ignored. I am grateful to Mr. P.L.N. Raju, In-charge Department of Geoinformatics, who provided me adequate infrastructure and environment to carry-out the present study. My special thanks to Prof. Vinod Kumar (IIT Roorkee) and Dr. M.L. Mittal (Deputy Director, NTRO), who helped me to clear my concepts on wavelet.

Not to forget I would like to extend my special thanks to two of my friends Rahul Raj and Navneet Kumar for their wilful help and sincere co-operation during my research. Furthermore I am deeply indebted to my friends Gaurav, Shashi, Jitendra, Amitava, Naveen, Richa (my roommate) and Rinki at IIRS.

I owe special gratitude to my family members, Bua ji (Prof. Bhuvan Chandel), Mamma (Ms Manju Devi) Bhaiya (Sumit chandel), Didi (Puja Chandel) for continuous and unconditional support of all my undertakings, scholastic and otherwise. Especially, I am grateful to my better half, Amit Chandel whose patient love always motivated me during this research work. Finally, I credit completion of this work to almighty Sai Baba, who gave me the strength and patience required during the tough phases of the last six months.

Alka Singh
IIRS, Dehradun
Uttarakhand- 248001
India, January, 2009

ABSTRACT

Tea plantation in India is more than 100 years old. In most of the gardens, the tea plants remains for more than 50 years. Such a long period of stand in the field results in soil quality degradation, water logging, and susceptibility of the plants to pests and diseases, pesticides contamination and nutrient deficiencies, as a result there is a decline in the yield. Thus it has become a pressing need to monitor these plantations. The main objective of this research is to monitor tea replantation from the time of uprooting till planting of new plants and extracting patterns using wavelet based approaches from satellite images.

Pattern analysis in spatial domain using conventional methods fails to depict the fine changes in the frequency. By using wavelet transform minor spatial changes can be extracted by using frequency domain information. Wavelets provide a natural way to summarize and visualize spatial data at different scales and to extract patterns in different directions. Different wavelets are compared at different levels of decomposition in this study. From the satellite images at different stages of replantation, meaningful patterns from the Haar, Daubechies and the Symmlets wavelets has been extracted.

Usually the replantation involves uprooting of old plants and leaving the land barren for about three months followed by the Guatemala plantation for 18 – 24 months in order to rehabilitate the soil followed by ploughing and levelling of the land for planting of new tea seedlings. For the analysis of these stages, different wavelets pattern were extracted from the vegetation indices of the image. The best pattern for each section was selected on the basis of spatial correlation and level of information required from the section. The anisotropic autocorrelation gives the constant spatial variation coming out at different scale and in different directions. In the study the topographic and hydrological parameters of the land were used to analyse the extracted patterns. Due to high management activities and little variation in elevation, topographical parameters were found less efficient in explaining the extracted pattern It had been observed that Daubechies-4 provides the better results for fine features extraction because they are unsymmetrical orthogonal wavelets therefore can be better correlated with the irregular patterns. Haar was found not suitable because of its blocky results. Symmlets-8 was suitable for smooth features extraction because of its symmetrical long support.

Keywords: Discrete Wavelet Transform, anisotropic autocorrelation, cross correlation, perpendicular vegetation index,

Table of contents

List of Figure

List of Tables

List of Mathematical conventions

General notations **Interpretations**

Fourier analysis

$$F(u,v)=\sum_{m=-\infty}^{\infty}\sum_{n=-\infty}^{\infty}f[m,n]e^{-j2\pi(umx_0+vny_0)}$$

FOUREIER ANALYSIS OF A SIGNAL

$F(u,v)$	Frequency at location (u,v)
$f(m,n)$	Spatial location in x, y axis
e	Natural exponent
x_0 and y_0	Number of pixels in x and y direction

$$F(m,n)=\frac{1}{UV}\int_0^u\int_0^v f(u,v)e^{j2\pi(umx_0+vny_0)}dudv$$

INVERSE FOURIER TRANSFORM (IFT)

$$f(x,y)\approx\sum_{m=1}^{M/2^j}\sum_{n-1}^{N/2^j}s_{j,m,n}\phi_{j,m,n}(x,y)+\sum_{j=1}^{j}\sum_{dir}\sum_{m=1}^{M/2^j}\sum_{n=1}^{N/2^j}d^{dir}{}_{j,m,n}\psi^{dir}{}_{j,m,n}(x,y)$$

DISCRETE WAVELET TRANSFORM

j	Dyadic scale
m,n	Dyadic translation in x and y axis

$s_{j,m,n}\approx\int\int\phi_{j,m,n}(x,y)F(x,y)dxdy$ Smooth wavelet transform coefficients at level j

$d^{dir}{}_{j,m,n}\approx\int\int\psi_{j,m,n}(x,y)F(x,y)dxdy$ Detail wavelet transform coefficients at level j in each directions

$\psi_{j,m,n}(x,y)=2^{-j/2}\psi(2^{-j}x-m,2^{-j}y-n)$ Mother function

$\phi_{j,m,n}(x,y)=2^{-j/2}\phi(2^{-j}x-m,2^{-j}y-n)$ Father function

$\Phi(x,y)=\phi_h(x)\phi_v(y)$ APPROXIMATION COEFFICIENTS

$\Psi^h(x,y)=\phi_h(x)\psi_v(y)$ HORIZONTAL COEFFICIENTS

$\Psi^v(x,y)=\psi_h(x)\phi_v(y)$ VERTICAL COEFFICIENTS

$\Psi^d(x,y)=\psi_h(x)\psi_v(y)$ DIAGONAL COEFFICIENTS

$\phi(.)$	low frequency part of the signal
$\psi(.)$	high frequency part of the signal

$$PVI=\frac{NIR-aR-C}{a^2+\sqrt{a^2+1}}$$

PERPENDICULAR VEGETATION INDEX

a	Slope derived from soil line
c	constant interception of soil line
NIR	Near Infra Red band
R	Red band

$$r_{a,b}=\frac{\mathrm{cov}(a,b)}{\sigma_a\sigma_b}=\frac{\sum(a_i-\bar{a})(b_i-\bar{b})}{(n-1)s_a s_b}$$

CORRELATION COEFFICIENT

$$\rho = \frac{n\sum p_i * p_{i+k} - \sum p_i * \sum p_{i+k}}{\sqrt{(n\sum {p_i}^2 - \sum {p_i}^2) * (n\sum {p_{i+k}}^2 - \sum {p_{i+k}}^2)}}$$

AUTOCORRELATION

P_i pixel value at i pixel location

P_{i+k} pixel value at *k* pixel further to i^{th} pixel

n number of point pairs to be compared based on cutoff.

$$\rho_{12}(h) = \frac{1/n\sum_{i=1}^{n} Z_1(x_i)Z_2(x_i+h) - m_{1-h}m_{2+h}}{\sqrt{\sigma^2_{1-h} * \sigma^2_{2+h}}} \in [-1,+1]$$

Cross Correlation

$Z_1(x_i)$ Value of variable-1 at x_i location

$Z_1(x_i + h)$ Value of variable-2 at a location separated at 'h' distance from x_i

m_{1+h} Mean of variable-1

m_{2+h} Mean of variable-2

σ^2_{1+h} Variance of varianble-1

σ^2_{2+h} Variance of varianble-2

List of Abbreviations

Abbreviation	Description
DEM	Digital Elevation Model
DWT	Discrete Wavelet Transform
FFT	Fast Fourier Transform
MATLAB	Software brand name from Math works Inc
PSI	Perpendicular Soil Index
PVI	Perpendicular Vegetation Index
STFT	Short Time Fourier Transform
TRA	Tea Research Association (Jorhat) Assam India
WFT	Window Fourier Transform

1. Introduction

1.1. General

The oldest non-alcoholic beverage known to man is Tea (*Camellia sinensis* L.; family Theacea) in the world. Traditionally tea plant can be propagated from stem cuttings or seeds, with an average life span of 100 years or more (Mondal et al., 2004). India is the largest producer and consumer of tea in the whole world. In the 18th and 19th centuries Europeans obtained the tea plants from China and carried plantations in their respective colonies (Susan Freeman et al., 2004). In India commercial production of tea was started by the British East India Company. Currently India faces challenges from countries like China, Sri Lanka, Kenya, Indonesia etc producing good quality tea. The domestic trend shows a decline in quality the tea production, due to various reasons such as rising costs, low production and also deteriorating tea quality which ultimately leads to the closure of many gardens. Indian tea industry has grown as one of the most extensive tea industries and is the second largest employer after the national railway system in the world. During recession in the industry, maintenance of hundred thousands of people working in the industry became a liability. Based on the above mentioned factors and to utilize the full potential of the industry and analyzing the reasons for decline in production became a pressing need.

1.2. Background of Tea Replantation:

In the beginning Tea was grown directly from the seed, which leads to geographical and morphological proximity to the main taxa, resulting in numerous hybrids by natural crossing (Banerjee, 1992a). This heterogeneity resulted in the variation in yield, quality for fermentation as well as disease and stress tolerance (Green, 1971). To produce the more suitable and improved varieties, tea seedlings are raised on a special nursery and then planted in the field.

Tea bushes remain in the field for more than 50 years. Such a long period of stand in the field results in soil quality degradation, water logging, and susceptibility of the plants to pests and diseases, pesticides contamination and nutrient deficiencies, as a result there is a decline in the yield. In this situation uprooting and replantation of the old degraded plantation with clonal cultivars were found to become necessary (Kamau, 2008). The figure 1-1 shows the general physical features (topography) of the Tea garden, which plays a key role in the growth of tea plant as well as in the drainage related problems.

Figure 1-1: General topography and the soil condition of the Tea Garden.

The tea research and extension activities for North India are generally undertaken by the Tea Research Association (TRA) which is located in Jorhat Assam since 1911. Around 75% of the total tea growing area of the N.E. India is covered by TRA member estates (http://www.jorhat.nic.in). TRA provides financial grants, technical, and research support to analyze the natural parameters contributing to the fertility of land. It also aims at improving quality, cost reduction, increase in bush productivity, soil biochemistry, irrigation, engineering and transfer of technology for product derivatives and diversification (Technical report 2007). This research is being carried out in collaboration with TRA.

the tea industry currently is in a consolidation phase. However plantation owners and farmers, have been reluctant for a long time to uproot and replant existing tea sections, due to fears of subsequent revenue loss. Since 2005 the industry has undertaken a massive rejuvenation and replantation process which involving uprooting of old tea plants and planting of new seedlings, by the year 2020. The uprooting and replantation process consists of 3 primary stages.

i. During the first stage the tea plants are uprooted and for 3 months approximately land is left barren.
ii. In the second stage Guatemala crops are planted for 18 – 24 months in order to rehabilitate the soil by increasing its fertility and nutrient contents.
iii. In the last stage land is once more left fallow with the Guatemala grass kept as a mulch followed by further ploughing and levelling of the land thereby making it ready for the tea seedlings to be planted.

The replantation process offers a unique possibility to relate and study the various patterns occurring in the soil, Guatemala stage and during seedling stage. The focus in current study is to monitor the replantation process from the time when uprooting takes place till the planting of the new tea seedlings. Here wavelet based analysis is done to quantify the patterns observed from satellite images.

1.3. Role of Remote Sensing

The spectral reflectance of a tea field always varies with respect to the phenology, moisture content and crop health. These factors could be well monitored and measured from the pixel intensity, derived from the radiance of the multispectral remote sensing sensors. Information obtained from different possible statistical observations of remotely sensed data can be combined with collateral data in Geographic Information System (GIS) provides various insights to the cultural practice being implied in the cropping system (Dutta 2008). The integrated tools of remote sensing image processing and GIS technologies can aid in identifying not only those tea crops which are affected by the stress conditions due to weather related damage, excess or deficiencies of moisture or contamination and infestations

but also phenological age of the plantation. The problems detected at an earlier stage, provides an opportunity predict the situations for the planters and to ameliorate the effects say for example by, deciding upon the correct type and amount of fertilizer, pesticides and irrigation, finally which can aid in improving the productivity and quality of the field, most importantly in a cost way.

Patterns are here defined as the non random distribution and arrangement of low and high values (Epinat, 2001). A pattern analysis is done on the basis of recognizing objects by analyzing their shape, size, orientation and location, for human beings which is a common activity and gets automated gradually. A pattern is defined in this study as a set of associated observable objects which reflect the repeated underlying real objects (on the basis of ontology). This definition also extends to the space-time domain, where events or objects may re-occur in a predictable manner within a spatial domain. Incorporating human expertise in interpreting the pattern by associating the real world knowledge with the computer assisted data mining can extract any continuous as well as discrete pattern. The bases of classical pattern recognition approach, largely depends upon inductive computer learning by using different statistical and algorithmic methods. They are primarily dependent on tone, colour, textural and upto some extent contextual information. The classifier may use a training data set based on a statistically well-separated feature space (Luo, 1998). Its aim is to classify or simplify data by observing different possible realization either on the basis of solid statistical method or prior knowledge provided by the user. This traditional approach simply does spectral transformation by creating new linear combination of pixel intensities at the same location (Schowengerdt, 1997). This approach fails for more complex patterns as it does not describe the structural information in the pattern. In such circumstances it will be more appropriate to carry out a hierarchical decomposition into sub patterns until reliable and meaningful information is obtained as done in wavelets. It has been observed in this study that the underlying patterns of each image which are relevant for tea growth using wavelet transformations can yield good results.

In the nineteen eighties J. Morlet (a geophysicist) did wavelet analysis in his work and used the term "ondelette" (French for small wave) first time, which changed subsequently into the term 'wavelet' for the analyzing function (Abbate et al., 2002). Wavelets can be considered as the modified version of the windowed Fourier transform (WFT). In Fourier transform the function is spread globally over the entire frequency domain, these infinite edges function is practically rather hard to conceptualize for real signals and fails to retrieve local changes. In 1987 S. Mallet and Y. Meyer combined the concept of Fourier analysis with a pyramidal multiresolution analysis, due to which the fast wavelet transformation algorithm was developed (Abbate et al., 2002). The WFT can automatically adopt different frequencies for different windows which can be localized simultaneously in space and time. In 1980's the concept of wavelets originate as an alternative to WFT. In Fourier and wavelets, spatial transformations is done by creating a linear combination of orthogonal function of spatial frequency and distance in place of the pixel values of a particular spectral band (Schowengerdt, 1997).

In recent times the use of wavelet analysis has tremendously expanded to numerous disciplines like the natural sciences (seismic events), engineering, astronomy (image processing), and medicine (ECG, medical imaging). In remote sensing, wavelets are applied regularly for classification of images, scaling dimensions (compression, band reduction in hyper spectral data), modelling multiscale phenomenon, denoising (SAR) and image fusion. It seems that there is no limit to the subjects where it can be used from signal processing to solution of statistics and partial differential equation (Resnikoff and

Wells, 2000). Wavelets provide a natural way to view the data at different scale hence it proves to be very useful in extracting the pattern revealed at different resolution.

1.4. Problem Statement

Tea plants starts yielding from the third year onwards and continues for more than hundred years in well managed garden. But peak yield is obtained during 10-30 years after plantation, as shown in the plot where the impact of age factor affecting the yield is drawn for all of the sections of Hope Tea garden for year 2002-2008. The declining trend observed may be a result of prolong monoculture of aged tea bushes, leading to degradation of soil and moisture condition of the land (Kamau, 2008).

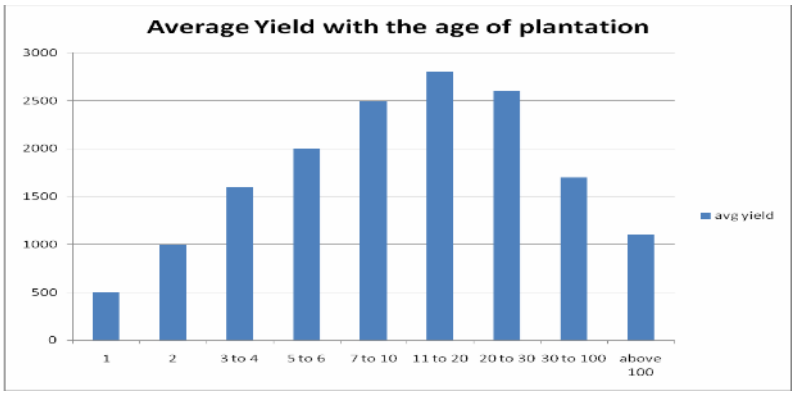

Figure 1-2 Plot showing average yield with respect to age of Tea Plantation of Hope Tea Garden.

The age after which tea plants don't respond well to the practiced agronomic application, in such case replanting and removal of the aged, diseased and pest infested plants and rejuvenation of the soil responsible for the decline in yield could give better quality and more profit.

1.5. Motivation

Based on above discussion, replantation seems to be a backbone for next 50-100 years of production period. Different stages of replantation have their own characteristics and feature, which are required to be analysed in a holistic manner. By realizing the importance of tea replantation and the lack of previous studies done with the help of remote sensing, motivated to carry forward this research work. The current study mainly involves monitoring of the entire tea replantation process at 4 different stages and analyzing their observed patterns. Wavelet analysis and geostatistical techniques are applied to monitor the plantation at different stages of replantation. The best pattern is then analyzed by using topographic and hydrologic parameter. This study involves monitoring tea replantation using high resolution satellite data and analyzing the patterns observed during the entire process using wavelet analysis.

Results from this study can help the garden managers to plan fertilization and distribution of nutrients in their field based on local needs. The study further helped to increase our understanding of the topographical and hydrological relationships as well as soil physical and chemical parameters, in relation to fertility and tea plant requirements during the different replantation stages.

1.6. Objectives

The main objectives of this research work are:

- To quantify patterns during different phases of tea replantation using wavelets.

- To find the natural and/or human induced causes for the patterns identified by wavelets.

This leads to the following research questions that are addressed in this thesis:

- Which level best represents the image during the different stages of replantation?
- Which particular wavelet is best during each stages of replantation?
- How to analyze for finding the causes of the observed pattern extracted from wavelets?

1.7. Structure of The Thesis

This thesis contains following six chapters:

- The first chapter gives a brief introduction about the tea replantation and importance of this research to carry forward along with the research objectives.
- The second chapter deals with the literature review.
- The third chapter describes the theory and concept of wavelets.
- The fourth chapter describes the study area, the data used and the methods followed in this study.
- The fifth chapter discusses in more details the analysis and results.
- The sixth chapter presents the conclusion and recommendations for future work.

2. Literature Review

In world India produces around 27.4% of tea, followed by China (24.6%), Sri Lanka (9.75%), and Kenya (9.4%).In 2004 the export of tea from India felt by 13% as reported by Food Health Organization Tea. (http://www.fao.org). Even after such huge decline, tea is the only industry in which India has retained its position as a leading producer in the world for past 150years. Considerable efforts were made by the government of India to regain the industries full potential and large scale replantation is one of the facets of it. Many researchers have analysed the different aspects of tea plantation but no significant work was carried out on replantation by using remote sensing data.

Ruan and Hardter (2001) analyzed the soil samples from various tea growing regions and found that most tea gardens in China are on red earth, containing marginal amount of potassium (K) and magnesium (Mg). In this research it was found that proper nutrient supply especially K and Mg is most important for tea growth, which not only increases the yield but also improved the quality related constituents in tea. Mondal et al. (2004) found that improvement of tea productivity of ageing tea plantation will come from better timing and dosing of nitrogen with proper management practices. Soil pH and organic carbon are weakly related to the productivity of the ageing tea plantation. It was also found that uprooting and replanting has been the most profitable way to solve degrading production. Dutta et al. (2006) analyzed the different resolution images as Landsat, LISS III and ASTER in monitoring tea bush health and field condition and found ASTER as the most efficient one. It has been described how the tea yield is affected by the health of tea bushes and observed that replantation can be one of the solution in the sections affected by different tea pests.

In this research wavelet has been applied as a tool to do multiscale analysis and analyze the extracted pattern of tea replantation. Wavelet is comparatively a new domain in digital image processing but still lots of work have already being done in different fields. Coifman and Wickerhauser (1992) used the Shannon entropy for best basis selection at low information cost. In this an adopted waveform analysis has been done, which uses a code book or a library of predefined orthogonal basis. Mallet et al. (1997) proposed adaptive DWT in place of standard wavelet basis. It has been tried for reducing the dimensionality in the classification of multi spectral data and optimizes the discriminatory information present in the image. Zhu and Yang (1998), measured the sensitivity of wavelet transform for classification of 25 texture types of relief images under the condition of different wavelet decomposition models, filter lengths, resolutions and mother wavelets. In this research it has been observed that with longer filter length, higher is the accuracy and best decomposition level is either 3 or 4 for the different decompositions. Pitter and Kamarth (1999) divided the wavelet coefficients into clusters for feature extraction in unsupervised mode. Neural network was trained by a set of representative signal records formed from these clusters. This reduces the size of input signal, retaining its accuracy and intrinsic information content of the measured signal. Amgaa et al. (2003) used wavelets for object separation from laser altimeter data, and found it successful for simpler cases of objects but not that much efficient for complex urban feature extraction. Bosch et al. (2004) made a comparison between Variogram and wavelets and found Haar wavelet transform more similar to experimental variogram and generalized variogram of different orders corresponds to complex wavelets in Daubechies family. It was found that wavelet variogram can accentuate long range trend and filter it out but fails for cross boundary local trends.

Lark (1999) illustrated the application of multiresolution analysis of discrete wavelet transform (DWT) on fairly small sets of soil sampled data. It was found the technique has been very efficient in revealing those local feature variations which had been lost in the traditional methods of analysis, and express them quantitatively both in scale and magnitude. Lark et al. (2007) extended their work and concluded that Discrete Wavelet Packet Transform (DWPT) is an advance wavelet technique compare to DWT as it works well for both stationary and non-stationary data sets. For the best basis selection among different packets they used entropy norm. This technique has been used for secondary soil data set in this research and recommended to be used for 2D satellite images. Gandah et al. (2000) suggested simple scoring technique based on millet hills above ground development. Score ranking is done ranging from 0 to8, to make estimates of millet yield. The scoring has been related with the soil data and the millet grain yield, at three different locations. The pattern comparisons had been done for two years by three different procedures i.e. stepwise regression, taxonomic distance and cross-correlograms. A sensitivity analysis was done by drawing random plot specific values for 200 times and then observing their cross-correlation. A significant correlation has been observed between the scoring and the yield.

Verhagen et al. (2000) used wavelets to compare the interpolated yield, of 10years for a 2.5 hectare field, with their respective rainfall distribution of growing season. The reoccurring pattern had been quantified, which can guide the irrigation in dry and wet years. Epinat et al. (2001) used wavelets for extracting patterns in phenological study of crop on high resolution Dutch airborne scanner images. To support the management recommendation for the farmers based on the conditions at the specific locations of the field. They compared Haar and Symmlets wavelets which are nearly symmetric orthogonal wavelets. It was observed that level-4 gives best pattern based on anisotropic autocorrelation.

Geerken et al. (2005) used Fourier filter cycle similarity (FFSC) method for classifying rangeland vegetation and described its superiority over traditional unsupervised classification. This method gives a synoptic visualization of vegetation coverage variation and is independent of background reflectance and scene statistics. Evans et al. (2006) extending the work of Geerken described the Discrete Fourier Transform as a computationally inexpensive and rapid method for rangeland vegetation classification with all FFCS capabilities. Immerzeel et al. (2005) suggested that multi-temporal NDVI imagery can be used in data scarce and inaccessible areas to study land use and precipitation. They found first two harmonic terms of fast Fourier transform of NDVI images, highly correlated with the amount of precipitation during the growing season. Based on these relationships NDVI behavior of upcoming season can be forecasted. Xu et al. (2008) detected relationships between vegetation and soil and topography in valleys of Himalayan region of China can explain 78% of total variation and first two accounted for almost 60%. It has been demonstrated that 70% of total variance in soil can be explain by soil clay content, as the soil water content is governed by the soil texture. The co-evolution of vegetation and soil and follow the natural succession sequence has been promoted.

In this research, the soil and topographic relationship with the greenness index (PVI) were applied to analyze the different replantation phases of tea, in order to find reasons for the patterns obtained from the wavelet analysis. Wavelet avoids the false precision by bringing all the image information at different scales and it also gives the directional change in features at all the scales. This thesis is caring forward the work of Epinat in a much wider sense by not only comparing Haar and Symmlets wavelets but also the Daubechies wavelet. The Daubechies wavelets are asymmetrical wavelet having fractal

characteristics which are suppose to represent the real world features with more precision. In general natural phenomenon are irregular and un-periodic at fine scale, so can be better captured by asymmetric wavelets. Further an attempt is made to analyses those natural causes which are responsible for the extracted patterns of different phases of tea replantation.

3. Wavelet Theory

3.1. Origin of Wavelets

Since the 1800's Fourier analysis serves as a backbone of all frequency domain analysis. This reveals information from the signal that was not perceivable in spatial domain. Let a finite spatial signal $f(m,n)$ limited between x_0 number of pixels in x-direction and y_0 number of pixels in y-direction, undergoes Fast Fourier Transform, gives frequency spectrum $F(u,v)$ where frequency location is represented by u,v for m,n location respectively.

$$F(u,v)=\sum_{m=-\infty}^{\infty}\sum_{n=-\infty}^{\infty}f[m,n]e^{-j2\pi(umx_0+vny_0)} \qquad \textbf{3.1.2}$$

Where 'e' is natural exponent. Lowest intensity is brought up at the centre as $f(0,0)$ by Fourier image which increases outwards. So it's relatively straightforward in identifying and removal of the noise concentrated in any specific part of frequency and the reconstruct it back. Hence for infinite duration periodicity signal Fourier analysis is the best tool. But for transient signal, localized and finite duration basis function is required while Fourier is global in nature. The fourier image can be reconstructed back to spatial domain by following expression.

$$F(m,n)=\frac{1}{UV}\int_0^u\int_0^v f(u,v)e^{j2\pi(umx_0+vny_0)}dudv \qquad 3.1.2$$

U=1/x_0 = sampling rate in *x* direction

V=1/y_0= sampling rate in *y* direction

The Window Fourier Transform (WFT) also known as Short Time Fourier Transform (STFT) gives both frequency and spatial resolution. The STFT include the Gobor transform as a special case with a Gaussian window (Abbate et al., 2002). In a Gabor transform, the one dimensional signal $f(x)$ is multiplied by a window slide function along the x axis, which is non zero for only a short period of time to get the signal information for that particular time interval, resulting into two dimensional representation of the signal $S(j,k)$.

$$S(j,k)=\int_{-\infty}^{\infty}\int_{-\infty}^{\infty}f(u,v)\varphi(x-k)e^{j2\pi(umx_0+vny_0)}dudv \qquad 3.1.3$$

In which *φ(k)* is the window function chosen by the user.

$\pi = 3.1416$

'j' is frequency parameter and 'k' is Translation parameter.

Some measures of goodness exist for making the choices on the window function. In order to extract high frequency feature i.e. more energy concentrated in a short space, window is needed to be adjusted to narrower width. Which result in reducing the frequency spacing of coefficients. If we want a constant spatial resolution then window size will increase, decreasing frequency resolution. The inverse STFT transform bring back the image to spatial domain from frequency domain. However everywhere

it is fixed on the plane, which causes difficulty in processing non stationary signals. From here the origin of wavelets, which localises the finite energy bases came into existences.

3.2. Wavelets: The State Of The Art

Wavelet represents the next logical step which solves the problems like signal cutting or limited precision by applying windowing technique with a variable sized regions. It's a mathematical tool which provides powerful framework for multiresolution images with an efficient insight into its spatial and frequency characteristics.

Gradually wavelet has shifted the attention of researchers from only frequency based analysis (Fourier) to a scale-based analysis. An image is decomposed in a wavelet representation, into different scales by an array of coefficients. The wavelet coefficients represent the scaling and shifting of a mother wavelet basis. Scaling of wavelet denotes the stretching or compressing of the mother wavelet function, with a higher scale corresponding to a higher stretching of the wavelets. A wavelet which is more stretched will represent a coarser portion of the signal, corresponding to a slow change, in other words: a low frequency signal. Wavelet shifting corresponds in delaying its onset. To represent wavelets we notice the following properties.

i. **L^2 inner product** of the two functions: the wavelet coefficients are computed by taking inner products of the function f with the wavelet functions

$$\| f \| = \sqrt{\langle f, f \rangle} = \sqrt{\int f^2(x)dx} \qquad \textbf{3.2.1}$$

A mother wavelet $\psi_{j,k}(x)$ convolve to a signal $f(x)$ to give a decimated coefficients as given in equation 3.2.2 (Ogden, 1997)-

$$d_{j,k} = < f, \psi_{j,k} > = \int f(x)\psi_{j,k}(x)dx \qquad \textbf{3.2.2}$$

ii. **Orthogonality:** It gives generalized notion of perpendicularity which ensures mutual independence of scaling function and wavelet basis. A sequence of functions $\{f_j\}$ is said to be orthonormal if the f_j 's are pair wise orthogonal and $\| f_j \|=1$ for all j (Ogden,1997). The inverse wavelet transform is reverse of the wavelet transform by adopting spatial resolution to the frequency.

iii. **Compact support**: wavelet describes spatially localized and transient variation by its compact support which takes none zero values only in some limited interval, which provides a local analysis of the signal for that interval. A vector $f \in L^2(\Re)$ is localized in space near x_0, if most of the components, except a few values of the compact support, are zero. To be noted here $\Re$ is a real number. This is opposite to the Fourier basis, whose vectors are dispersed evenly as possible (Frazier, 2000)

iv. **The Integral of the wavelet must summarize to zero**, As wavelet function has zero average i.e. DWT vanishes at zero frequency. In the words of Ogden any function $f \in L^2(\Re)$ can be approximated arbitrarily well by a finite linear combination of the mother wavelet $\psi_{j,k}$.

$$\int_{-\infty}^{\infty} \psi_{j,k}(x)dx = 0 \qquad 3.2.3$$

v. Admissibility condition: the set of all signals have finite energy, as shown in the equation 3.2.4

$$\sum_{n \in Z} |x[j]|^2 < +\infty \qquad 3.2.4$$

Here Z is integer and j is the level of dilation. The square integrable function which satisfies the above condition is analysed first and then without loss used for reconstruction of a signal. For meaningful convergence, x shouldn't be too large. (Frazier, 2000).

vi. **Regularity:** more regularity means more vanishing moments. Wavelets must have some concentration and smoothness in both frequency and space domain. The smoothness of the basis functions is beneficial in reducing the approximation error, getting proper features and estimating function in nonlinear regression analysis.

vii. **Symmetry:** To get a symmetric wavelet, its filter must have a linear complex phase and odd number of vanishing moments. Haar is the only symmetric as well as compactly supported orthogonal wavelet.

viii. **Vanishing moment:** The number of vanishing moments of the analysing wavelet decides the order of a wavelet transform. The increase in vanishing moment had direct impact on degree of polynomial and compact support increases, this leads to regularity and smoothness of wavelets. The wavelet had n-vanishing moments, if it satisfies the following equation

$$\int_{\omega} f(x)x^j dx = 0 \qquad 3.2.5$$

Where j= 0, 1, 2.....n number of vanishing moments
ω = supported bounded region

3.3. Discrete Wavelet Transforms (DWT)

Unlike the discrete Fourier transform, a discrete wavelet transform (DWT) includes large number of absolute but related transformations of mother wavelets for different frequencies at limited duration. Due to this reason wavelets are localized in space with a compact support, which is adequate for analysing local and complex pattern analysis. It is in contrast with Fourier decomposition, which is more suitable for stationary signals and more global information extraction. Between different wavelets trade off can be realized in terms of their compactness versus its smoothness, on the other hand Fourier transform remains always unique. A DWT is based on wavelet functions of a fixed family, confined within a finite domain giving an appearance like a wave, due to this reason it is named 'wavelet' (Strack et al., 1998).

When the signal is recorded on a very fine scale or in a continuous manner, CWT is often used. The interpretation of CWT is easier due to redundancy in coefficients which reinforce the traits and make the information more visible. It does not lose information in terms of saving space, so it's especially good for very subtle information. But this is also a disadvantage of CWT, which at every scale generates an awful lot of redundant and unmanageable data. The DWT decimations are more efficient and accurate as it uses dyadic scales and positions i.e. every decomposition is based on power of two.

In simple words a wavelet is compared with a section of original signal and the correlation of energies of the two are computed known as correlation coefficient. Results will depend on the shape of wavelet and original signal which can be adjusted by stretching wavelet at different dilation levels. A wavelet is defined by the wavelet function and scaling function. The wavelet functions are generated by Dilations and translations of the "Mother function" $\psi_{j,m,n}(x,y)$.

$$\psi_{j,m,n}(x,y) = 2^{-j/2}\psi\left(2^{-j}x - m, 2^{-j}y - n\right) \quad 3.3.1$$

The Scaling function $\phi_{j,m,n}(x,y)$: The scaling function is primarily responsible for improving the coverage of the wavelet spectrum.

$$\phi_{j,m,n}(x,y) = 2^{-j/2}\phi\left(2^{-j}x - m, 2^{-j}y - n\right) \quad 3.3.2$$

where the dilation parameter 'j' is the scale factor, which increases with the power of 2 with increase in level and determines the width of wavelets, how narrow or broad it will be along x-axis and the translation parameter 'm, n' = integers, known as shift index and are responsible for the location of wavelet function along the x-axis and y axis respectively.

$2^{-j/2}$ controls the height or amplitude of the wavelets. The reason for choosing this normalised factor is to keep energy of the daughter wavelet constant (Abbate et al., 2002).

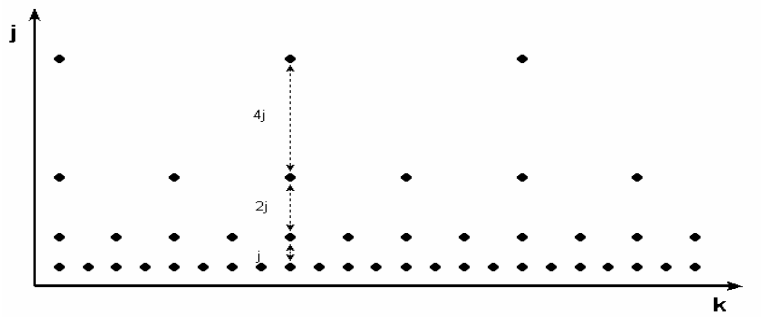

Figure 3-1: Dyadic grid of discrete wavelets localization.

The Orthogonality of the components is ensured at every step of translation by taking alternate values from the convolution as shown in the figure above. For low frequency we need fewer samples as shown at 4j level of decimation in the above figure 3-1 and vice versa. The two dimensional wavelet analyses apply the above approach twice, once along the horizontal *x*-axis and once along the vertical *y*-axis of the coordinate space, which yields four different types of two dimensional wavelets, as shown below:

Approximation coefficients: $\Phi(x,y) = \phi_h(x)\phi_v(y)$ 3.3.3

Horizontal coefficients: $\Psi^h(x,y) = \phi_h(x)\psi_v(y)$ 3.3.4

Vertical coefficients: $\Psi^v(x,y) = \psi_h(x)\phi_v(y)$ 3.3.5

Diagonal coefficients: $\Psi^d(x,y) = \psi_h(x)\psi_v(y)$ 3.3.6

$\phi(.)$ represents smooth (low frequency) part of the signal

$\psi(.)$ represents detailed (high frequency) part of the signal

An important contribution in wavelets was made by Mallat in 1998 by making a transition from mathematical theory to filters. The study on filter banks is known as 'sub band coding'. Here the term filter denotes a convolution operator, which will cut out those frequencies for which associated wave-

let multiplier is zero and convolve the non zero part of filter with the input signal (Frazier, 2000). Initially two filters are designed in sub band implementation which is scaled to form a filter bank. Generally by using two filters it's convenient to construct the wavelet transforms (Abbate et al., 2002). To obtain wavelets function from high pass filter and dilated scaling function from local weighted averaging low pass filter, there corresponding impulse responses are used (Abbate et al., 2002).

In every next level of decomposition they are down sampled to its half. The approximation crystal contains the low-frequency content of the signal and the highest energy distribution, hence it's the most important part of the signal which gives identity to it. The high-frequency content of the input signal is delineated in the detail crystals which gives the quality to the signals. High frequency means the signal which varies at a very short range in terms of geostatistics gives fine scale information. It seeks to analyse our data between frequency mean i.e. zero and the nyquist frequency (highest frequency that one can detect in the data i.e. $\frac{1}{2}x_0$). The basic computational step in DWT convolution followed in decimation is shown below in figure 3-2:

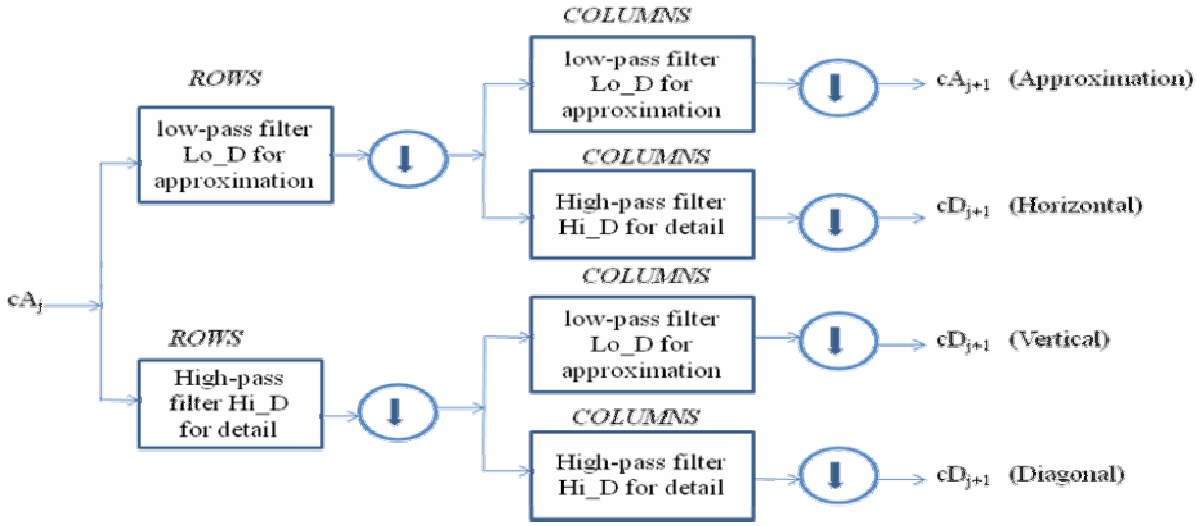

Figure 3-2: Two Dimensional DWT

The process iterate only on the approximation crystal i.e. each level is calculated by passing the previous approximation coefficients through a high and low pass filters bank as shown in the figure 3-2 which decomposes the input signal into next four lower scale. Because of which the approximation window became narrower with every dilation step and high frequency component occupies wide range of decimated frequency. After each decimation the input signal are represented as four separable two-Dimensional wavelet crystals, as one approximation and three detail functions (in horizontal, diagonal and vertical direction). As the index j runs from small to large, in the same way the corresponding approximation runs from coarse to fine (Ogden, 1997). The original signal can be reconstructed back, by summing up j^{th} level of approximation and all detail coefficients.

$$f(x,y) \approx \sum_{m=1}^{M/2^j} \sum_{n-1}^{N/2^j} s_{j,m,n}\phi_{j,m,n}(x,y) + \sum_{j=1}^{j} \sum_{dir} \sum_{m=1}^{M/2^j} \sum_{n=1}^{N/2^j} d^{dir}{}_{j,m,n}\psi^{dir}{}_{j,m,n}(x,y) \qquad 3.3.7$$

Where

$s_{j,m,n}$ Smooth wavelet transform coefficients at level j. Approximation crystal includes coefficients 's', which only occur at last level i.e at level j. The coefficients $s_{j,m,n}$ are given by expression 3.3.8

$$s_{j,m,n} \approx \int\int \phi_{j,m,n}(x,y)F(x,y)dxdy \qquad 3.3.8$$

Similar expression applies for $d^{dir}{}_{j,m,n}$ detail wavelet transform coefficients in each direction (horizontal, vertical and diagonal) at level j. These coefficients were grouped into crystals. Hence the smooth image at level j-1 of multi resolution approximation can be derived from sum of the smooth and detail images at resolution level j.

$$s_{j-1}(x,y) = s_j(x,y) + \sum_{dir} D_j^{dir}(x,y) \qquad 3.3.9$$

3.4. Multi Resolution Analysis

Mallat and Meyer in 1986 formulted Multiresolution analysis (MRA), it provided a natural framework to understand the logic behind the concept of wavelet basis, which ultimately become the tool for constructing new wavelets. MRA provides the ability to change the resolution according to the need, similar as using a microscope (with different magnification levels). In recognising the pattern it can be of great help (Abbate, 2002).

The sequence of subspaces for a function space $V_j, j \in Z$ posessess the following properties (Ogden, 2002) Here Z is a integer:

i. A sequence of embedded closed subspaces:
$$\ldots \subset V_{-2} \subset V_{-1} \subset V_0 \subset V_1 \subset V_2 \subset V_3 \ldots \subset L^2(\Re); \qquad 3.4.1$$

ii. Emptiness i.e. no information or no detail and completeness i.e. whole space of square integrable function respectively as
$$\cap_{j\in Z} V_j = \{0\}, \overline{\cup_{j\in Z} V_j} = L^2(\Re); \qquad 3\text{-}3.2$$

iii. Scale invariance $f \in V_j$ If and only if $f(2\cdot) \in V_{j+1}$; 3.4.3

iv. Shift invariance $f \in V_0$ Implies $f(\cdot - k) \in V_0$ for all $k \in Z$ 3.4.4

3.5. Different Wavelet functions applied

Different wavelet families make different trade-offs between the compactness of the basis functions in space and their smoothness.

3.5.1. Haar wavelet

Haar in 1909 replaced the sine and cosine functions of the Fourier transform with very simple orthonormal basis function using dyadic scaling known as 'Haar' (Abbate et al., 2002). It is the first known and the simplest square wavelet which opened the routes leading to the concept of wavelets. Major disadvantage of Haar is its discontinuous basis due to which it is not differentiable and hence not optimal for approximating a continuous function. But due to this it is useful for extracting discontinuity. The Haar wavelet's mother wavelet function $\psi_{j,k}(x,y)$ can be described as:

$$\psi_{j,k}(x,y) = \begin{cases} x + \pi, -\pi \le x \le -\pi/2 \\ \pi/2, -\pi/2 \le x \le \pi/2 \\ x - \pi, \pi/2 \le x \le \pi \end{cases} \qquad 3.5.1$$

and it's scaling function $\phi_{j,k}(x,y) = \begin{cases} 1, 0 \le x \le 1 \\ 0, otherwise. \end{cases}$ 3.5.2

Haar wavelet has a support given by equation 3.5.3

$$\Psi_{j,k} = [k2^{-j}, (k+1)2^{-j}] \quad 3.5.3$$

For 1st decimation level and no shift means j=1 and k=1 Haar wavelet support will be $\Psi_{1,1} = [2^{-1}, (1+1)2^{-1}] = [0.5, 1]$

The scaling and wavelet function of Haar and their respective decomposition and reconstruction high and low pass filter are represented in figure 3-3.

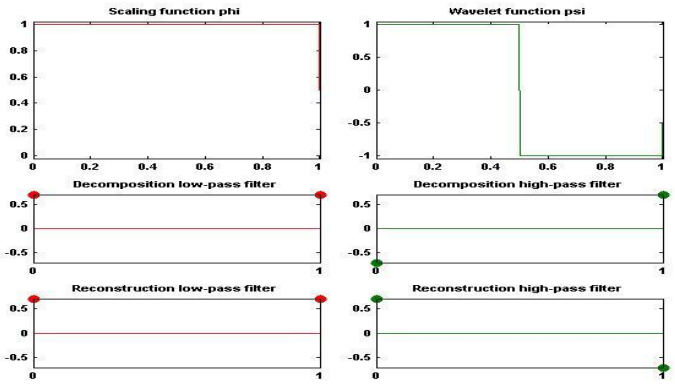

Figure 3-3: scaling and wavelet function of Haar wavelet.

Daubechies (1988) point out that Haar is the only real valued wavelet that has Orthogonality, compact support as well as fully symmetrical properties, with its poor frequency localization (Ogden, 1997).

3.5.2. Daubechies wavelet

Daubechies introduced the concept of compactly supported orthonormal wavelets and theory of frames in 1988. It is a compact continuous orthogonal wavelet, characterized by a maximal number of vanishing moments for some given support. It is an asymmetric wavelet basis having fractal structure. There are 10 family members in Daubechies, out of which first member db-1 is 'Haar' wavelet. These members are distinguished by the number of coefficients and the level of iterations, smoothness of the functions increases with increase in number of coefficients.

Db-4 wavelet used in this research has eight coefficients (0.1629, 0.50547, 0.4461, -0.019788, -0.13225, 0.021808, 0.023252, and -0.0074935) and four vanishing moments. The scaling and wavelet function of db4 and their respective decomposition and reconstruction high and low pass filter are represented in figure 3-4.

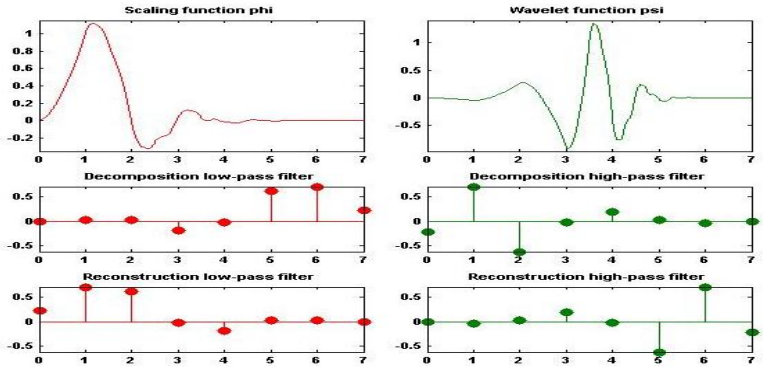

Figure 3-4 Scaling and wavelet function of daubechies-4 wavelet

Daubechies wavelets use overlapping windows, so all high frequency changes get reflected in the high frequency coefficient spectrum. Daubechies family of wavelets and scaling functions are derived from filter coefficients. The sequence of elements of a filter is derived as-

$$h_k = \int \phi(x)\sqrt{2}\phi(2x-k)dx \qquad 3.5.4$$

Daubechies approach to constructing orthogonal compactly supported wavelets begins with defining the 2π periodic trigonometric polynomial associated with the filter $\{h_k\}$. The wavelets and scaling function are written in terms of $m_0(\omega)$ function.

$$m_0(\omega) = \frac{1}{\sqrt{2}}\sum_{k\in Z} h_k e^{-ik\omega} \qquad 3.5.5$$

A new family of wavelets can be obtained by constraining this function to give Orthogonality and smoothness. The different wavelets make different trade-offs between smoothness of the wavelet and their compactness of the basis function localised in the space. Daubechies gives more emphasis on localising compactness hence is one of the most unsymmetrical wavelet family having a fractal structure. If any part of it is zoomed in, it will give the same structure as that of whole wavelet. This self similarity is a prominent feature of Daubechies wavelet.

Daubechies wavelets are very asymmetric because they are constructed by selecting the minimum phase square root, which had its energy concentrated in the beginning of their duration support (Abate, 2002). Db-4 has comparatively very short basis function hence can better isolate signal discontinuities i.e. fine details.

3.5.3. Symmlets Wavelets

Symmlets are nearly symmetrical wavelet proposed by Daubechies in 1992 as a modification of db family. It also has compact support Orthogonality, capable of exact reconstruction. Sym-8 wavelet used in this research has sixteen coefficients (0.0013364, -0.0002142, -0.010573, 0.0026932, 0.034745, -0.019247, -0.036731, 0.2577, 0.54955, 0.34037, -0.043327, -0.10132, 0.0053793, 0.022412, -0.00038335, -0.0023917) and eight vanishing moments. The scaling and wavelet function of sym-8 and their respective decomposition and reconstruction high and low pass filter are represented in figure 3-5.

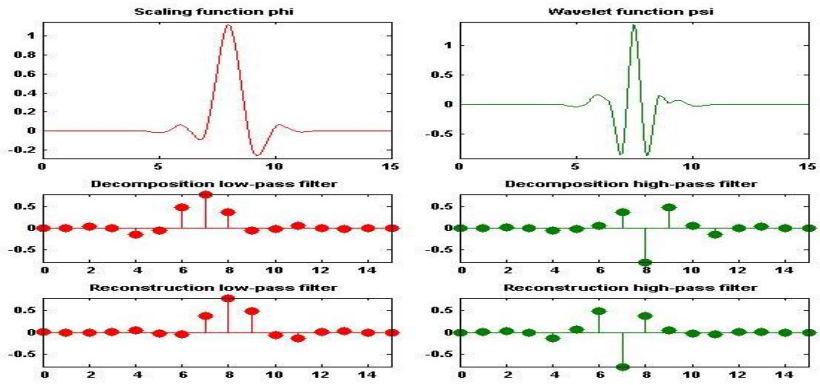

Figure 3-5 scaling and wavelet function of Symmlets-8 wavelets.

As seen in figure 3-5 symmlets is an almost symmetrical and smooth wavelet, hence have comparatively weak compactness.

4. Study Area and Data used

4.1. Location

The 'Dooars' valley extends between the north eastern part of India and also at the foothills of the Himalayas. Dooars means door which is a gateway to Bhutan, at an altitude ranging between 90-1750 m . Dooars region politically constitute the whole of Jalpaiguri (West Bengal) and Dhubri, Kokrajhar, Barpeta, Goalpara and Bongaigaon Districts of Assam, the plains of Darjeeling District and upper region of Cooch Bihar Districts of West Bengal. To the north of West Bengal, the Dooars valley constitutes a vast texture of dense forests, interwoven with lush green Tea gardens, stretching from River Teesta on the west to the River Sankosh on the east. Because of innumerable streams and rivers flowing through the region and suitable climatic conditions, the region is blessed by dense vegetation cover, showing the fertility of the land. There are more than 600 tea gardens in this region, out of which this study is based on two tea gardens of Jalpaiguri district as shown below

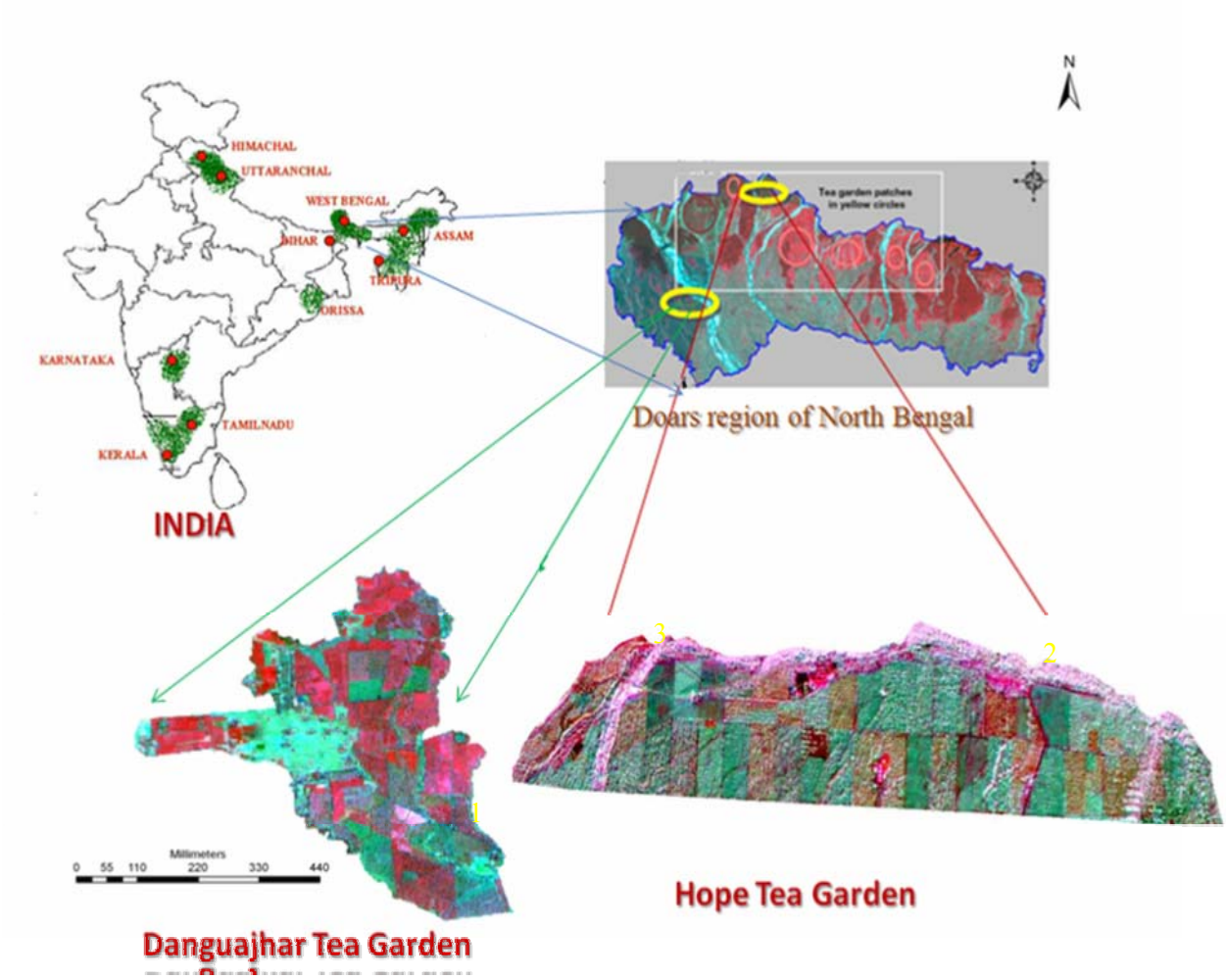

Figure 4-1: Study area.

4.2. Data Used

This study was carried out by using remote sensing and ancillary data mentioned in the following sections. For pattern analysis of small sections of tea garden of 10-13 hectare area high resolution remote sensing data was required. So google earth image was captured at 1m spatial resolution. Due to non availability of high resolution satellite data for the region, LISS III (23.5m) was fused with cartosat-1 (2.5m).

4.2.1 Remote Sensing Data

In Indian earth observation programme Resourcesat (IRS-P6) was lounged in 2003 for land and water assessment, which is consist of AWIFS, LISS III and LISS IV sensors of respectively 55, 23.5 and 5.8 meter resolution, shown in figure 4-2(a). Panchromatic stereo imaging Cartosat-1-1 was lounged in 2005 for cartographic purposes, shown in figure 4-2(b) . Following satellite data were used for this study.

Figure 4-2: (a) Resoursesat satellite and (b) Cartosat-1-1 satellite

4.2.1.1. LISS III Image

Liss III image of the Hope Tea garden acquired on 9th December 2005 from IRS.-P6 sensor was used. LISS III consists of spectral range from 0.45 to 0.86 micro meters, which is captured in 4 bands as green (0.52µm-0.59µm), red (0.62µm- 0.68µm), near infra-red (0.77µm-0.86µm) and middle infra-red (1.55µm- 1.7µm). It revisited 141 km swath in 24days with 23.5 meter spatial resolution.

4.2.1.2. Cartosat-1-1 Image

Cartosat-1-1 stereo image for Hope tea garden acquired on 26th December 2005 and for Danguajhar tea garden on 18th April 2008 to generate DEM were used. The stereoscopic mages were generated by capturing the same area at 5 degree tilt in AFT band and 26 degree tilt in FORE band. The panchromatic Cartosat-1-1 images covers 30 km swath at 2.5 meter ground resolution.

4.2.1.3. Google Earth Image

High resolution google earth image were downloaded from website for the region. The images were dated to be acquired on 26th October 2006 for Hope tea garden and 17th December 2006 for Danguajhar tea garden, which was resampled to bring at nearly 1 meter spatial resolution.

4.2.1 Ancillary Data

Tea Research Association provided the following ancillary data:

- Daily rainfall record for last 10 years from 1997 to 2006.
- Random soil samples collected for the sections under the study, without geographic coordinates.

- Section wise data of age, yield, soil pH, organic carbon, Nitrogen %, potassium %.

4.3. Sections of study

In this study whole tea replantation process was analysed in 4 different stages as just after uprooting, after guatemala plantation, when guatemala was mature and finally just before replanting of tea seedlings. This study required multitemporal dataset of the same section for proper analysis but due to non availability of remote sensing data of the region, these stages were taken from different sections. Again only 2-3% section of the whole garden undergoes replantation every year, so all stages were not there on the acquired date in only one garden. Therefore one stage was taken from Danguajhar and other three stage from Hope Tea Garden.

4.3.1. Danguajhar Tea Garden

Danguajhar is under Goodricke Tea Industries limited, having 962.41 hectares area under plantation. It is situated adjoining to the Teesta River with latitude and longitude extending between 26°35'44.21"N and 88°41'12.94"E to 26°32'45.98"N and 88°40'0.37"E.

4.3.1.1. Just after uprooting of Tea plants

For nearly 3 months, the field is left fellow after proper leveling and ploughing as shown in figure 4-2(a). On 17th December 2006, when the image was captured Section 8b is in the first stage of replantation. The section was well drained and almost flat covering 13.07 hactares area.

4.3.2 Hope Tea Garden

Hope Tea Garen has 432.12 hacts area under plantation and is divided into two divisions i.e, West Division and East Division. It is situated Near to the Bhutan border with latitude and longitude extending between 26°57'49.16"N and 88°54'1.64"E to 26°57'8.39"N and 88°57'5.93"E.

4.3.1.2. Young Guatemala

Guatemala remains on field for nearly 18-24 months, its young plantation can be seen in section 18 of the garden in december 2005.The area of the section is 10.41 hactares and is of irregular shape,a part of which is taken for the study as shown in figure 4-2(b).

4.3.1.3. Mature Guatemala

Full grown Gwatemala is shown in 4-2 (c) which is section 4N in LISS III and Cartosat-1 fused image for december 2005. The average yeild of the section was also low as compared to the expected estimation. It was planted in 1886. It was expected to yield 2000 kg per hectare but its yield decreased to 684 kg per hectare by the end of 2002 and the average yeild of the section was 1153 kg per hectare. So the section was uprooted in the year 2003 and replanted in 2006.

4.3.1.4. Fellow land just before replanting the Tea

The field is ready for new plantation as seen in the figure 4-2(d), which is the section 4N of the Hope Tea Garden in october 2006, acquired from google earth. The area of the section is 9.61 hectares and is located in the West Division. The plants were planted at a spacing of 105x65feet.

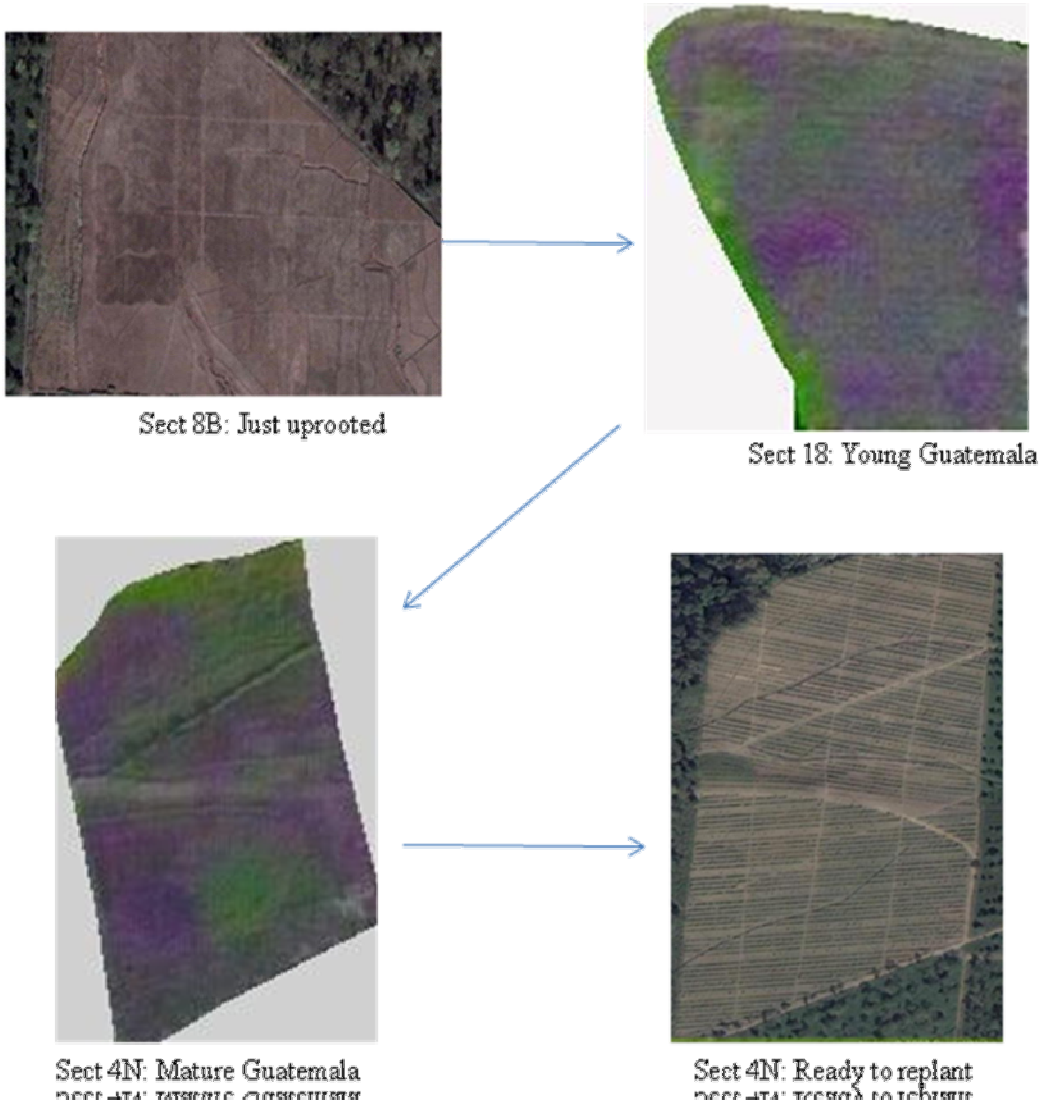

Figure 4-3: stages of replantation in a. Section 8b, b. Section 18 and c. and d. of Section 4N.

4.4. Ecology

The word Jalpaiguri means a place where olive is grown. Jalpaiguri is one of the most prominent wildlife areas in India and bears the best Sal forest in the country. The main forest cover comprises of Semi-Moist-Deciduous vegetation with grasslands which nourishes a wide spectrum of wildlife. The region provides shelter and protection to various species of wildlife included in the Red Data Book (RDB) and appendices of CITES (Convention on International Trade in Endangered Species) of wild Flora and Fauna (www.jalpaiguri.nic.in).

4.5. Climate

Dooars region falls in the sub-tropical climatic zone, characterised by high monsoon rainfall. The region is blessed by 7-8 months of long rainy season from March to October as shown in the chart for last 10 years from 1997 to 2006. The average maximum and minimum temperature is 31 and 10 degree celcius repectively. Average annual rainfall the area is about 3,500 mm. Summers are mild and humid and constitutes a vey short period of the year. Winters are cold and dry with foggy mornings and nights.

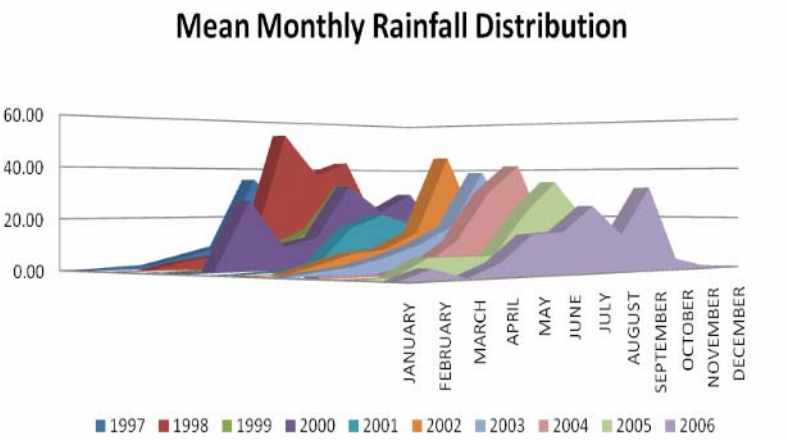

Figure 4-4 Mean monthly rainfall distribution of Dooars region.

Heaviest rain occurs from mid of May and continues till the end of September due to moisture laden south-west monsoon towards the Eastern Himalayas. Such a heavy rain provides natural irrigation and suitable climatic condition for tea growth but on the other hand it also causes flood espacially in Brahmaputra and Teesta rivers. Overflowing of rivers is a common phenomenon during monsoon in this region, causing sedimentation in the adjoining gardens.

4.6. Economy and population

The district is primarily rural with more than 80% of rural population (www.jalpaiguri.gov.in). Economy of the region depends on the 3 T's as Tea, Tourist and Timber. The region is famous for Tea gardens planted by the Britisher's. For working in the gardens and developing the forest into tea villages, British imported labour from the adjoining areas. These people are now granted scheduled tribe status leading to high percentage of SC/ST population. Apart from them many thousands of people are engaged in the tea estates and factories directly or indirectly.

The vast texture of dense forests with turbulent rivers battling out of the steep gorges in panoramic grandeur of the Himalayas is specially noted for its wild life sanctuaries, having fascinating diversity of flora and fauna making it a paradise for nature lovers and ecotourism. But a major potential of it still remains unexploited. Timber smuggling is other major business in the region with the increasing population.

5. Methods Adopted

5.1. Data Preparation

High resolution good quality google earth data was available for the region. But it doesn't have spectral information, required for vegetation study. So multispectral LISS III data was used, but it has very poor spatial information for precision agricultural studies. High resolution satellite imagery was required to capture the dynamics of complex landscape within a small field; hence Liss III image was merged with the Cartosat-1 data, carrying high spatial resolution information.

5.1.1. Preprocessing of Google image

The downloaded google earth image loses its coordinated when captured in the JPEG format. So it was georeferenced to assign the rows and columns of the image with a real world X, Y location using UTM WGS 84 North projection and 45 zone with less than 0.40 RMSE (root mean square error). The geometric correction of the images was done with the help of the more than 30 ground control points, collected from google earth and then accurately located in the image. The image was resampled to assign the DN values to the transformed grid by using nearest neighbor (NN) interpolation algorithm, because NN closely preserves the spectral information of the original image.

5.1.2. Image Fusion of LISS III with Cartosat-1

LISS III image was fused with AFT image of fine resolution panchromatic Cartosat-1 because of its near nadir acquisition angle. It brought 23.5 meter spatial resolution to 2.5 meter in ground. Data fusion is the process of merging multi-source data with different characteristics in terms of spatial and spectral resolution by using image fusion algorithm in order to get enhanced or better quality of information in one image. A general definition of image fusion is given as "Image fusion is the combination of two or more different images to form a new image by using a certain algorithm" (Pohl and Genderen 1998).

According to Pohl and Genderen Van (1998), there are many advantages of Image fusion such as it enhances certain features not visible in either of the single data alone by complementing and substituting the missing information. It not only improve geometric corrections and the sharpen images but also provides stereo-viewing capabilities for stereo photogrammetry. In general, the pixel based image fusion techniques can be categorised as under:

- IHS (Intensity Hue Saturation): In image fusion using IHS transformation method. First the three bands of the image (with lower spatial resolution) in RGB is transformed into three components, I(Intensity),H(Hue) and S(Saturation). The image of higher spatial resolution is then contrast stretched to match the variance and mean of the Intensity image. Then the intensity component among the I, H and S is replaced by higher spatial resolution image. This new IHS image is again transformed to RGB by using inverse IHS transformation.
- Principal Component Transform: Similarly in PCA method principal components are derived from the image of lower spatial resolution where each component is uncorrelated with one another. The image of higher spatial resolution is then contrast stretched to match the variance and the mean of the first component image is substituted for the same and transformed back to RGB using inverse PCA transformation.

- Brovey Transformation: Brovey Transformation method uses algorithm to combine the images in which three bands are used according to the following formula:
  [DNB1 / DNB1 + DNB2 + DNB3] × [DN high res. image] = DNB1_new
  [DNB2 / DNB1 + DNB2 + DNB3] × [DN high res. image] = DNB2_new
  [DNB3 / DNB1 + DNB2 + DNB3] × [DN high res. image] = DNB3_new
  Where: B(n) = band (number)
  i.e each of the three multispectral bands used for RGB display are first normalized and then multiplied with the higher resolution cartosat-1 data. This causes increase in the contrast of the image but the radiometry of the image was no more preserved after the fusion and makes the resulting image visually more appealing by increasing the contrast between the features of interest.

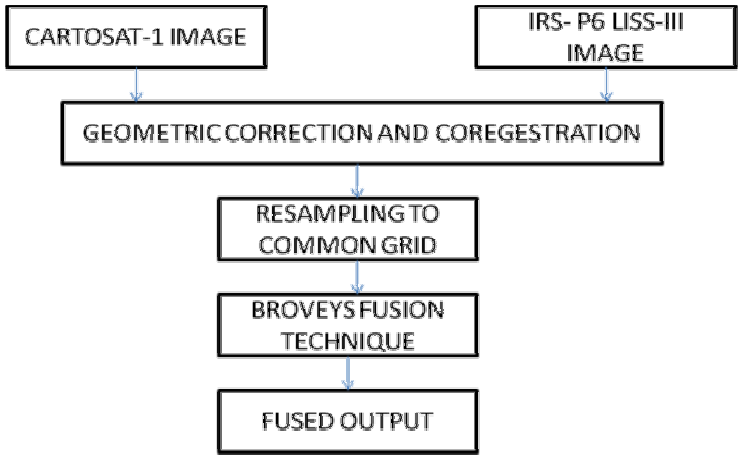

Figure 5-1: Methodology adopted for image fusion.

Among the above mentioned techniques Broveys transformation was used in the present study to fuse LISS III and Cartosat-1-1. Because in this transformation band wise fusion takes place due to which the comparative identity of each band was preserved. While in other image fusion processes such as PCA and IHS transformations the higher resolution image replaces one of the bands of the original image. As a result of which the originality of the image bands no more exits. In this transformation among various resampling techniques such as nearest neighbour, bilinear interpolation and Cubic convolution, cubic convolution resampling technique was used.

In nearest neighbour resampling technique, the grey value from the closest pixels were interpolated and assigned to the centre pixel. In bilinear interpolation and cubic convolution, the grey level from the weighted average of the four closest pixels and 16 closest pixels respectively is assigned to the specified pixel. Among these resampling methods cubic convolution was found better for this study because in this method, optimal trade off between the interpolation accuracy and the computational complexity was done. This technique resulted sharper images than produced by bilinear interpolation and no blocky appearance as in case of nearest neighbour interpolation.

5.2. Perpendicular Vegetation Index (PVI)

To identify and to assess the pattern of vegetation distribution is one of the primary goals of remote sensing. Most commonly used vegetation index is NDVI (normalized differential vegetation index), but it requires near infra red and red spectral bands. In the study high spatial resolution of the fused image is obtained at the cost of spectral information of the image. So neither the fused image nor the google image had the spectral information required for NDVI computation. In 1977 Richardson and

Wiegand developed perpendicular distance to the soil line as a measure of vegetation development known as perpendicular vegetation index. Generally a greater amount of vegetation is observed on the points farther away from the soil line toward its left (Curran 1983). This distance based vegetation indices can detect the features of the vegetation cover by eliminating the effect of brightness of soil background.

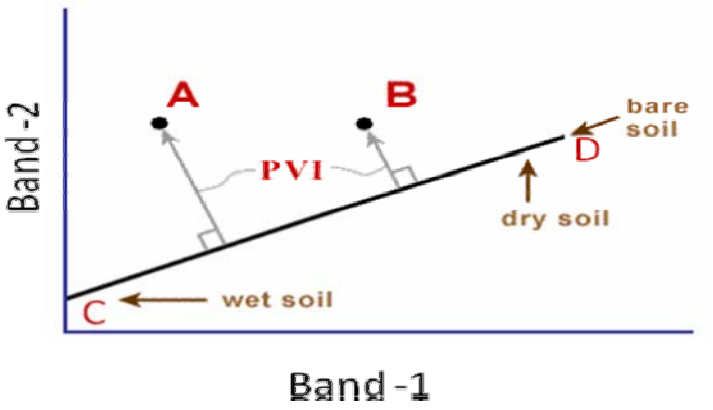

Figure 5-2: Perpendicular Vegetation Index plot.

A line is drawn between two extreme points of dry (D) and wet (C) soils existing in the scatter plot. Point A and B show the vegetated areas respectively for dry and wet soils. The soil line represents variation in the two dimensional Kauth- Thomas soil brightness value index (SBI). PVI is generally calculated using NIR and Red band and the equation uses constant accordingly. Columbus et al. (2001) described the formula, where constants are derived from the soil lines generated between wet and dry soil, as described in equation.

$$PVI = \frac{NIR - aR - C}{a^2 + \sqrt{a^2 + 1}} \qquad 5.2.1$$

Where NIR = Near Infrared band (band giving highest reflection to vegetation)

R = Red (band giving lowest reflection to soil)

a = slope derived from soil line

c = constant interception of soil line.

In the study as no NIR spectral information exist because either it was lost due to fusion or not available in google earth image. Taking the same soil line concept, a linear regression is drawn between the bands which better represents the vegetation against the band representing the pixels of bare soil. This distance based vegetation index is designed to detect the feature of vegetation cover and eliminate the background soil brightness.

5.3. Digital Elevation Model (DEM) Generation

Cartosat-1 being a multi-view high resolution stereo data of 2.5 meter pixel size provides a unique capability of surface mapping with hight accuracy, in the meter range. DEM generated from Stereo image is a most common method of elevation modelling, consisting of steps described in this section.

5.3.1. Interior and Exterior Orientation

To generate DEM from stereo Cartosat-1 data Lieca Photogrammertic suite (LPS) version 9.1 was used. Interior orientation defines the internal geometry of the sensor, existed during the capture of image. The images are radio-metrically corrected and supplied with the rational polynomial coefficients (RPC) model, with the Cartosat-1 datasets in text format. The information defining the internal orien-

tation is read form the coefficients existing in the RPC file. Then external orientation defines the position and angular orientation of the sensor at the time when image is capture. For this geometric model of UTM WGS-84 projection in zone 45 was selected and then georeferenced from the RPC files. The registration by RPC method computes the polynomial adjustment model for each image, to build a correlation between the pixels and their ground locations, but having nearly 100 meter positional accuracy. To improve the accuracy of the extracted DEM, ground control points collected from the google earth were attached as shown in the figure 5-3.

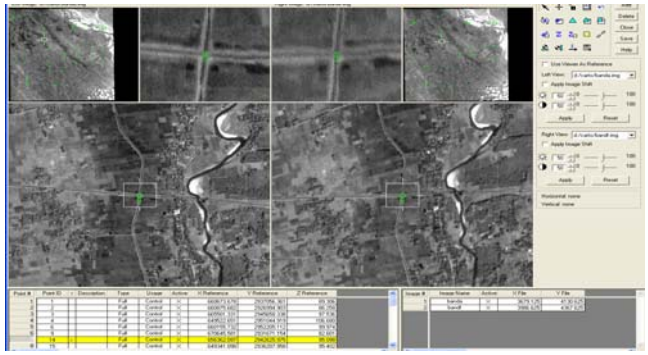

Figure 5-3: GCP's applied in stereo model using LPS.

5.3.2. Tie point generation and Triangulation

The tie points were generated by automated image matching procedure on both the images, whose ground coordinates was not known and were calculated during the triangulation. The location accuracy of the points was checked and then report was generated to assess the accuracy of the triangulation. The systematic offset of the RPCs in location was removed by triangulation using the GCP and tie point information. The points giving high error in the residual report were eliminated and new control points with more accuracy were used. Then bundle adjustment was updated. Again the report was generated and the process iterates till overall root mean square error for GCP's reaches 0.3 pixel accuracy. DEM was generated at 10 meter cell size with contour lines as shown in figure 1-4, which can be of immense use for topographical analysis of the field.

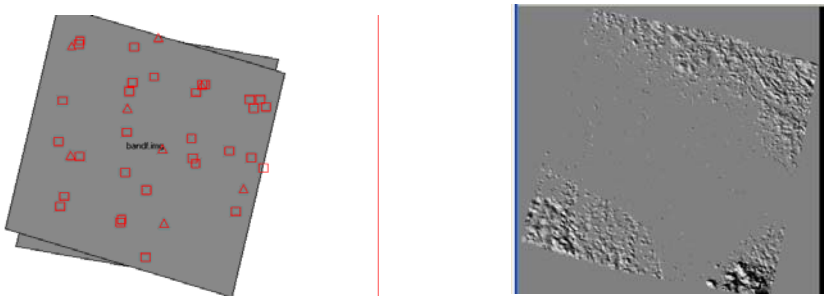

Figure 5-4:) Block details of stereo model and b) Generated relief map.

The above stated procedure for DEM generation was adopted for Hope and Danguajhar Tea Garden, as both gardens are not coming in one Cartosat-1 image. Then the subsets of the sections, under analysis were taken to get elevation information from the DEM.

5.4. Wavelet Decimation

The subset of the sections were taken from the perpendicular vegetation indices images, generated from the google earth and fused image. The image needs to have some pre-processing before entering into wavelet analysis.

Wavelets works like a kernel movement, hence had the same problem at edges as filters in spatial domain. The boundary pixel problem is well known constrain of wavelets, it requires square or at the most rectangular image. But in reality fields are irregular and wavelet considers the no-data value outside the area of interest and hence the features at edge get distorted. This effect increases going down the decimation, as shown in the figure 6-1of horizontal details.

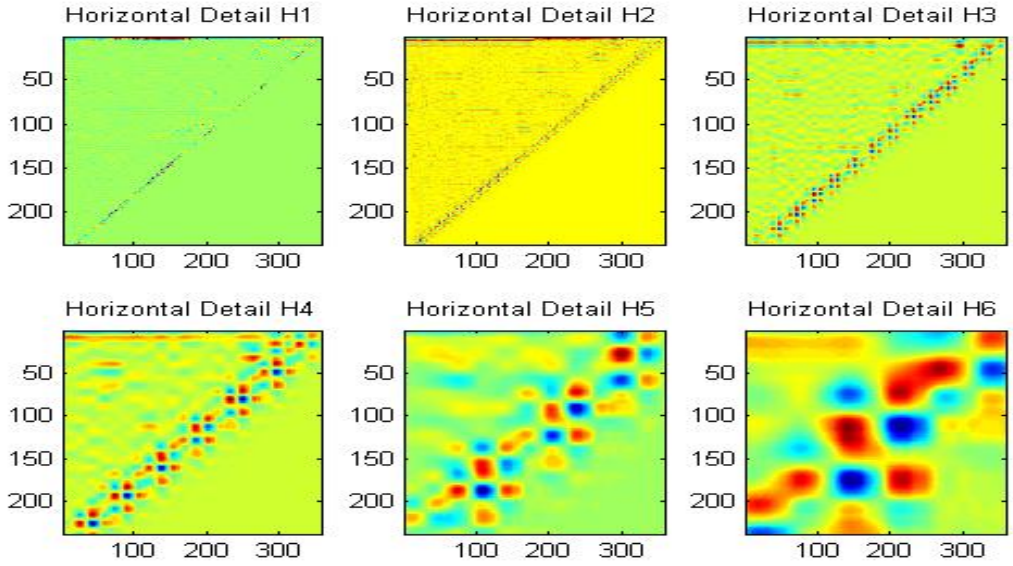

Figure 5-5: Horizontal details showing the edge effect problem.

To solve the boundary pixel problem two approaches is possible:

a. Reduce the size of field to bring it upto near square shape. But this will leads to loss of section area to be analysed. For the case like India fields are very irregular and hence may be major part of section will be lost and cannot be analysed, as shown in the figure 6-2.

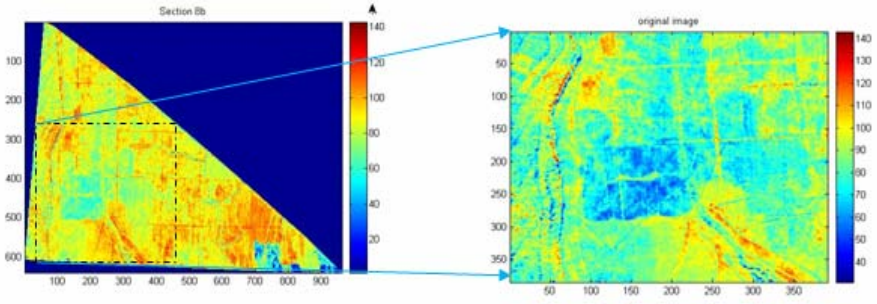

Figure 5-6: Subset to resolve edge effect problem

b. Cosmetic correction: Three different methods were tried. By extending the border pixel to all of the vacant sides, as seen in the figure it develops an artefact in the image and is the worst solution. Replicating the image on its edges so that a mirror image of it can fill the zero pixels but it was also found to generate false features. The last option tried and then finally selected was replacing all zero pixels outside the edges of the section by an image average value. It will

decrease the abrupt change in the features on the border as well as will not generate any false features. Epinate et al. (2001) also assigned the average NDVI value in the pixels outside the field to avoid bias.

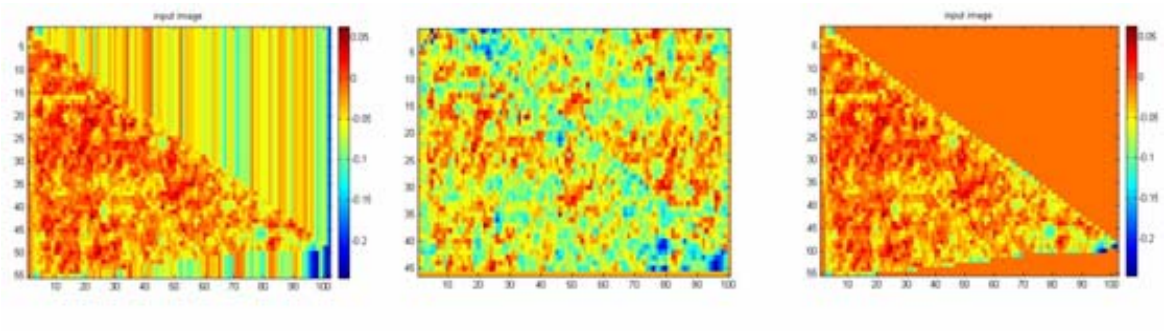

Figure 5-7: Cosmetic correction to resolve edge effect problem.

Another issue was to reduce the artifacts and error at the boundaries during reconstruction. DWT works faster when dimension of image is in powers of two. It was found advisable to work with square images, so that filtering will be same in both directions i.e. even after transposing the matrix. The discrete convolution of the function (as shown in equation below) i.e. a kernel of filter and input signal *g(x, y)* need to do extra padding for proper reconstruction.

$$\text{Length of each decomposed crystal} = \frac{floor(l-1)}{2} + N \qquad 5.4.1$$

Where l = length of original signal

N= length of filter (wavelet)

The kernel needs to be extended to have same length of signal by padding it with zeros or periodic repetitions or symmetric padding as the mode specified, to accommodate edge effects during reconstruction. In this research symmetric padding was done to increase the pixels during the slide of neighborhood block. This method assumes that the images can be recovered from outside the original support by replication of boundary pixel values.

After all these pre-processing images of the sections were decimated upto six levels by using Haar, Daubechies and symmlets wavelet coefficients using MATLAB wavelet codes. Based on the level of information required for the general pattern, most suitable level was selected from the decimated approximations. From the selected level, best suitable wavelet among the three was analysed for the reason of the upcoming pattern. The Detailed coefficients generated in each direction were analysed by anisotropic autocorrelation. The level having highest repetivity in the autocorrelation image was selected, which shows that the image has highest spatial dependence for that frequency.

5.5. Geostaistical Technique

5.5.1. Correlation

Correlation is a measure of strength of linear relationship between two variables, based on this relationship prediction of other variable can be made. Its value lies between -1 to +1. Pearson product correlation coefficient is calculated by dividing covariance of two variables *a* and *b* by the product of their standard deviations.

$$r_{a,b} = \frac{\text{cov}(a,b)}{\sigma_a \sigma_b} = \frac{\sum (a_i - \bar{a})(b_i - \bar{b})}{(n-1)s_a s_b} \qquad 5.5.1$$

σ_a = standard deviation of variable *a*
σ_b = standard deviation of variable *b*
$\bar{a}$ = sample mean of variable a_i
$\bar{b}$ = sample mean of variable b_i
s_a = sample standard deviation of variable a_i
s_b = sample standard deviation of variable b_i

5.5.2. Cross Correlation

Pearson correlation indicates the strength of a linear relationship between the two variables, but its value alone cannot evaluate the relationship properly. While cross correlograms provides the strength of correlation between the variables and the extent of distance upto which the correlation is significant. For spatial exploration of data, which is consist of looking at the cross dependence between measurements of different attributes, cross correlograms were calculated as described in equation 5.5.2 (Goovaerts, 1997).

$$\rho_{12}(h) = \frac{1/n\sum_{i=1}^{n} Z_1(x_i)Z_2(x_i+h) - m_{1-h}m_{2+h}}{\sqrt{\sigma^2_{1-h} * \sigma^2_{2+h}}} \in [-1,+1] \qquad 5.5.2$$

m_{1+h} Mean of variable-1

m_{2+h} Mean of variable-2

σ^2_{1+h} Variance of varianble-1

σ^2_{2+h} Variance of varianble-2

5.5.3. Anisotropic autocorrelation

A phenomenon is said to be anisotropic when its pattern of spatial variability changes with the direction (Goovaerts, 1997). When the pattern of decrease varies in the autocorrelation graph with the direction for all point pairs, the discrepancies reflects the correspondence of data distribution in a particular direction. This behavior signifies the presence of anisotropy in the data. Anisotropy discerns the directional differences in autocorrelation. In other words, when variation in the data, changes more rapidly in any particular direction, it signifies anisotropy in dataset. The results obtained from the wavelet decimation in detail frequency crystals, divides the fine changes occurring in the space, in horizontal, vertical and diagonal directions. Thus the existence of anisotropy is sure in the detail directional crystals.

The overall pattern between proximity and similarity of pixel values were evaluated by autocorrelation providing an indication of the local homogeneity of a data set.The fundamental assumption in the method was stationarity of the data. This means that any two locations at a similar distance and direction would have similar variance.

$$\text{Autocorrelation} = \rho = \frac{n\sum p_i * p_{i+k} - \sum p_i * \sum p_{i+k}}{\sqrt{(n\sum {p_i}^2 - \sum {p_i}^2) * (n\sum {p_{i+k}}^2 - \sum {p_{i+k}}^2)}} \qquad 5.5.3$$

Where

P_i= pixel value at i^{th} position in map.
P_{i+k} = pixel value at k pixel further to i^{th} pixel.
n = number of point pairs to be compared based on cutoff.
Autocorrelation is unitless.
Spatial autocorrelation measures dependence or correlation among nearby pixel values in a spatial distribution. The adjoining variables are supposed to be correlated because they are affected by similar processes or phenomena. By plotting the difference of squared values of point pairs against the distance, the spatial autocorrelation existing among the data can be seen. Point pairs which are closed together in distance should have less difference squared values, showing high spatial dependence. And the distance beyond which the difference squared value levels out, the point pairs are considered to be uncorrelated.

5.6. Methodology Adopted

For precision agricultural studies high resolution data is required so in this study google earth data at 1m resolution and fused LISS III and Cartosat-1 data at 2.5m spatial resolution was taken. These data do not had spectral information required for calculation of NDVI so PVI (perpendicular Vegetation Index) was calculated as a greenness index. After undergoing required pre-processing as discussed in section 5.4, the images of each stage of replantation was bought in wavelet domain. After decimation from the approximation as well as detail crystals best suitable representation of each section as well as detail informative crystals were selected based on correlation and autocorrelation respectively. The general characterstics of garden as well as the section under study was analysed. The topographical and hydrological parameters were derived from Digital Elevation model generated from the stereo cartosat data. Derived parameters were correlated and analysed with the extracted pattern from wavelets. Analysis was supported by the ancillary information like soil and climate. The overall methodology followed in this study was shown in figure 5-8:

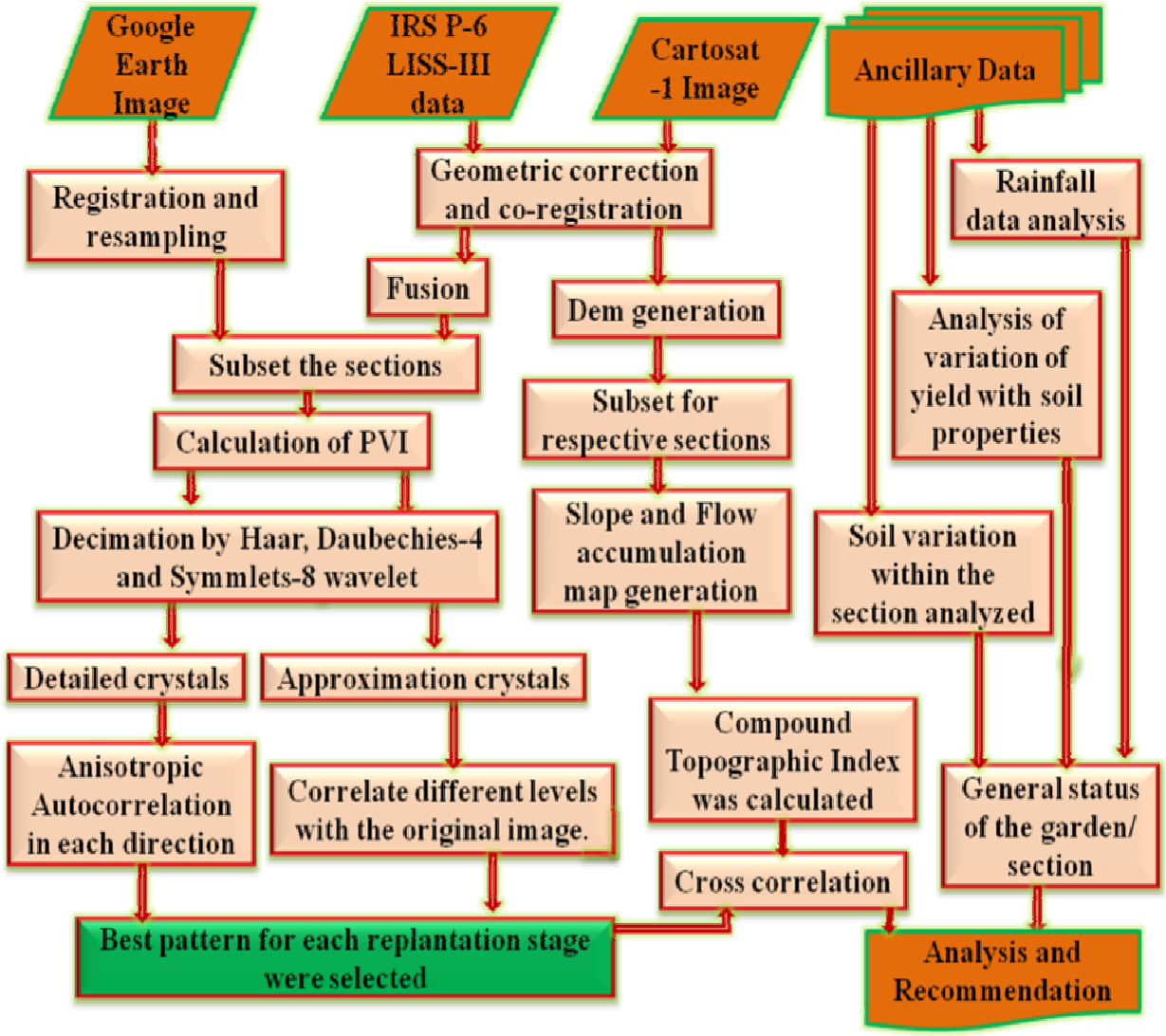

Figure 5-8: Methodology adopted

6. Results and Analysis

In the study the analysis was done on four different development stages of tea replantation. Based on the required stage, sections were selected from the available images of different acquisition dates, as multi-temporal images were not available. Greenness index/ soil brightness index was calculated in the form of PVI/PSI images at different stages of replantation (taken from different sections). After resolving boundary issue discussed in section 5.4 of thesis, the images were decimated upto six levels using Haar, Daubechies and Symmlets wavelets.

6.1. Just after uprooting of Tea plant (Section-8b of Danguajhar tea Graden)

Just after uprooting of tea plant, the section was left open to kill the micro-organisms present due to prolong shade and moisture conditions of more than 100years, as well as to absorb the nutrients supplied during this stage. In general every year 2.5% area of the garden was targeted to replant and priority was given to least producing section to maintain the age balance of the estate. Tea was deep skiffed (5-10 tones organic matter/ha) before uprooting (Replantatation processes, TRA). During the first stage contour survey, identification of catchments, marking of drainage lines and filling up unwanted drains and shade stump holes was done. The ideal pH for tea growth is 4.5 to 5.5, to increase approx. 0.5 unit of pH, 2 tones of dolomite was applied. Sub-soiling to break pans (if exist) was done for aeration. Drains were dug with a comprehensive plan considering the pattern of runoff. In the section 8b (figure-6-1.a) clear drain lines can be seen, and it seems that some were still not completely dug. The wavelet analysis was done to analyze the pattern at this stage of the section, to see how far remote sensing with wavelets is capable to monitor the stages of replantation.

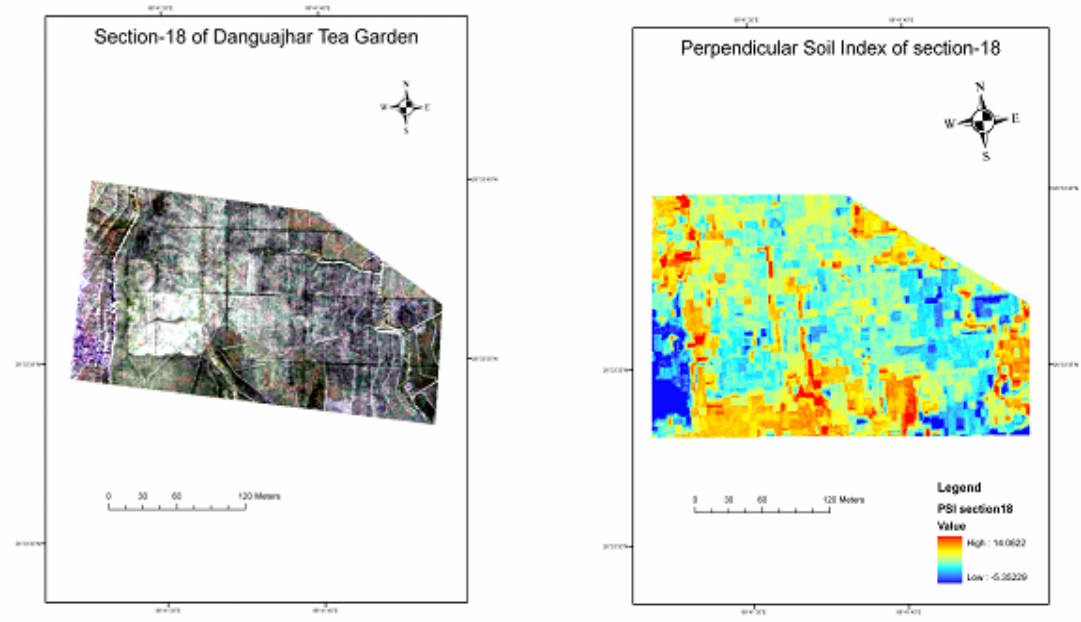

Figure 6-1: Section 18 of Danguajhar Tea Garden and b. its Perpendicular soil index.

The subset of the section was rotated to two hundred fifty five degree to align the management lines horizontally and to reduce the area of no data value. The section was a bare land with small patches of vegetation. The image was taken from google earth, having no NIR (near infrared wavelength) infor-

mation, so NDVI (Normalised Differential Vegetation Index) of the image gave meaningless results. Based on the concept of PVI (Perpendicular Vegetation Index, discussed in division 5.2 of the thesis), soil index was drawn among the set of spectral bands which shows highest variation between vegetation and soil (figure 6-2). To calculate PVI linear regression line was drawn between highest dry and wet vegetation points in the feature space. Then all other points were shifted to be drawn on this regression slope line, by calculating the euclidean distance between the points and the perpendicular intercept to the regression line. Distance based soil index was designed to enhance the soil brightness. PSI (perpendicular soil index) of the Section-8b of Danguajhar Tea Garden was shown in figure 6-1b.

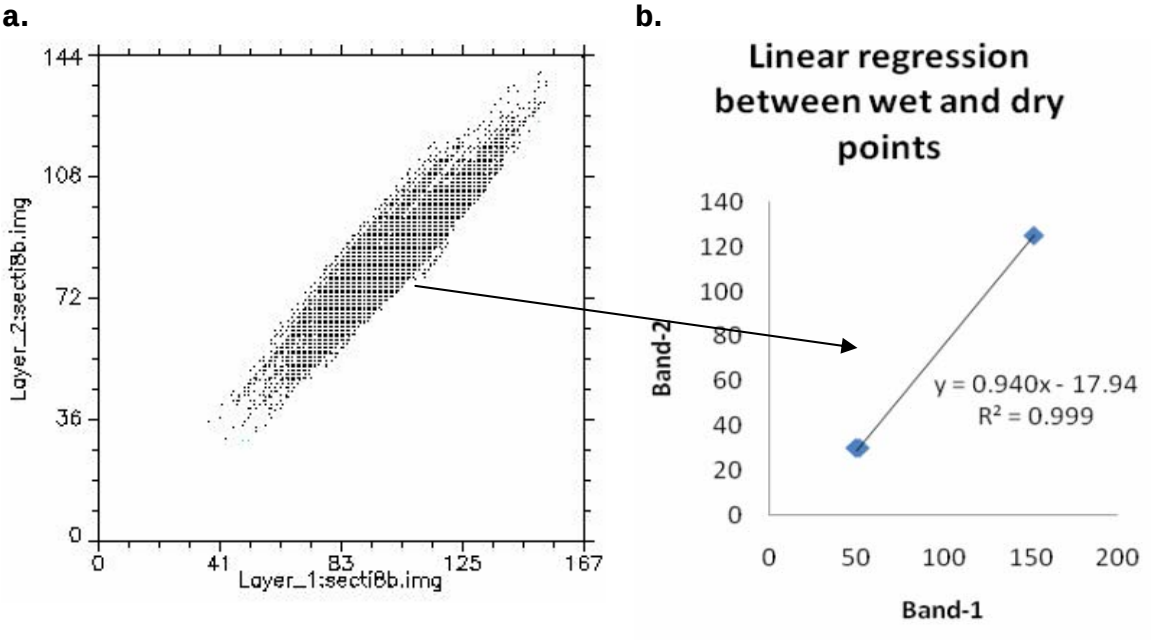

Figure 6-2: a. Scatter plot between bands of max variation among vegetation and soil, b. regression line drawn between most wet and dry vegetation points (In case of PVI it is soil line).

6.1.1. Wavelet analysis of the section

The PSI of the section was calculated at 1meter resolution, which was decimated upto level six to give a coarsest resolution of 64 meters on the ground. But after reconstruction this coarser information was brought to the same number of pixels, as was in the input image. Hence only information content of the image was reduced without making it pixel-ate.

6.1.1.1. Smooth wavelet transformed coefficients

The approximation crystal at different levels of decimation has the identity of the image at that scale, in the form of smooth wavelets coefficients. The coarser resolutions i.e. level5 and level6 were of less use for pattern extraction because upto that level, much of the information content was lost (as shown in figure 6-4 and in table 6-1). The correlation drawn between the crystals of all six levels and the input PSI image (table 6-1) for db4 wavelets deduced to 71% at level-5 and 63% at level-6. So, in this study, only first four levels of decimations were analysed from different wavelets.

Table 6.1 Correlation matrix between different levels of approximation with the input Perpendicular Soil Index of section 8b.

	a1 db4	a2 db4	a3 db4	a4 db4	A5 db4	A6 db4	PSI
a1 db4							
a2 db4	0.97						
a3 db4	0.92	0.94					
a4 db4	0.87	0.86	0.91				
a5 db4	0.76	0.8	0.85	0.9			
a6 db4	0.65	0.69	0.73	0.77	0.87		
PSI	0.98	0.96	0.9	0.83	0.71	0.62	1

Going down the decimation levels high frequency details were reduced accordingly and hence its correlation with the input image goes down. Table 6-1 shows that from level-4 to level-5 correlation was reduced from 87% to 76%, this shows heavy loss at level4. To get best level out of them a trade off was done based on the extent of information required. In this study a general pattern needs to be extracted by deducting the noise in the form of high frequency details. At upper levels, crystals of each level were highly correlated to their next, but level4 gives comparatively less correlation with its previous and next level. In section 8b, level-4 was found better correlated as well as visually similar (figure 6-1and figure 6-3) with the input PSI image. Correlation was drawn for all the three wavelets at level4 between the approximation at different levels with input PSI image (table 6-2).

Table 6.2: Correlation matrix for different wavelets at level3 with the input Perpendicular Soil Index of section 8b.

	PSI	A4haar	A4db4	A4sym8
PSI				
A4haar	0.75			
A4db4	0.87	0.9		
A4sym8	0.87	0.92	0.99	

Haar being the simplest wavelet, having only 2 coefficients gives blocky pattern, which can not be the real feature on the ground. The blocky results from Haar increases going down the level, so upper levels decimation was found better to extract pattern using Haar Wavelet. For the section 8b, Db4 and sym8 gives almost similar results at first four levels of decimation, shown in figure 6-3 and table 6-2. The difference among them (db4 and sym8) increases as going down the levels. Because in upper level crystals, frequency was higher and the section was almost smooth. So the shape of wavelet plays very less role, as wavelet basis are very compact at upper levels and basic shape of both of them are nearly same (as symmlets is derived from Daubechies). By going down the level, wavelet gets more and more flatten and hence at lower levels impact of shape of each wavelet was more pronounced. Section 8b was a stationary smooth field, both db4 and sym8 was found to be suitable but Haar because of its blocky pattern (which was not natural) got rejected. For further analysis sym8 level-4 was considered because it had comparatively larger range of wavelet coefficient values (figure 6-2h).

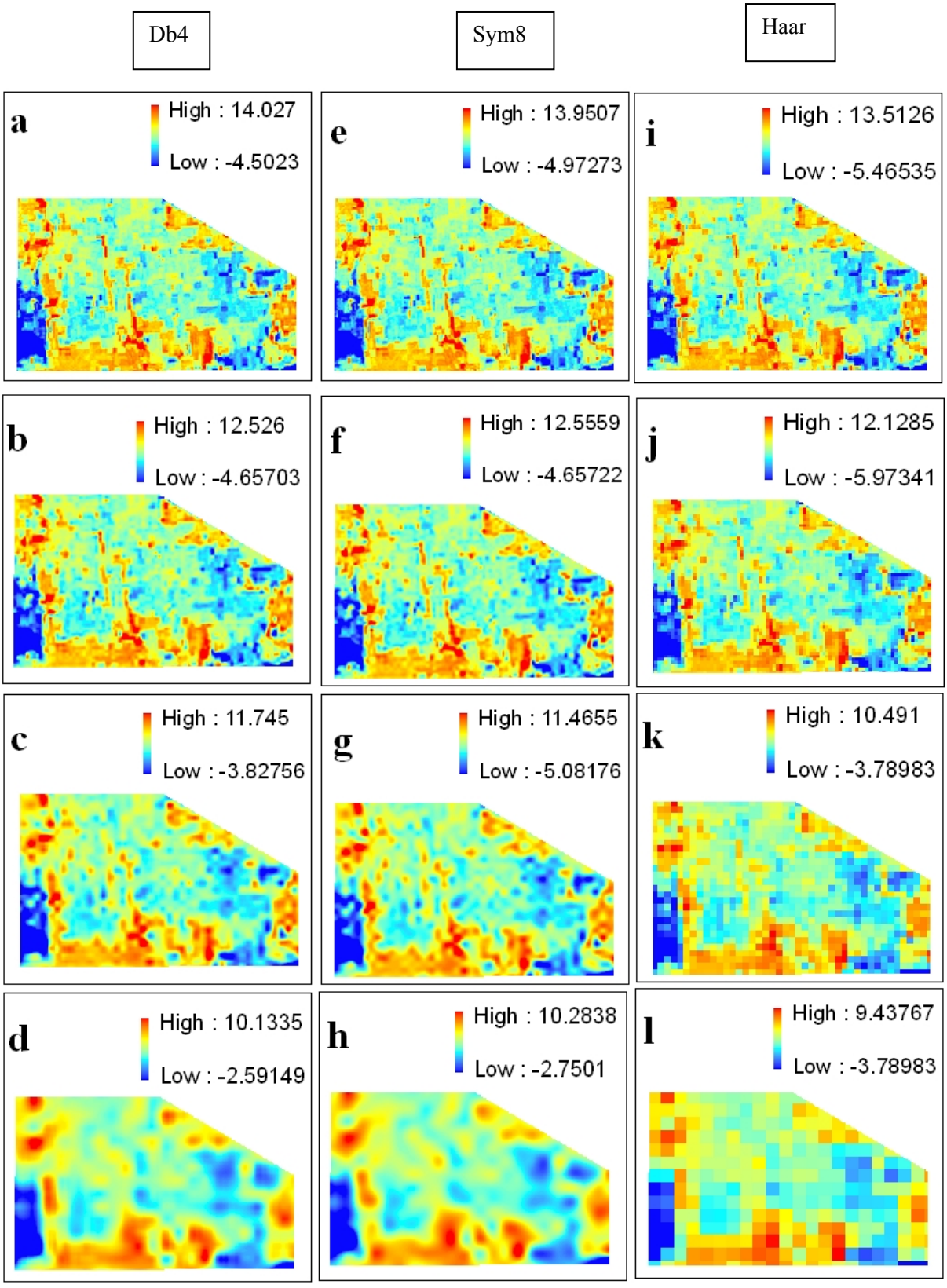

Figure 6-3: Approximation crystal from level-1 to level-4 by db4 wavelet in a, b, c and d; bySym8 wavelet in e, f, g, h and by Haar wavelet in i, j, k and l.

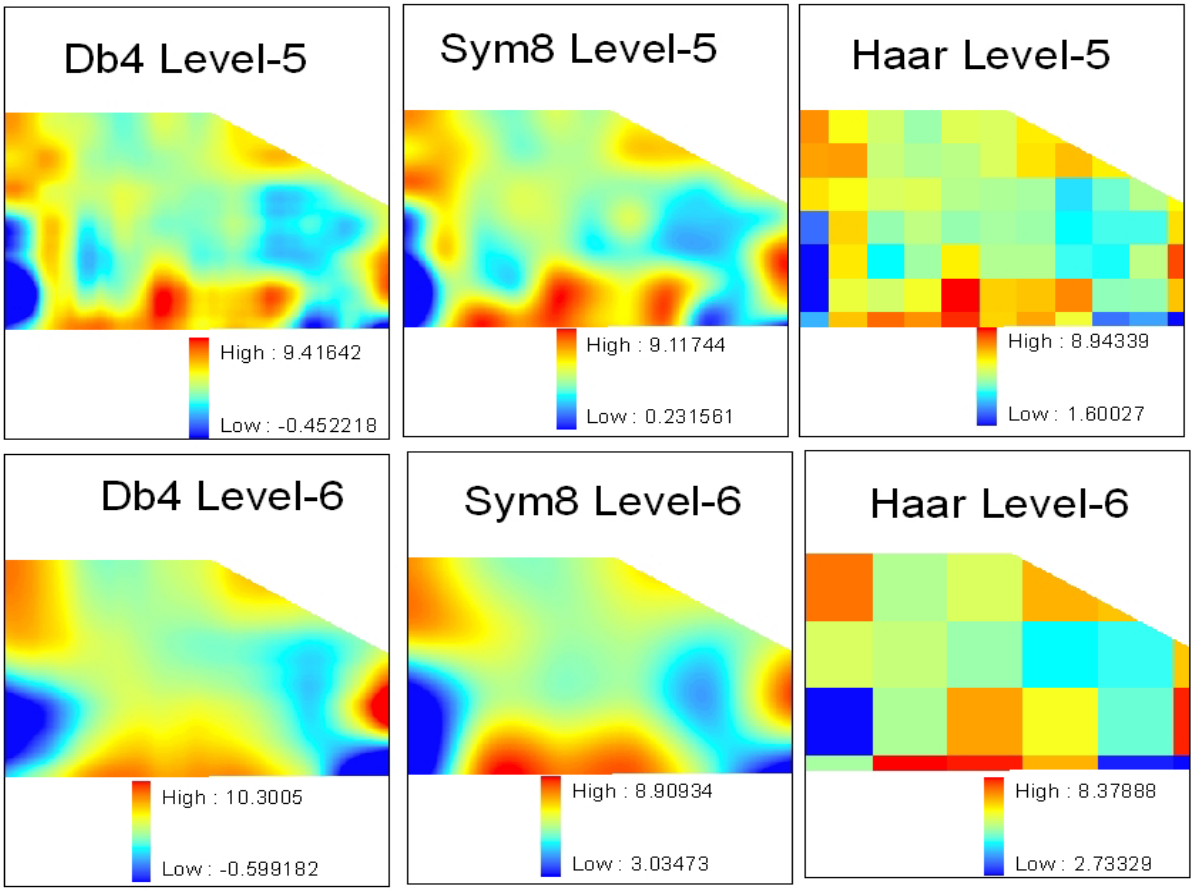

Figure 6-4: Approximation crystal for Level-5 and 6 by Db4, Sym8 and Haar wavelet.

The cause of the extracted patterns at level-4 was analysed by topographical and hydrological characteristics of the section. The section was not very undulating, having height range from 86.5 to 90 meter and maximum slope of 20%. The soil index of input PSI image was from -6.9 to 14 with mean 7.023, which was generalised at level-4 by sym8 with coefficients ranges from -2.7 to 10.28 having same mean and different standard deviation (1.5). Pattern extracted from level-4 sym8 was correlated with slope, compound topographical index (CTI) and flow accumulation to analyse the reason for out coming pattern.

The section was just uprooted after more than 100 years of long monoculture, so land was left open to kill the microbiological activities going on the field due shade and moisture. In the western part of the section ploughing lines can be seen where levelling was still left and drain lines were in the stage of development in the section. The Digital elevation model of the section gives the impression that some central and northern parts were at higher relief compared to the other part of the section, can seen in the contour lines. The slope map shows that except red region, steepness of the slopes was less than 10percentage, which determines the speed of water flow and thus the velocity of material flowing down the slope or infiltrating into soils, irrespective of the direction. Flow accumulation map determines the cumulative hydrological flow i.e. contribution of each pixel to water outlet and determines the natural drainage pattern of the section based on flow directions.

To describe the effects of topography on location and size of saturated moisture areas the compound topographic index (CTI) has been used (Moore et al. 1993). The wetness index is based on slope gradient for runoff generation. It is a refinement of upslope catchments area (area of land draining to a particular pixel) that better characterizes the spatial variability of soil properties due to surface hydrology (Moore et al. 1993). Compound topographical index shows the level of wetness i.e. saturation in

the soil. The image was acquired in the month of December 2006, which had only one rainy day of 0.4mm rainfall. Almost no moisture was there in the field due to natural cause, and November was also dry, so soil gives bright reflectance (red colour in the figure 6-4a.) due to aridness.

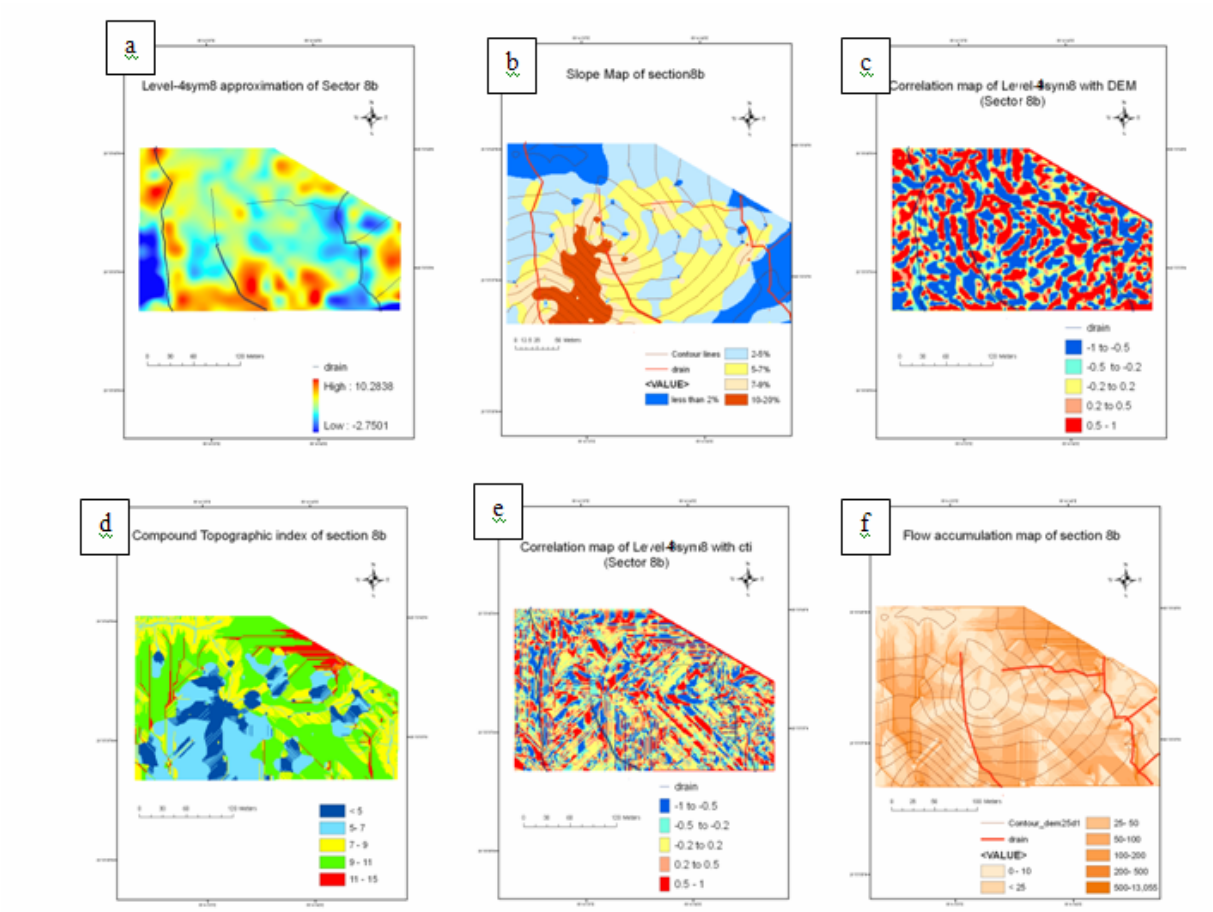

Figure 6-5: a. level4 approximation by sym8n wavelet with drainage lines, b. DEM, c. Correlation map with slope, d. CTI map, e. flow accumulation map and f. Correlation map with CTI for section 8b.

Blue colour in approximation map shows some vegetation; in the west of PSI approximation image had lowest wavelet coefficient value, indicates that these parts had most healthy situation for vegetation growth. The pattern in section-8b mainly followed the drainage line (especially in the east). The section was found 11% correlated with DEM, 6% correlated with wetness index, 5% correlated with slope and 2.5% correlated with flow accumulation. The results shows pattern of the field was very weakly correlated with the topographic parameters.

The traditional regression or multivariate approach had a drawback that they ignore data location and spatial structure of data distribution (Kravchenko, 2003). To visualise which part of the section gives better correlation with these parameters correlation map was generated. For which mean and std dev of each 3x3 pixel sliding window was calculated on both the images 'a' and 'b' and then the centre pixel value was replaced by cov(a,b)/(std a*std b). The generated correlation map between the extracted pattern with the DEM and Compound topographic index was shown in figure 6-4 c and e respectively. Map shows that DEM was more correlated than CTI, but no specific area was found to be better explained by correlation map.

Correlation can be considered as an evidence for a possible casual relationship, but it did not indicate the relationship prevailing there. Hence cross correlogram was drawn, which helps to evaluate strength and direction of relationships between the variables, with their spatial aspect. Cross correlograms were

also found informative in delineating the size of potential management zones for site specific harvesting (Kravchenko and Bullock, 2002b).

a.

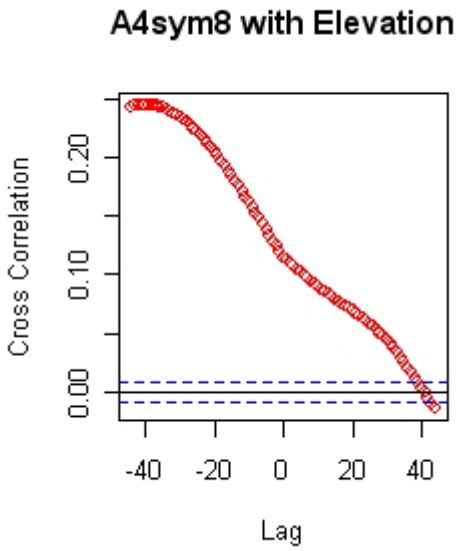

b.

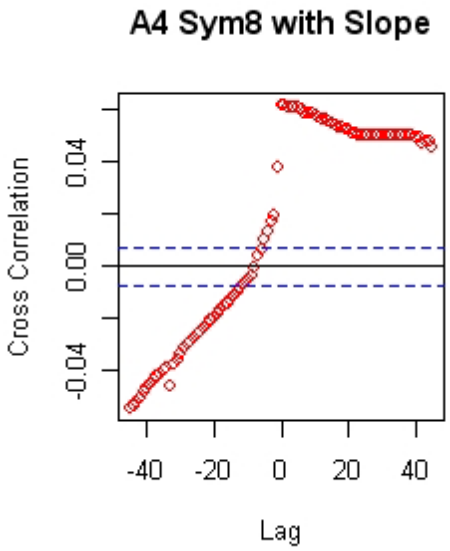

c.

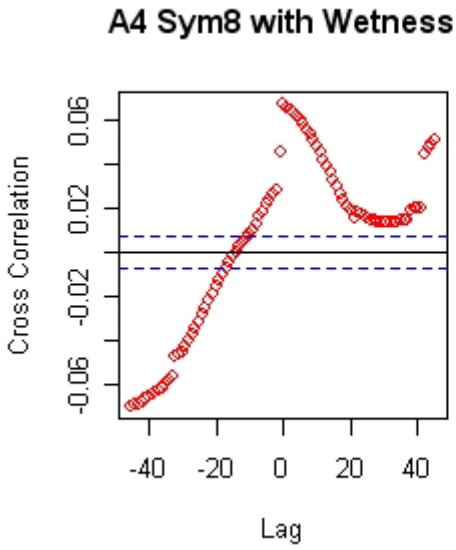

d.

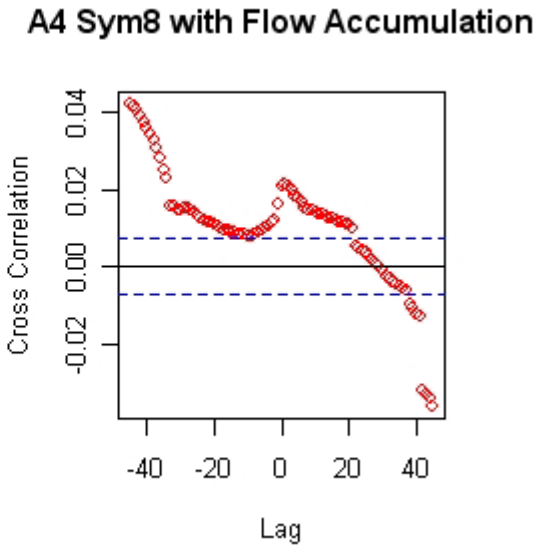

Figure 6-6: Cross correlation plot of Selected level-4 approximation by sym8 wavelet with a. Elevation, b. Slope, c. Wetness Index and d. flow accumulation.

The plot 6-6(a) shows that positive correlation exists between elevation and soil brightness, which gradually goes down to zero at 40m distance (because 1 pixel = 1m, therefore 1lag = 1m) and seems to be distributed normally. Though correlation between the two variables was weak (nearly 11%), but their spatial correlation range was strong, which indicate that it will be easier to manage this relationship on a site specific basis. Typically cross correlograms has its maximum value at zero lag distance and gradually decreases until it became statistically insignificant. Correlation of slope with the soil brightness doesn't decrease much with lag distance, therefore had very long range, hence it was a more stable relation than elevation. Sedimentation and wetness shows their obvious relationship and had

comparatively small range (nearly 20m) of correlation, because section was almost plane, having no rising and falling to have longer impact range.

Vegetation followed the drainage line (especially in the east), which indicates that management activities were the major driving force in a small section of 4.5m height variation. Some central and southern part of the section have more soil reflectance as the moisture condition was low due to high elevation and low flow accumulation.

6.1.1.2. Fine frequency wavelet coefficients

Fine variation in the field can give features of minor importance for precision farming. These fine frequency coefficients, captures the detail information at different resolution level in each direction. Figure 6-7 shows the details extracted at different scales in horizontal direction by db4 wavelet. It was found that first level gives very noisy information and the fifth and sixth level give very general information about the change in horizontal direction. So analysis was done on the levels in between to extract dominant pattern in each direction.

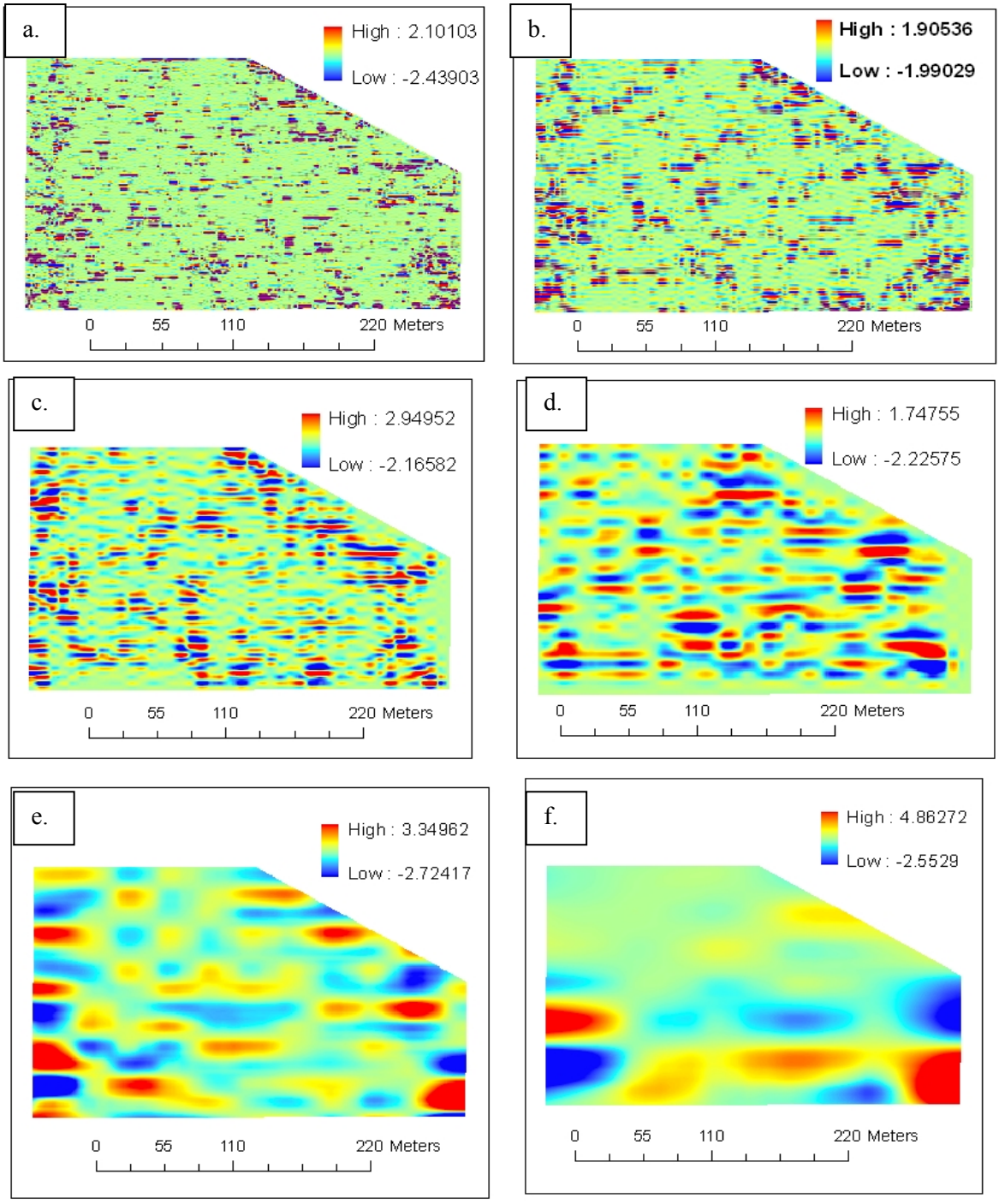

Figure 6-7: a. to f. Horizontal details at six levels of decimation by db4 wavelet respectively.

To select most informative level in all three directions i.e. horizontal vertical and diagonal by Haar, db4 and sym8 wavelets, autocorrelation graph was used and energy of the crystals was also analysed. Energy gives the contribution of each crystal to the reconstructed image, which is the sum of the squares of the coefficients of that crystal, divided by the sum of the squares of the pixel values of the whole image. Approximation crystal contains more than 96% of energy and rest of the energy was distributed in three directions, so energy content of each level was very less in detail crystals. The distribution of energy among all decimated levels in different wavelets was shown in figure 6-8.

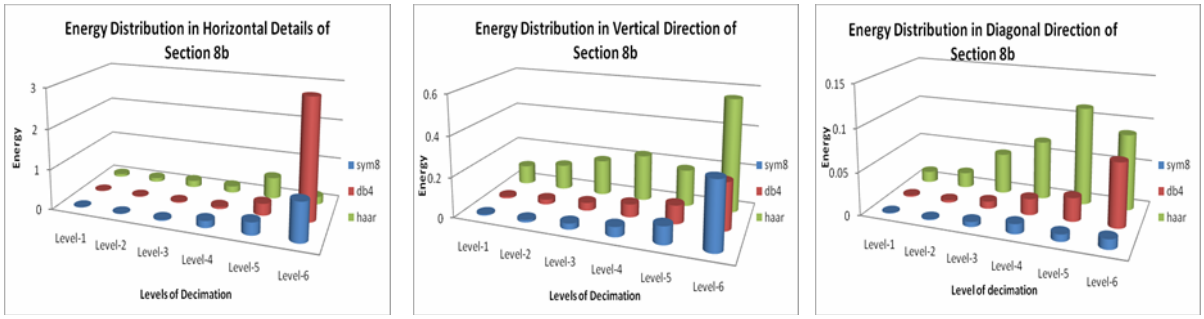

Figure 6-8: Energy distribution in different levels by sym8, db4 and Haar wavelet in three directional details.

It was found that lower level crystals generally had highest energy content and they follow increasing trend, because coarser resolution will gradually have comparatively smooth frequency information which contains higher energy than the previous levels of decimation. The fifth and sixth level details give general approximation rather than the detail information as shown in the figure 6-4. On the other hand first level captures very fine details which are generally considered as noise (figure 6-3). But energy does not give any information about the spatial structure and in this study spatial pattern needs to be extracted, hence energy was not considered on deciding the best representation. So, the crystals at the second, third and fourth decimation were analysed by their autocorrelation graph and surface, irrespective of energy of that crystal.

Wavelets gives variation at several spatial scales and autocorrelation gives the constant values, extent and magnitude of variation. To analyse the difference among different wavelets, autocorrelation graph was drawn as shown in figure 6-9.

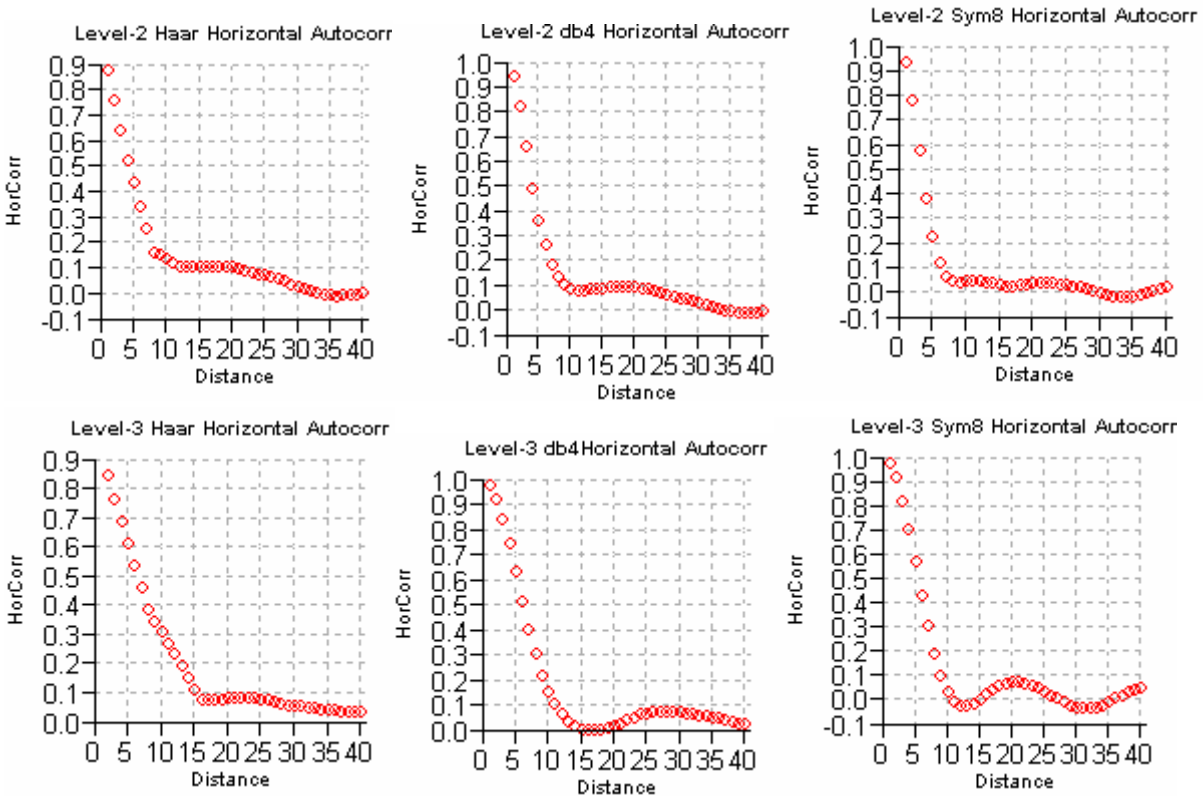

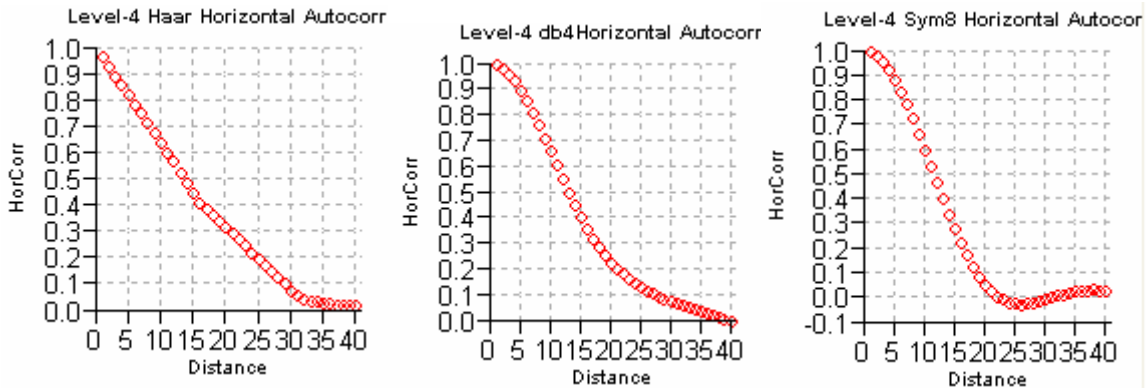

Figure 6-9: Autocorrelation for Level2 at top, for Level3 at middle and for Level4 at bottom by using Haar, Daubechies and Symmlets wavelets.

The Level-2, 3 and 4 autocorrelation graph shows that spatial correlation exist upto 8, 15 and 35 pixels when the wavelet transform coefficients corresponds to 4m, 8m and 16m on ground respectively. Level-2 gives comparatively fine variation with respect to distance and has less extent of spatial correlation. Hence the anisotropic autocorrelation surface, only for level-3 and level-4 by all three wavelets were drawn (figure 6-10, 6-11 and 6-12 respectively in horizontal, vertical and diagonal direction).

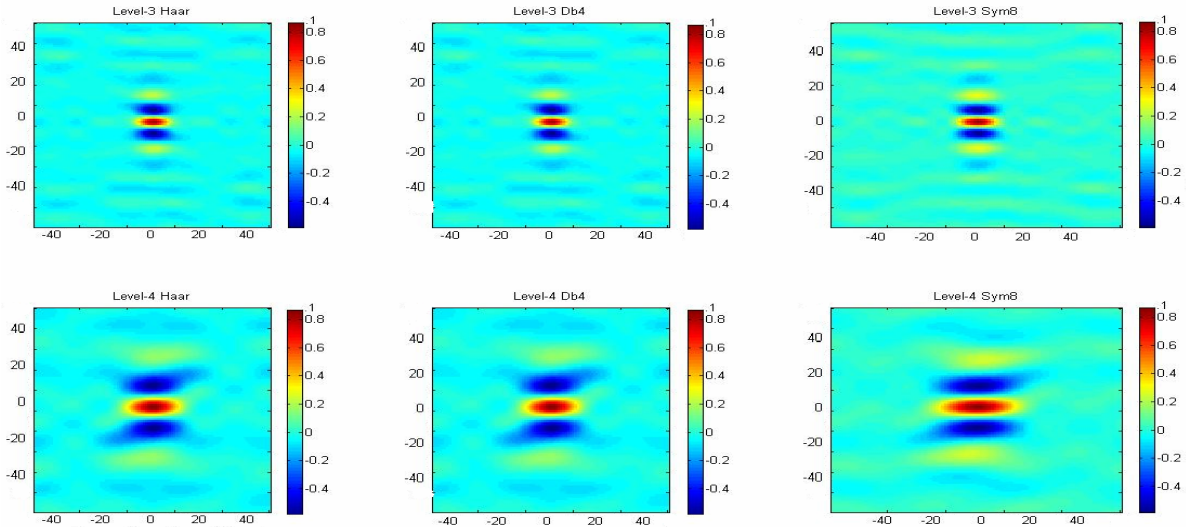

Figure 6-10: Horizontal anisotropy by Haar, db4 and Sym8 in level3 and 4 of decimation.

The figure 6-10 shows that though very strong horizontal structure was not present in the section but some repetivity was found in level-3 (figure 6-7 c.), which corresponds to the information at 8meters on the ground at 1m pixel size. Autocorrelation surface for db4 and Sym8 wavelets shows better spatial correlation, than Haar. The correlation of sym8 and Haar with the input PVI image was better than db4 (table-6-3) and horizontal line of sym8, though had very low autocorrelation value but had a bit better repetivity than db4 and Haar (figure 6-10). So, level-3 by sym8 wavelet found as a better representative of horizontal features in the section 8b.

Table 6.3: Correlation between different wavelets at level3 and level4.

	PVI	h3db4	h3haar	h3sym	h4db4	h4haar	h4sym
PVI							
h3db4	0.01						
h3haar	0.19	0.01					
h3sym	0.18	0.03	0.24				
h4db4	0.02	0	0.01	0.02			
h4haar	0.22	0	0	0.17	-0.05		
h4sym	0.22	0.04	0.29	-0.03	0.08	0.39	

The extracted information shows that some features repeats at 10m distance on field and can be seen in the grid of anisotropic surface (figure 6-10). Section8b was a stationary open field having few track lines and drain. The features extracted by sym8 at level-3 mainly depict these track lines. Similarly Vertical details were extracted and analysed to get the most informative level.

In vertical direction sym8 level-3 gives better results (figure 6-11) with the repetivity of feature at 30 meters distance. These are the tracks drawn by the farmer for proper management of field. The south west vertical line shows high frequency change as some grass or vegetation was grown in that part.

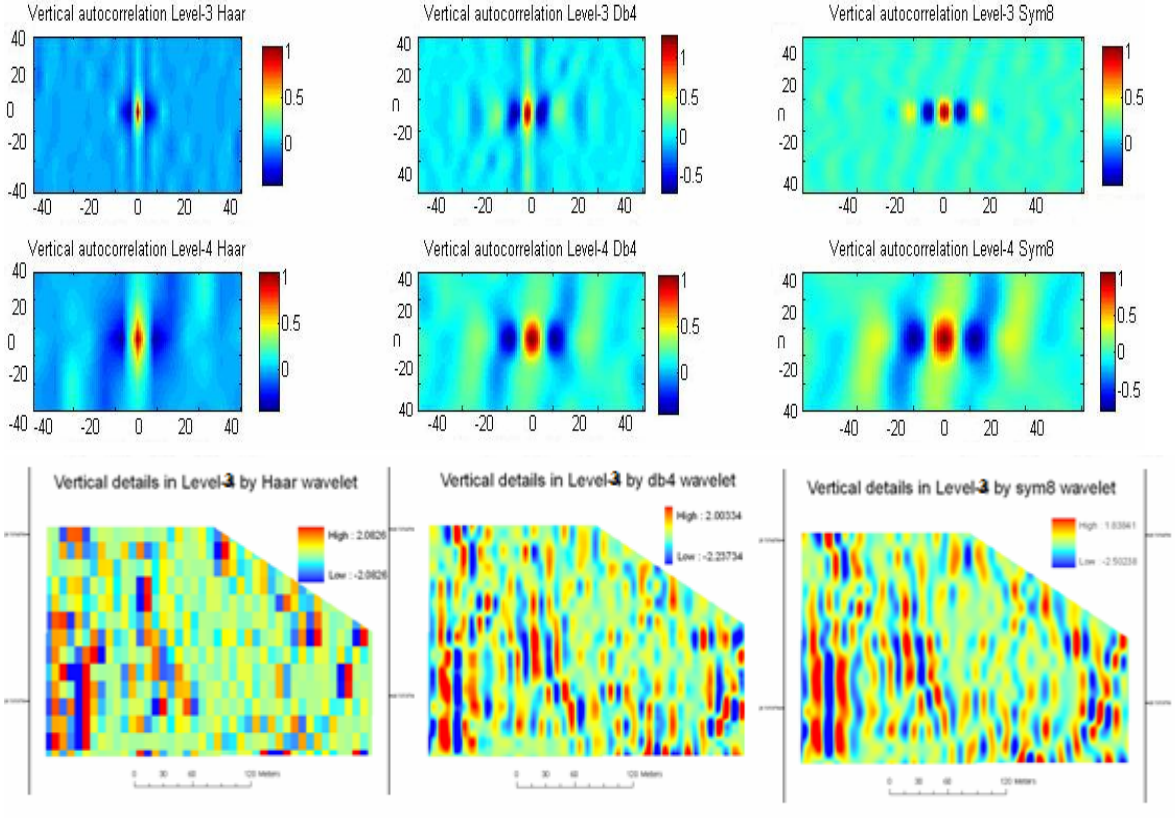

Figure 6-11: Vertical details at level-3 by Haar, db4 and sym8 wavelets with their respective anisotropic maps.

Similarly diagonal details were also extracted and found that sym8 level-3 best represents the diagonal features on the field which repeats at 15meter distance (figure 6-12). These patterns were not visible in the input image, which shows that some diagonally varying features exist in the section.

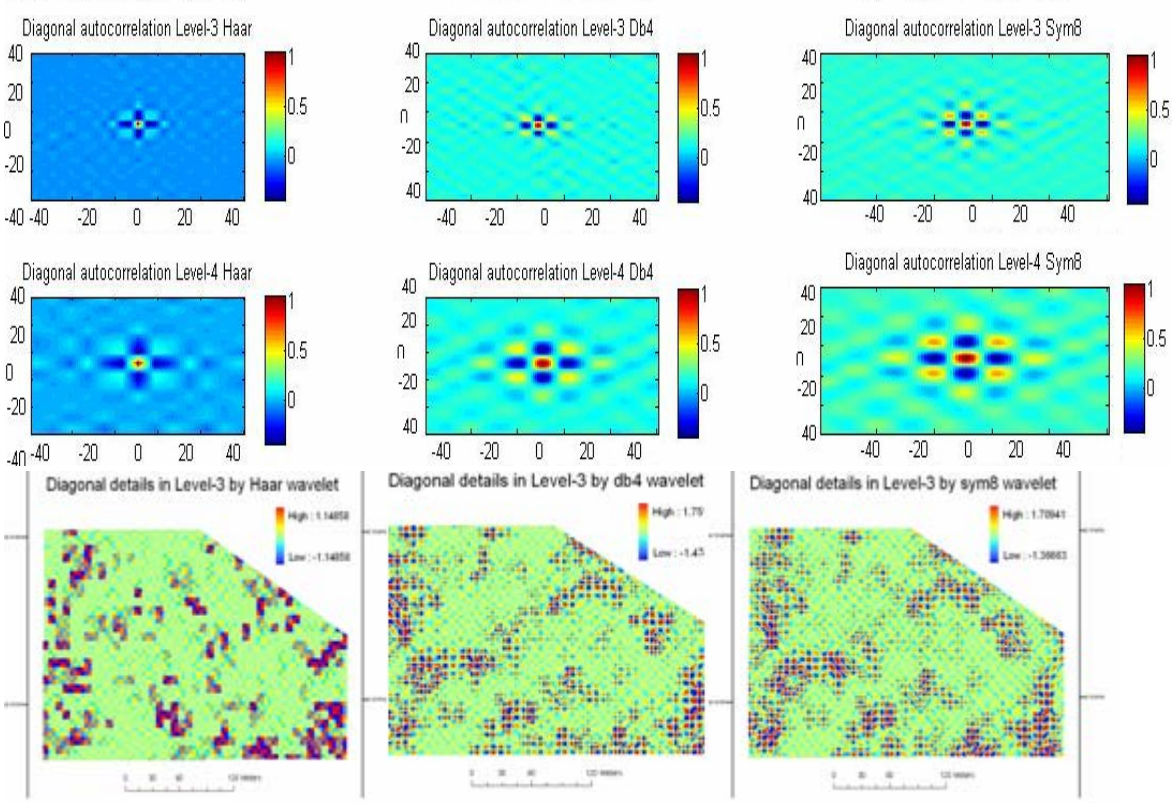

Figure 6-12: Diagonal details at Level-3 by Haar, db4 and sym8 wavelets with their respective anisotropic maps.

To analyse the natural or man made cause for these extracted pattern in different directions, fine spatially varying secondary information was required , for the case, good sampled soil data can reflect the cause of these features coming at level-3 in horizontal and vertical and diagonal direction by sym8 wavelet. Sym8 gives better representation of the details in the section because of its smoothness and nearly symmetric nature, as the section was not dominated by fine frequency change and can be considered as stationary.

6.1.2. Impact of climatic parameters on the yield

In 2006 when section was uprooted it was giving production of less than 1400 unit, far below its standard expectation. Yield of a field is a highly complex and multi dependent variable. Soil characteristics (a micro-level parameter), climatic condition (which is almost constant within a garden), terrain (which changes comparatively in a smooth manner) and the condition of the crop are major driving force. So any parameters alone cannot explain the variability in the tea yield. The variation in soil water content (SWC) with time is mainly affected by the fluctuation in rainfall and temperature, which decides plant water requirement. The impact of rainfall on the yield was shown for the section for last nine years (figure 6-13).

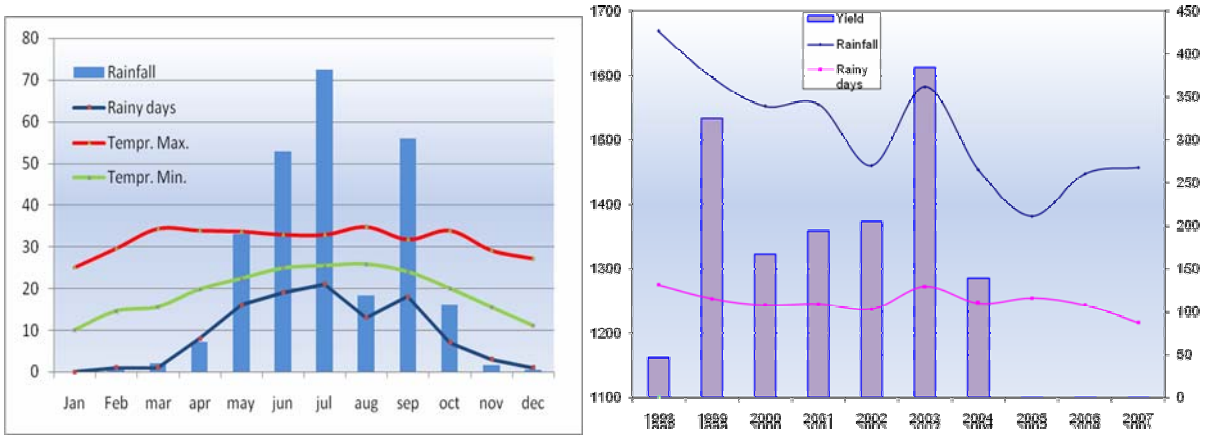

Figure 6-13: a. Climatic condition of 2006 and b. Impact of rainfall on yield in last nine years.

Precipitation and temperature were the most useful weather variable for tea production. The region had almost constant mean annual temperature range of 32 °c max to 18°c minimum for these years, so it had suitable temperature range for tea growth. This could be due to prolong rainy season from the month of March to November (figure 6-14). In dry months of December to February, temperature range increases a bit and they jointly acts as a yield limiting factor.

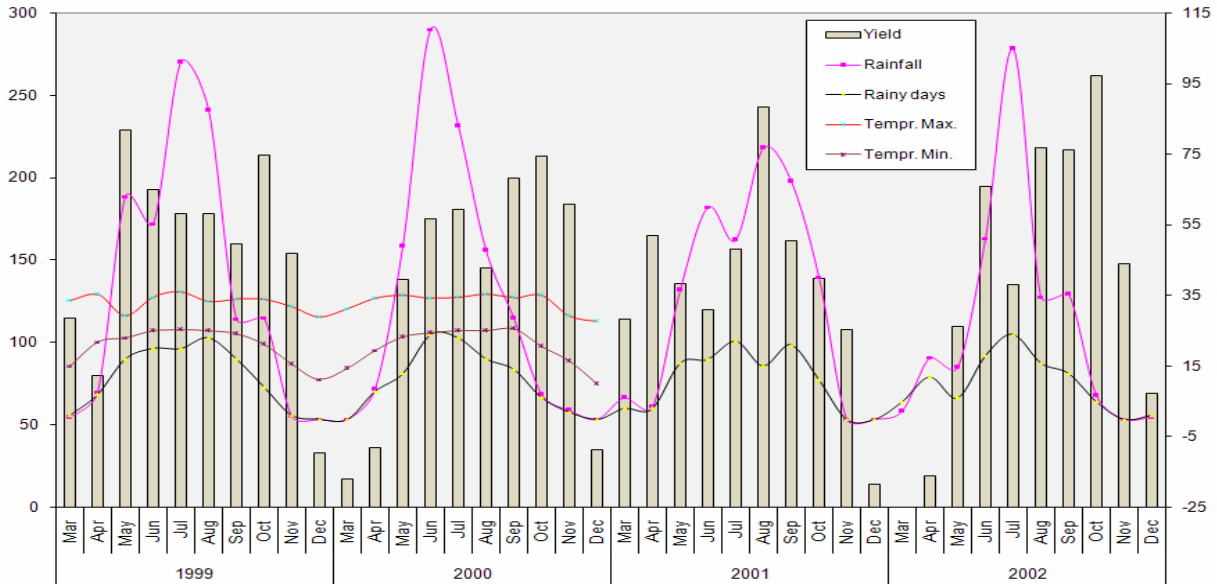

Figure 6-14: Monthly Variation in yield of section 8b with respect to climatic condition.

The yield shows direct relationship with the rainfall, it shoots up and down monthly based on amount of precipitation. Before uprooting, the section had highest yield of 1650 unit in 2003 between last nine years (figure 6-13), because of higher rainfall and most suitable climatic condition. For tea yield good soil moisture condition is required but not heavy rainfall, so for the month having not very high rain, production was better. The region got 5-8 rainy days with more than 100mm rainfall, that too mainly in the month of July and September. These heavy rains became hazardous, not only causing flood but also causes severe soil erosion (which has prime importance for the field having crop for more than 100years).

6.1.3. The Soil Variability

Other then climatic condition and terrain parameters, tea yield also depends on chemical composition of soil. To analyse the need of the soil and condition of the section, regress soil sampling was done during this stage of tea replantation, when field was open and having least vegetative activities. Fifty samples were collected for the section, by TRA to observe within-field variability of the soil properties. But as the samples were lacking coordinates so there spatial analysis was not possible. The descriptive statistics of the samples shows that skewness and Kurtosis of all of the parameters was normal (table 6-4).

Table 6.4: Descriptive statistics for the section 8b from 50 soil samples.

Statistics	pH (Top)	pH(Sub)	O C %	Potash %	sulphur%
Mean	4.3104	4.2702	1.95216	0.01524	0.0906
Std. Devi.	0.01524761	0.01597	0.02968	0.0002921	0.00119522
Variance	0.00023249	0.00025	0.00088	8.5306E-08	1.4285E-06
Skewness	0.07392019	-0.1279	-1.2375	0.1290073	0.01494036
Kurtosis	-0.6708707	-1.5097	-0.4608	-0.6602268	-0.7576595
Range	0.06	0.04	0.071	0.0009	0.005
Percentiles					
25	4.29	4.25	1.94725	0.015	0.09
50	4.31	4.27	1.969	0.01525	0.091
75	4.32	4.29	1.971	0.0153	0.092

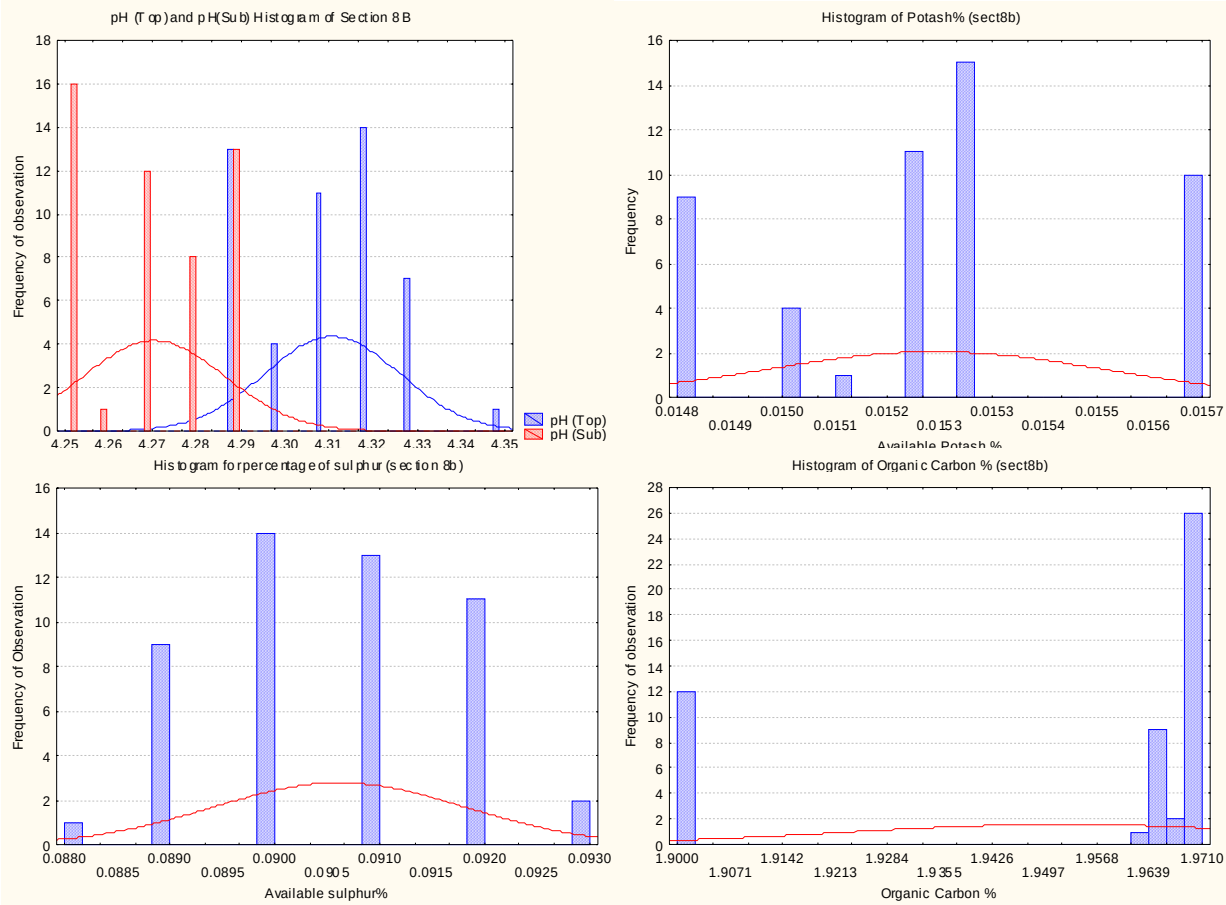

Figure 6-15: Histogram of Soil Variables a. pH, b. potash, c. sulphur and d. organic carbon in section 8b.

The general variability of the soil properties in fifty samples, given in figure 6-15 and standard deviation in table 6-4 shows very low variability in the soil properties within the field. Among the different soil parameters analyzed, ideally tea yield is highly dependent on the soil pH and availability of Potash and organic carbon. So to analyse the extent, to which the collected samples were unlike, QQ plot was drawn, which can give the reason for the variation in spectral signature captured by image.

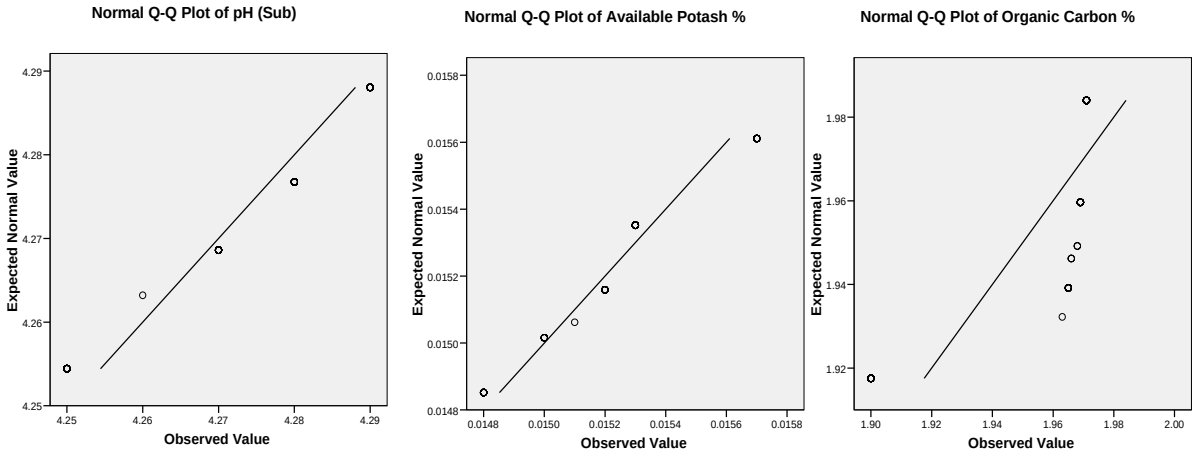

Figure 6-16: Quantile-Quantile plot for pH, Potash% and Organic carbon% of the 50 samples.

Percentage of potash was almost constant as shown in table-6-4 and almost normally distributed, because its source was from the insitu rocks. Organic carbon has highest variability in it, because it directly depends on health of tea bush and is very much local in characteristics.

6.2. Young Guatemala (Section 18 of Hope Tea Garden)

In the next stage of replantation, sections were rehabilated by large deep rooting grasses. Section 18 was uprooted in 2005 after 117 years of tea crop and was under young Guatemala plantation in Dec2005 when image was acquired. Multiplication baris were required at the rate of 0.1- 0.2 ha for each hectare uprooted per year (Replantatation processes, TRA). Ideally 60cm X 100cm planting space was managed and Guatemala was planted into tilled, moist soil which was infilled and weeded by hand or cheel hoe. Guatemala was left on field for 18-24 months and repeated fertilizer and lopping was done. First lopping was practiced at 60 cm ground measure of crop and will have basal dose of 60 kg N as 2:1:2. After each round lopping at 15 cm, 30 kg N as 2:1:2 was practiced. Potash was applied in form of 2:1:3 NPK mixtures, where soil potash was less than 100 ppm (part per million). Due to heavy rainy season no lopping was done after mid September. The section was uprooted in mid 2005 and replanted in 2007. It is naturally well drained field, no drain lines were observed in the section.
In the present study, from here onward, if not specified otherwise the red regions of the PVI image will be max vegetation part of the section reflecting healthy soil and blue region as minimum vegetation part reflecting stress soil condition, and rest as parts are in-between condition.

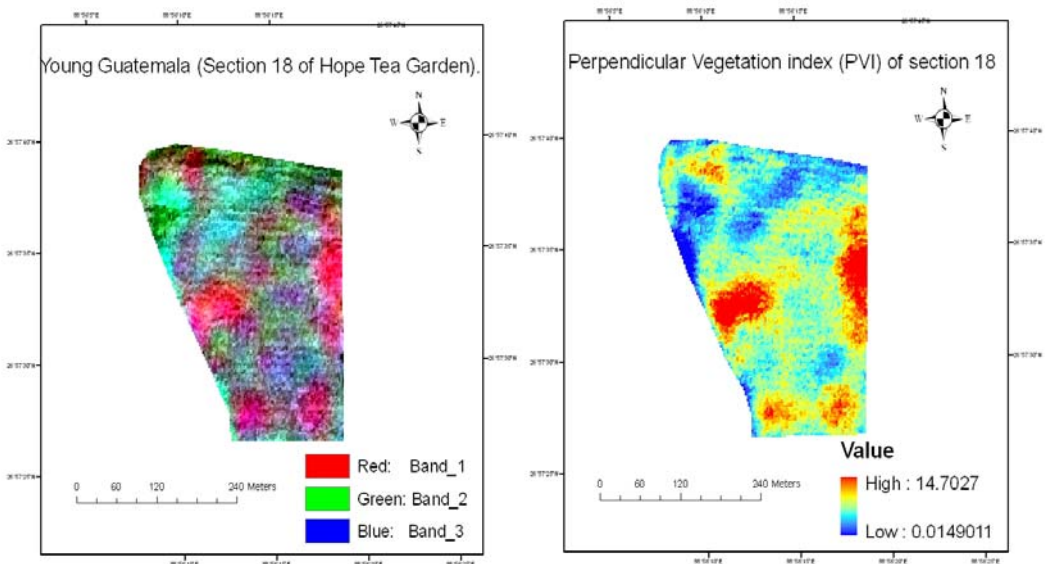

Figure 6-17: Section 18 at Young Guatemala stage and its calculated PVI image.

The perpendicular vegetation index (PVI) was calculated for section-18 (figure 6-17). The PVI of section-18 had mean 7.34 and 1.8 standard deviation, which shows sufficient variability and therefore features exist in the section. The PVI image was decimated upto level-6 and the approximation crystal of level-2, 3, and 4 were only analysed, due to reason explained in the section 6.2.1.2. These levels decimated by the Haar, Daubechies and Symmlets were correlated with the original PVI image. It was found that from level-3 onwards the loss of information was comparatively more having less than 90% correlation with the PVI.

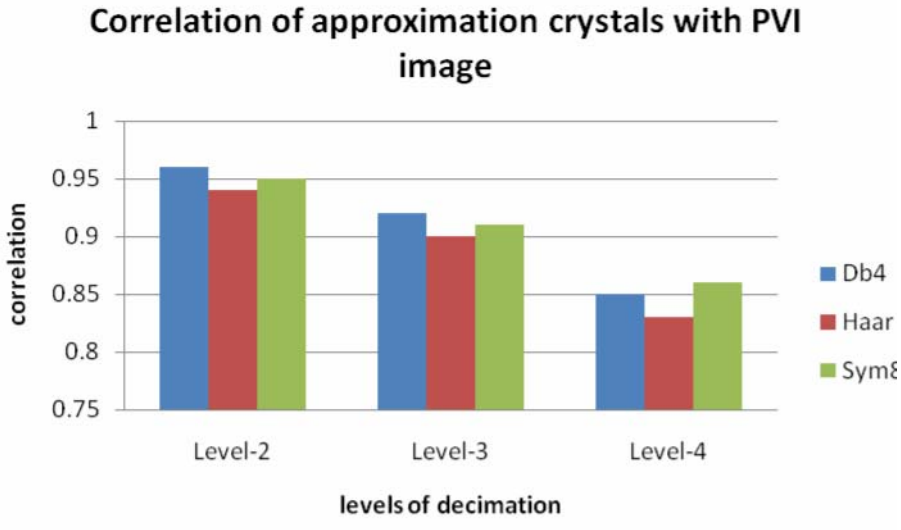

Figure 6-18: Correlation of Haar, Db4 and Sym8 wavelets with the input PVI at level 2, 3 and 4.

Figure 6-1 shows the very strong changes were not observed at different levels in correlation for all the wavelets. This shows image was dominated by smooth features. At level-4 the information content get reduced to 40m ground resolution scale. So only level2 and level-3 approximations were compared, (figure 6-19) decimated by Haar, db4 and sym8 wavelet.

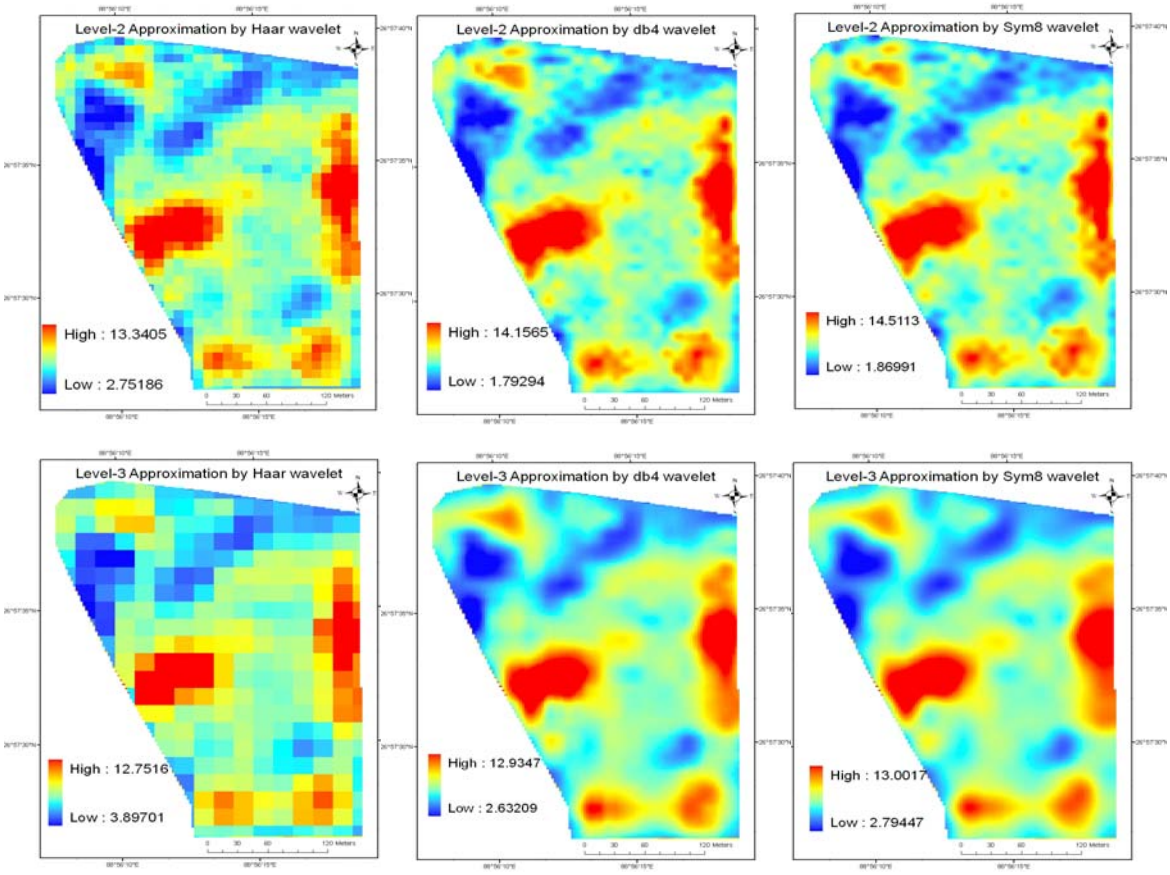

Figure 6-19: Level2 and 3 approximation by Haar, db4 and sym8 wavelets for section 8b.

Figure 6-19 shows almost similar approximation by db4 and sym8 but sym8 has larger range and better correlation with the input PVI image (figure 6-18), therefore it will considered in further analysis. Hence Level-3 sym8 crystal gives better representation of section-18 vegetation, with 7.3 mean and 1.6 standard-deviation in wavelet coefficient value. This shows that features in the section was not very fine and can be generalized at 20m ground information level. The input image was at 2.5 m resolution after fusion of Liss III with cartosat, so at level-3 it gives 20m resolution information. The generalised information extracted at level-3 by sym8 was correlated with slope and CTI.

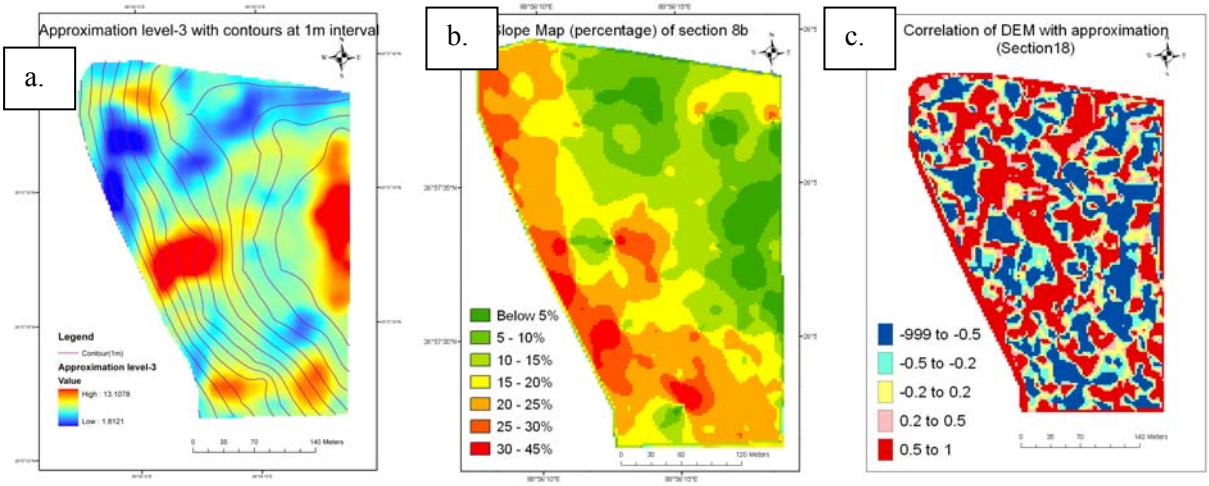

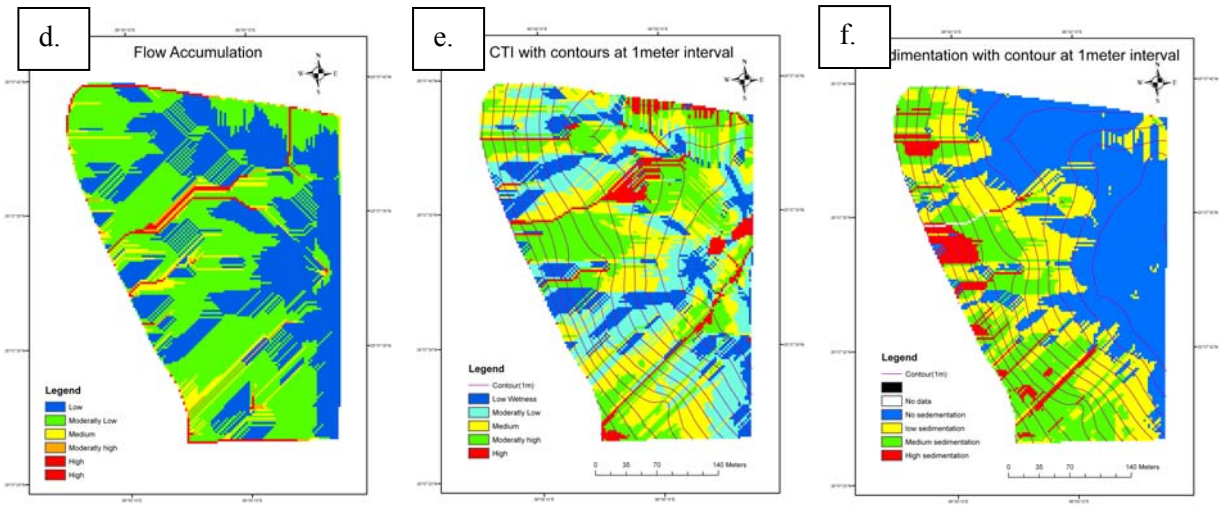

Figure 6-20 a. level3 approximation by db4 wavelet with contour lines, b. Slope map, c. Correlation map with slope, d. CTI map, e. flow accumulation map and f. Correlation map with CTI for section 8b.

The eastern part of the section was at the highest elevation and almost flat as seen by the contour lines and slope map. Vegetation had better correlation with slope for this region, can be seen in cross correlation figure 6-21 c. While correlation map (figure 6-20 c.) doesn't show this relation, explicitly. Northern and eastern part of the section has least flow accumulation and this inverse correspondence can be seen between the flow accumulation and vegetation in the figure 6-20. The sedimentation index was also calculated for the section because it had significant slope percentage. Clear correspondence with the slope gradient, higher sedimentation was found in the western part of the section hence can cause greater variability in vegetation, while eastern part was more or less stationary.

The section had comparatively better topography than section 8b, having elevation range from 412m to 424m height above mean sea level and 45% slope. So the topographical relations were also better, as seen in figure 6-21. Flow accumulation was nearly 12% correlated and had a range longer than 40 pixel, which means 100m on ground. Similarly slope, wetness, sedimentation and elevation had shown very good range (80-100m on ground) though are at weak correlation (less than 10%) but followed a symmetric trend. So the relationship can be better modelled and considered as stable.

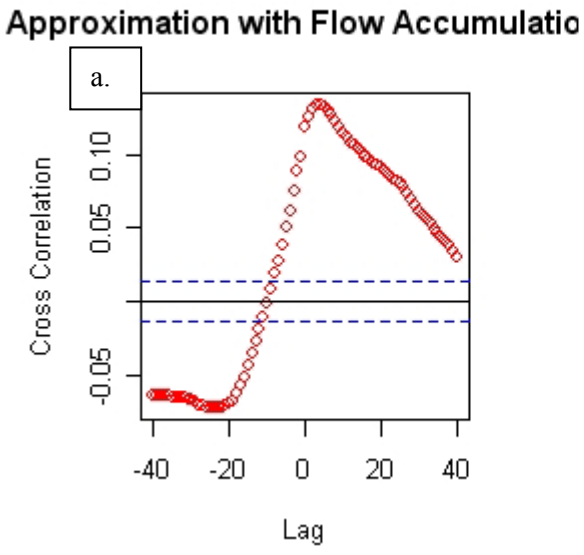

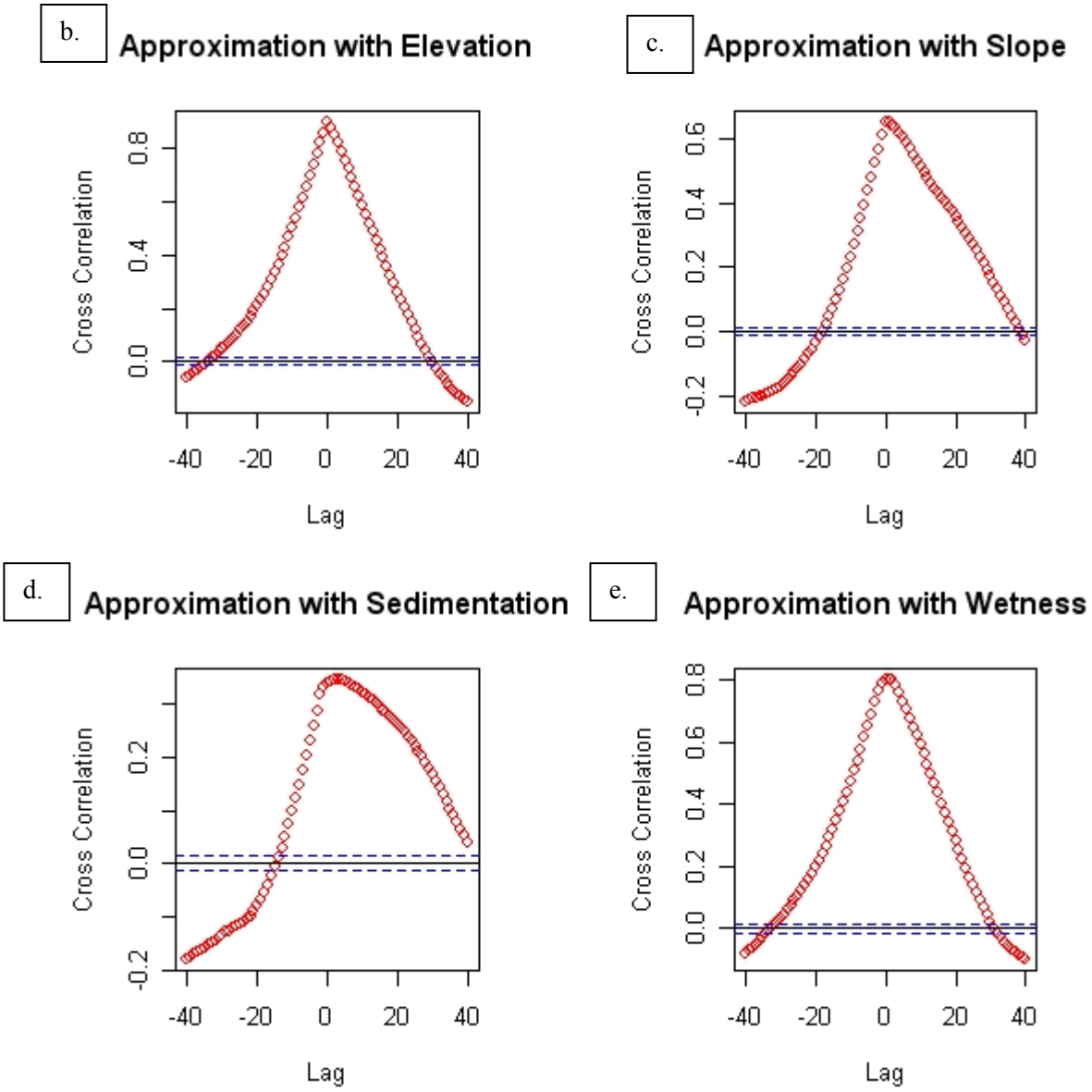

Figure 6-21: level3 approximation by sym8 wavelet was cross correlated with a. flow accumulation, b. Elevation, c. Slope map, d. sedimentation map, and e. CTI (wetness index) for section 8b.

6.2.1.1. Fine frequency wavelet coefficients

Again fine details of the section were extracted at different levels and then compared to get the most prominent directional information from them. The section was covered by young Guatemala, so ploughing direction was the major feature existing in the field. Clear horizontal lines can be seen in the image and strong horizontal autocorrelation was found. From the level-1 strong horizontal autocorrelation emerged. Level-2 db4 gives the best information about the horizontal repetivity of the features at 4 pixel distance on image i.e. 10 meter distance at ground. By going down to level-3, no spatial correlation was found (figure 6-22).

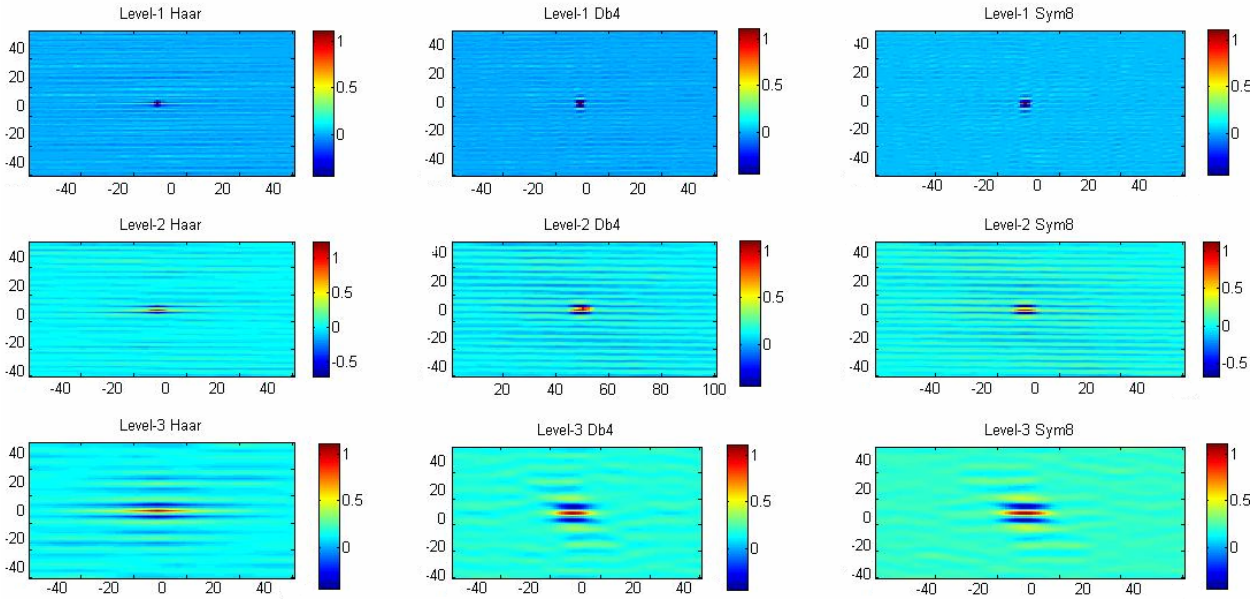

Figure 6-22: Horizontal autocorrelation of section 18 by Hara, db4 and sym8 wavelets.

Similarly vertical and diagonal information was also extracted. Though in these directions features were not that much strong, but some repetivity was found in vertical direction at 20 pixel distance i.e. 45m at ground, that may be the management lines. In diagonal direction spatial correlation was found at 25meter ground distance (figure 6-23).

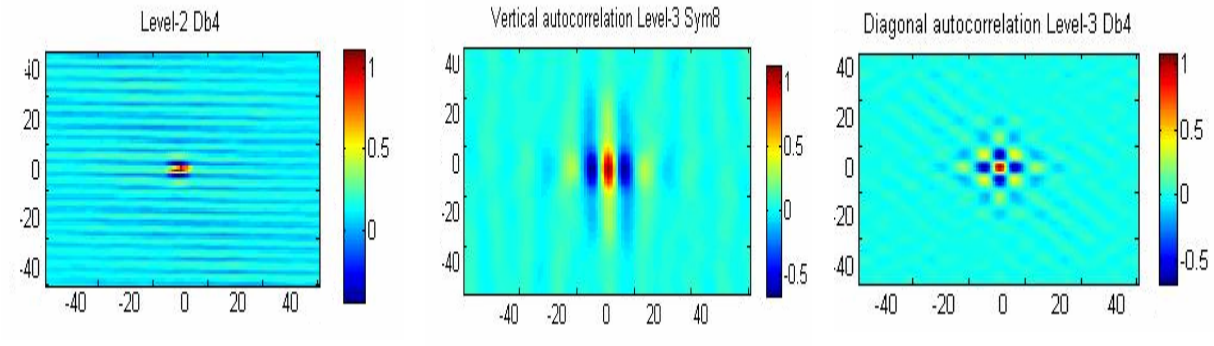

Figure 6-23: Best anisotropic autocorrelation found in the section 18, in horizontal, vertical and diagonal direction respectively.

The features extracted by db4 at level-2 for horizontal direction, at level-3 for diagonal direction and by sym8 at level-3 for vertical direction were shown in figure 6-24.

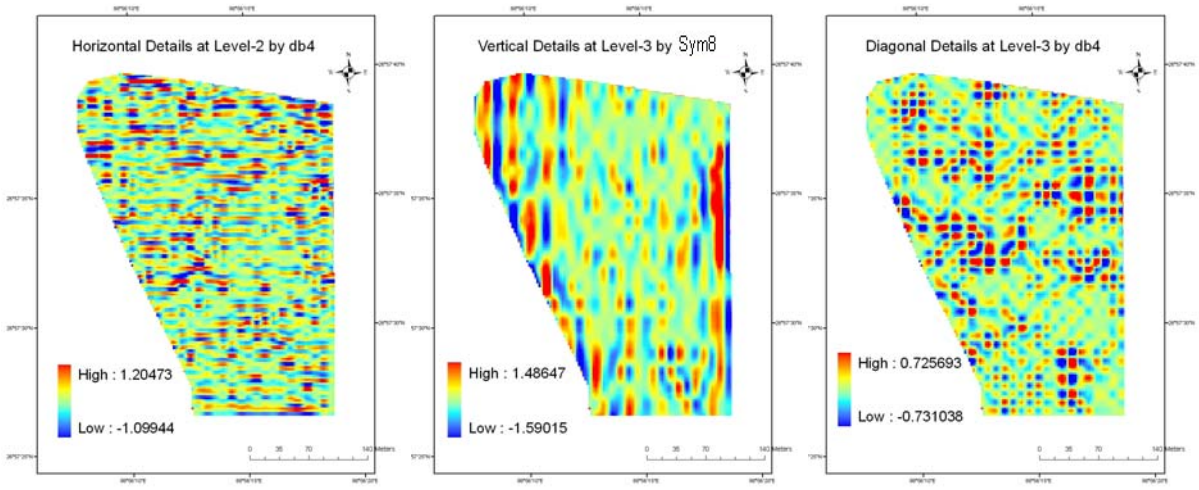

Figure 6-24:Horizontal, Vertical and Diagonal details of the section 18.

6.3. Mature Guatemala (Section 4N of Hope Tea Garden)

Fertilizer and lopping were repeated till Guatemala matures. Rehabilitation completes when the growth of the grass crop was over 2 m, thick and even and root penetration reach 90- 100 cm. The section 4N was uprooted in dec2003 after 117 years of tea crop and was at the mature stage of Guatemala in Dec 2005. The section had two rounds of subsoil, plough and lopping. Guatemala was planted at 65x105cm spacing and remained on field for 22months. It was a well drained section having field drain of 3inch and main drain of 4inch depth size (figure 6-25).

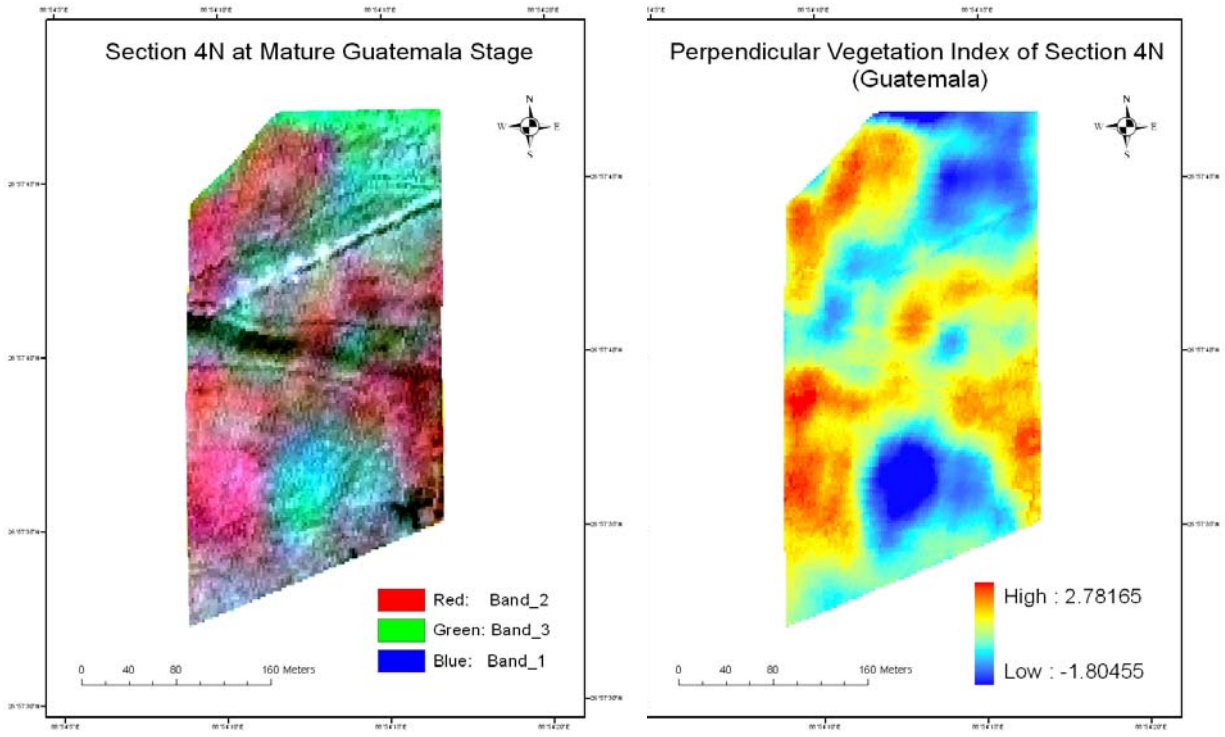

Figure 6-25: Section 4N at mature Guatemala stage and its calculated PVI.

Calculated perpendicular vegetation index has mean 0.79 and standard deviation 0.844, which shows relatively less variability in the section. May be at the time of acquisition of image, section had undergone lopping of Guatemala plantation. The PVI image was decimated and correlated with the input image (figure 6-26). It was found that very low change in information happened with every next level, which means the section has very low fine details. So level-3 was found to be better representative of the image, which generalizes 40m ground information at 2.5m pixel size.

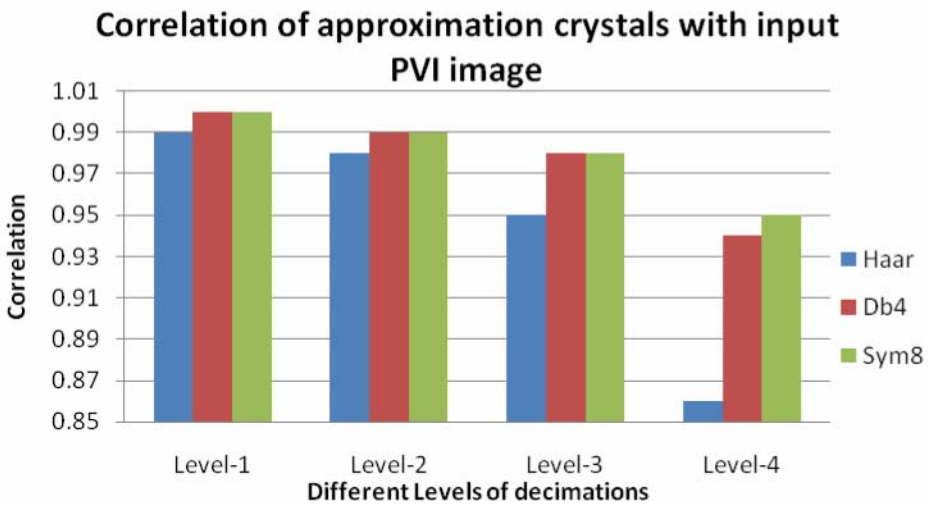

Figure 6-26: Correlation of input PVI with the different levels approximation crystals by Haar, db4 and sym8 wavelets.

To select among wavelets, 3D mesh plot was drawn for level-3 Haar, db4 and sym8, as here again sym8 and db4 gives equal correlation with the input image (figure 6-26). Colour of the plot determines the height, which reflects the wavelets correlation coefficient's value. Blue colour maps the minimum data value and red colour the maximum data value by linear transformation. By observing minutely at blue tail of the plots (figure 6-27), db4 found to be more similar to input image plot, as it has comparatively large range. In this study further analysis was done on db4 level-3 approximation for this section; though both of them can work equally well in approximation of the section.

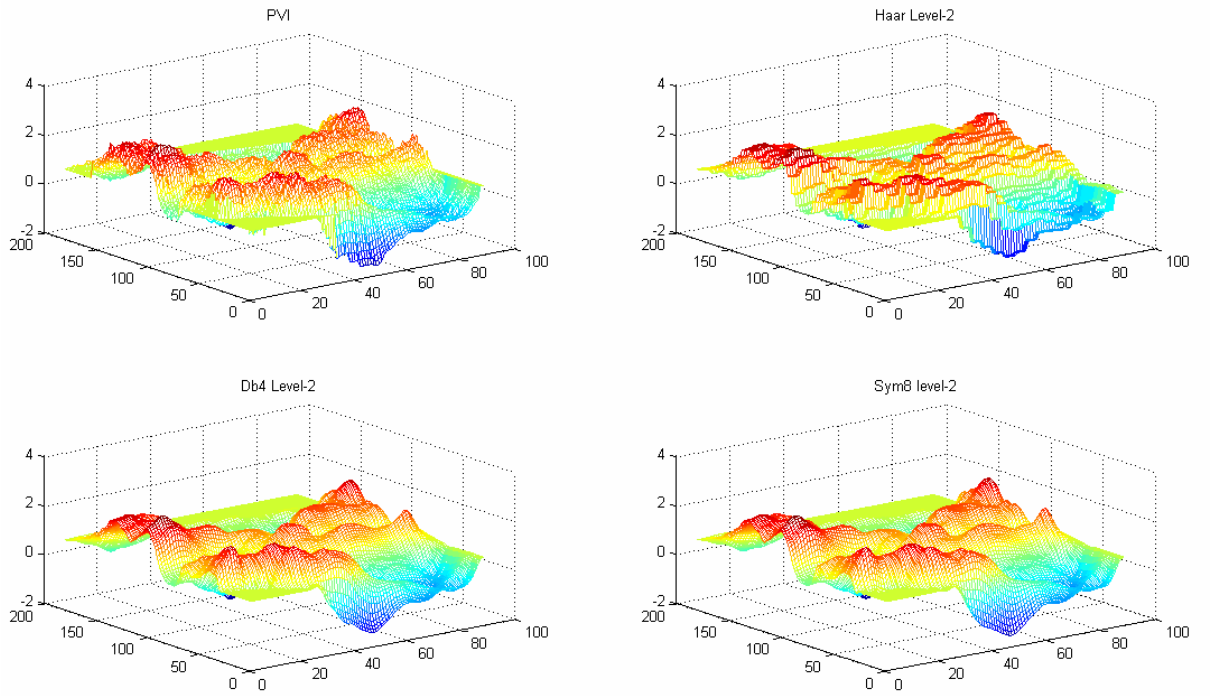

Figure 6-27: Mesh plot of PVI image, Level-2 approximation by Haar, db4 and sym8 wavelets

The analysis of the extracted pattern was done along with next stage, as both stages were taken from the same section, so better temporal aspect can also be seen.

6.3.1.1. Fine frequency wavelet coefficients:

As discussed above, at this stage of replantation section had very low fine details. Only prominent pattern was found in the diagonal direction, which may be the loping direction. Some features were also found diagonally at 7-8m distance on ground as extracted at level-2. Level-4 was also found to have some diagonal spatial correlation with repetivity at 20 pixels i.e. 50m ground distance. Db4 was found to be the better wavelet among these three to extract the pattern in diagonal direction as well s horizontal direction and sym8 vertical direction(see appendix). The autocorrelation map of selected best levels in each direction was shown (figure 6-28). At level-2 some repetivity was found in vertical direction at nearly 15m ground distance at 10 resolution level. In horizontal and vertical direction weak repetivity was found at level-3 i.e. 10m resolution at25m ground distance and at level-2 respectively.

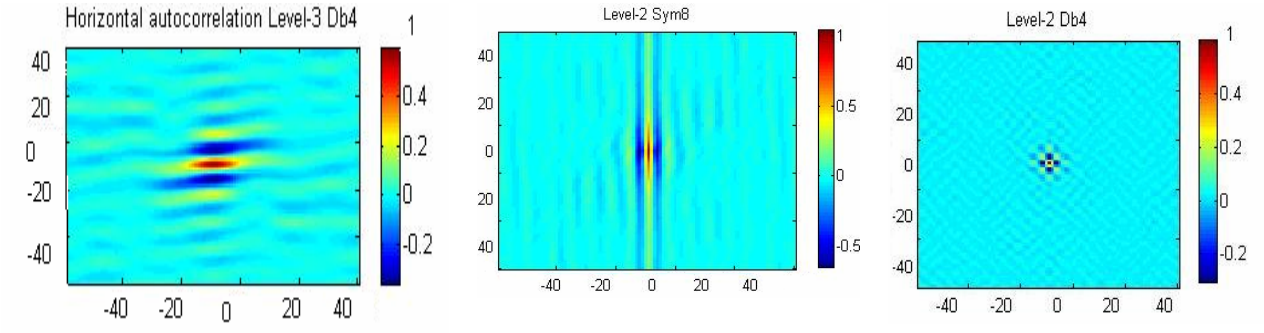

Figure 6-28: Autocorrelation of Vertical and Horizonatal details in section 4N at Guatemala stage.

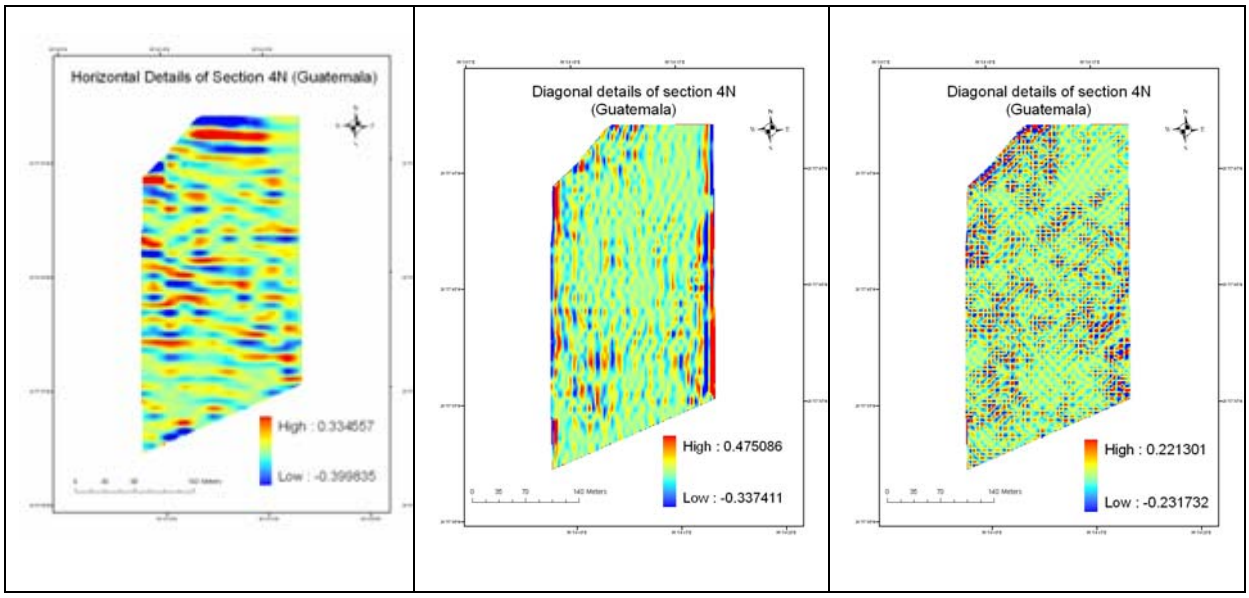

Figure 6-30: Horizontal, Vertical and Diagonal details of the section 4N (Guatemala).

6.4. Field ready to replant new seedlings (Section 4N of Hope Tea Garden)

In the last stage of replantaion soil was left bare after uprooting of Guatemala for 2-3months to keep crop materials for mulch and to absorb the nutrition. In 2006 the section 4N was replanted at the rate of 14600 plants per hectare. The image was acquired in the month of October2006, the stage when field is just ready to plant new seedlings, clear lanes and holes/ pits are visible (figure 6-31).

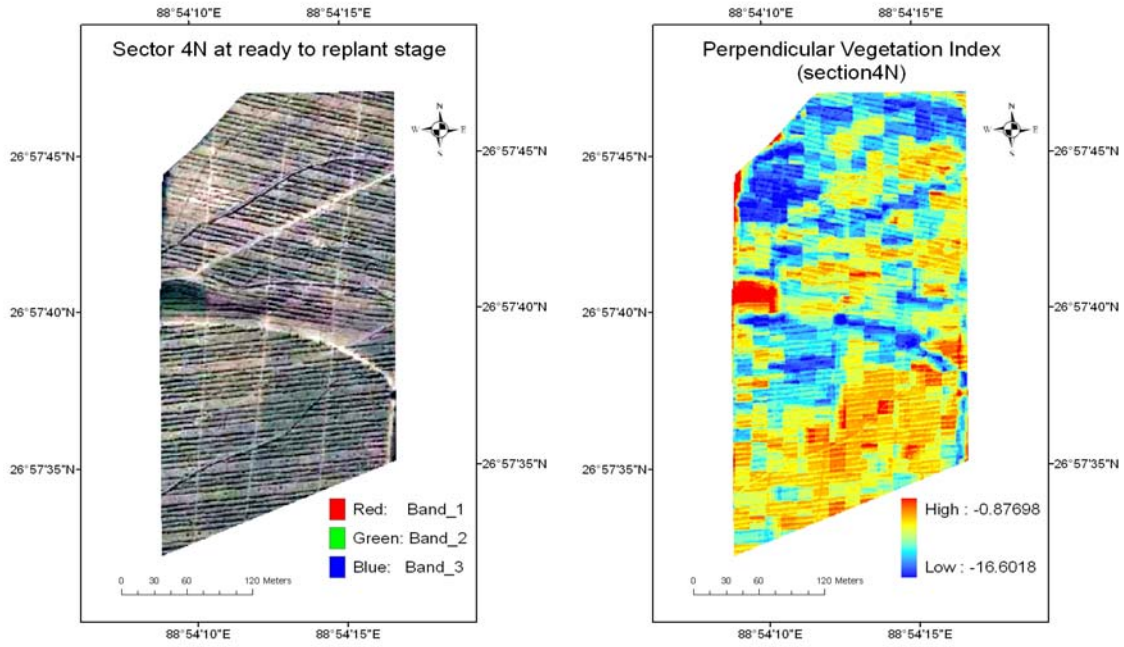

Figure 6-31: Section 4N, just before replanting and its calculated PVI.

Section was barren, with few patches of small grasses, showing that image was captured 10-15 days after completion of ploughing and levelling. Following the same process stated above, PVI calculated for the section has -9.38 mean and standard deviation 1.86 for the PVI image. This shows section had

very low vegetation cover and high variability. By wavelet decimation, level-4 was found to have most sufficient generalization of the section with 16m ground information. Figure 6-32 shows that level-4 was 89% correlated while level-5 correlation reduced to 73%, showing significant loss in information. With every next level, steep decrease in correlation was found which shows that the detail crystals must have some significant information. These are the ploughing lanes, which can easily be seen in the input raw image.

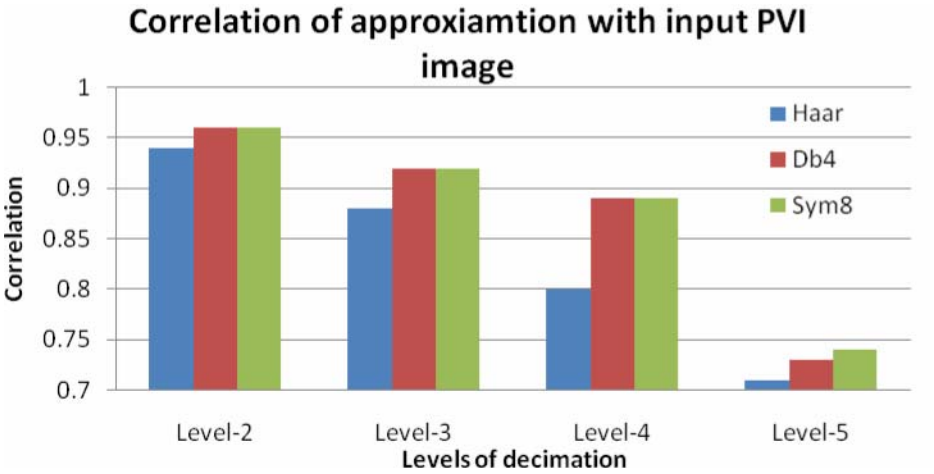

Figure 6-32: Correlation of input PVI with level-2 to level-5 approximation crystal

At each level, both db4 and sym8 are equally correlated with the input PVI image and Haar has slight difference. At the level-5 sym8 gives better performance than db4 because of its long support size and symmetric shape. To compare among the wavelets in the same level mesh plot was drawn (figure 6-31), which shows db4 a bit more similar at the blue ends. Though both sym8 and db4 has almost identical plot, so any of the two can work equally well for 16 m generalization of the section, in this study db4 was preferred.

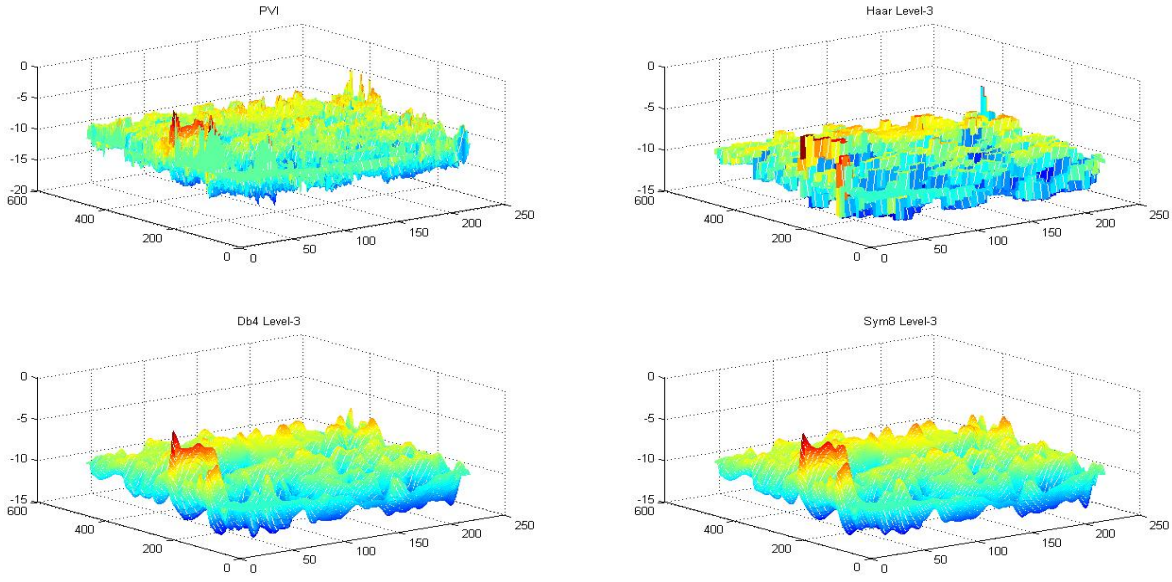

Figure 6-33: Mess plot of input PVI and Level-3 Approximation by Haar, Db4 and sym8

The level-4 approximation by db4 has same wavelet coefficient mean as that of input PVI image, only standard deviation was reduced from 1.86 to 1.5. The section 4N has elevation range from 345 m to 356 m and 352m mean. The section had maximum 44% slope as well as large almost fat region in central and eastern part, having highest altitude (figure 6-34).

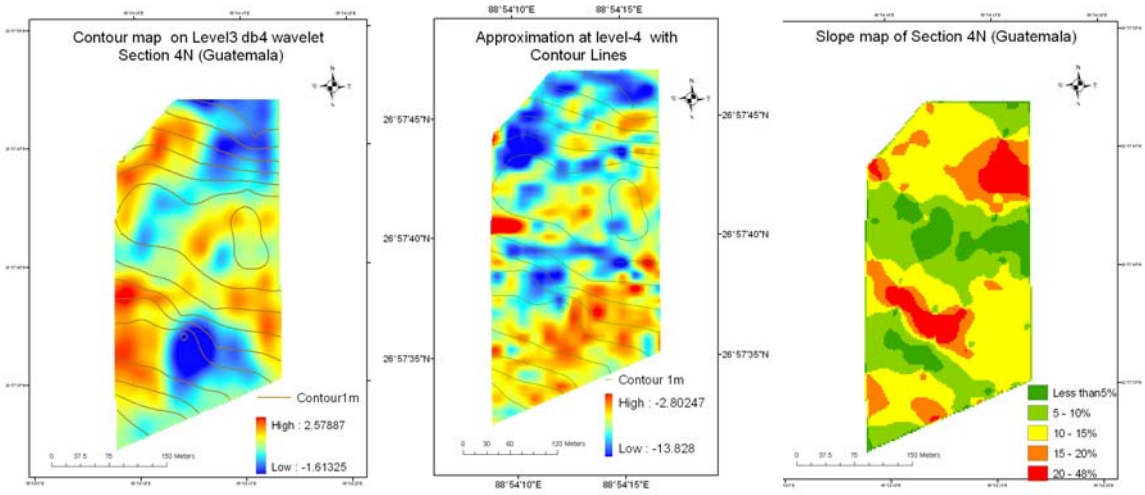

Figure 6-34: Section 4n approximation with contour lines at a. Guatemala stage and b. ready to replant stage and c. slope map.

The Slope and sedimentation of the section was 10-12% correlated with the guatemala variation while no correlation was found between the same parameters on the same section, which shows the impact of human induced changes. In the figure 6-34 only north east part of section (low vegetation) and the flat central part had same correspondence in both the stages. Here change in pattern and relationships can be seen with the change in stage of replantation. The range of the topographical parameters was nearly 20 pixels, i.e. 50m ground distance, when section was under Guatemala plantation. This shows that topographic variation has some contribution, though quantitatively it was very less.

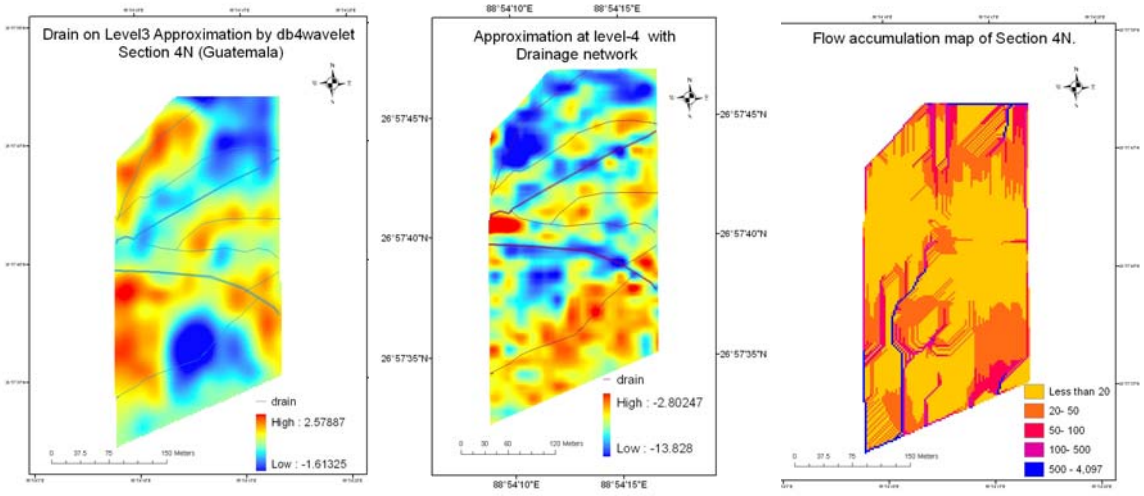

Figure 6-35: Section 4n approximation with drain lines at a. Guatemala stage and b. ready to replant stage and c. flow accumulation map.

The section was rich in drain lines (figure 6-35), so has significant contribution in the pattern by drainage network. Drain lines were dug in the first stage of replantation hence was present in both the stages. But the impact was more pronounced and clearly seen in the stage when section was barren. The two main drain lines shown with 1m buffer and have inverse relation with vegetation. This can be due to the drain were dry at that time and being bigger in depth acts as a dividing lane and vegetation could not cover it properly. Other field drains were positively related with the vegetation in both the stages. The section in Guatemala stage has better vegetation for the area having more flow accumula-

tion, though it was less than 6% correlated, because in the north eastern part section shows stress condition, which was not due to moisture but some soil condition. So these topographic parameters needs well sampled soil information to explain the features existing in the field at different stages.

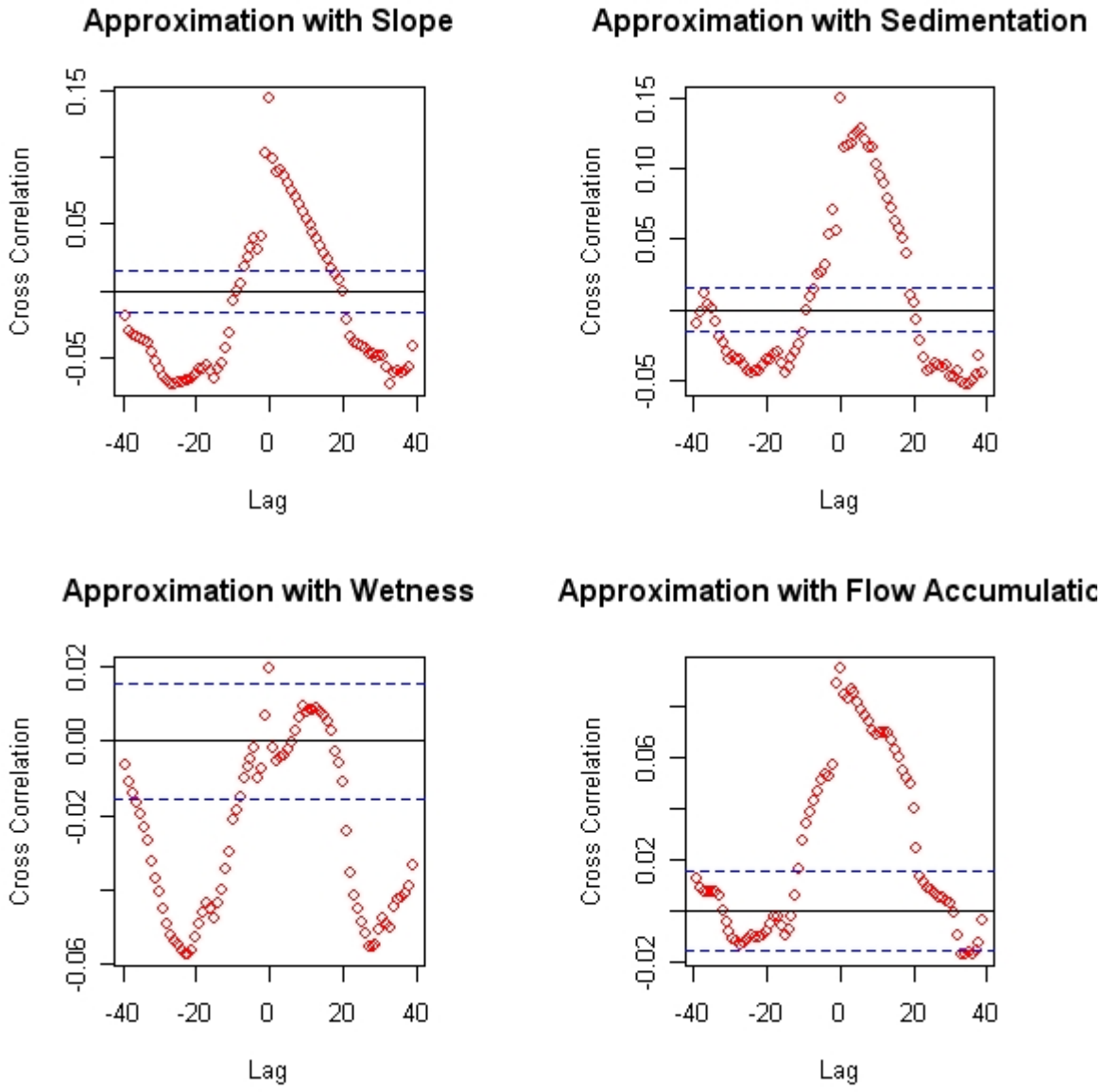

Figure 6-36: Cross correlation of level-3 guatemala stage with slope, sedimentation, wetness and flow accumulation.

Table 6-5 gives the quantitative correlation of each stage of replantation between topographic parameter (slope, elevation, wetness, sedimentation and flow accumulation) with their selected approximation. Elevation has maximum correspondence with the pattern on the field. In general slope is inversely related with vegetation, which was not found in the sections under analysis. The hydrological influence on vegetation due to elevation or slope was neither exclusively positive nor negative. As the value correlation was very low, so only on the basis of it nothing meaningful can be drawn. So cross correlation was found better in explaining the relationship.

6.5: Pearson correlation coefficient between the selected approximation crystal for each stage and DEM, Slope, Wetness index and Sedimentation index of the respective section.

Stage of Replantation	DEM	Slope	Flow accumulation	Sedimentation index	Wetness index
Just after uprooting	11%	5%	2.5%	6%	6%
Young Guatemala	9%	6%	12%	2.7%	8%
Mature Guatemala	22%	10%	-4%	-6%	3%
Ready to replant tea seedlings	30%	1.5%	1.5%	1.2%	1.7%

Guatemala stage of the section showed better topographical relationship (cross correlation) than ready to replant stage of the same section (figure 36 and 37).

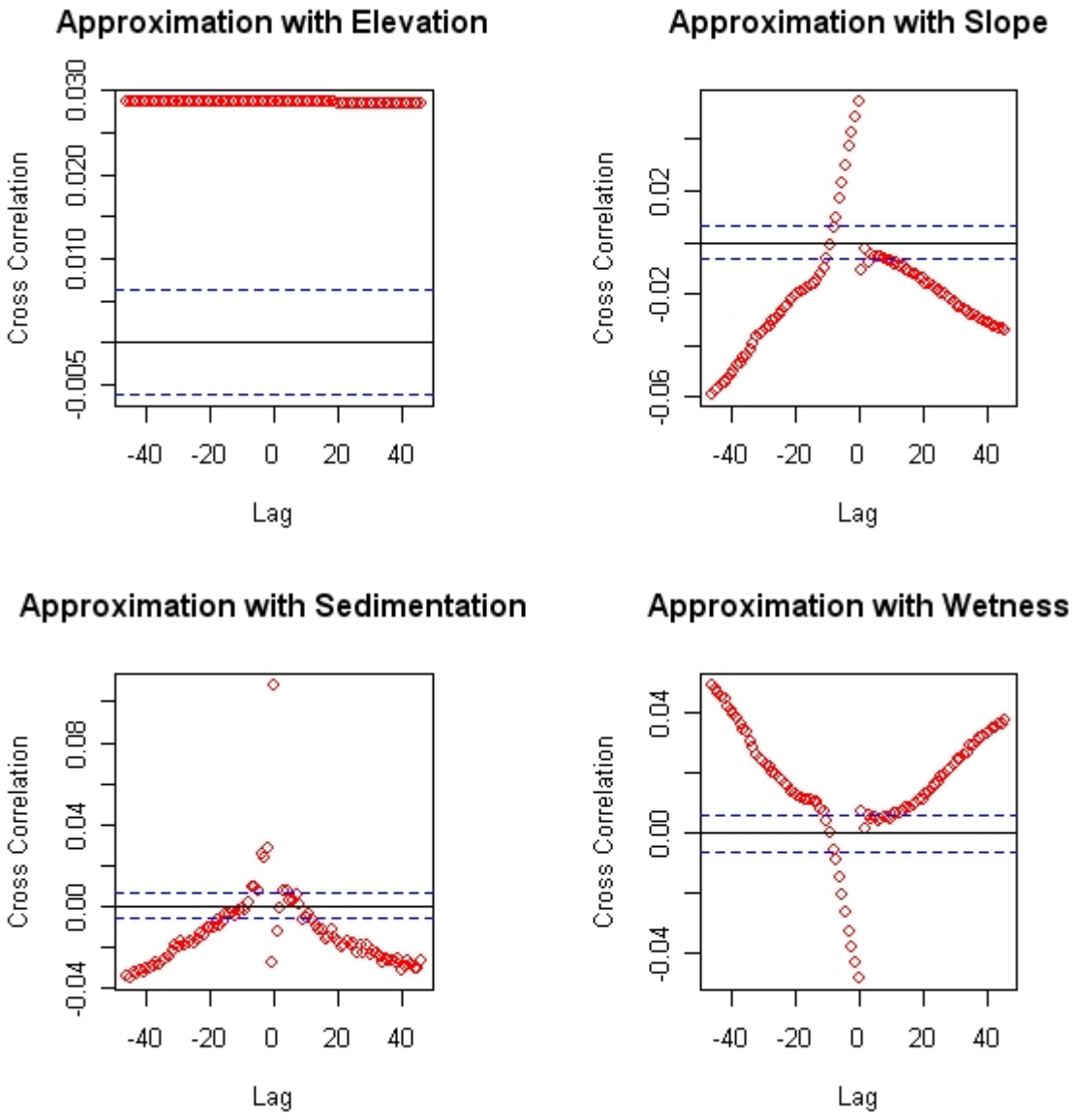

Figure 6-37: Cross correlation of level-3 guatemala stage with slope, sedimentation, wetness and flow accumulation.

6.4.1.1. Fine frequency wavelet coefficients

In contrary to the previous stage of the same section, the stage-just before replanting tea, very significant information was present in the detail crystals. By analysing the anisotropic autocorrelation of the detail crystals, very interesting and prominent horizontal features were extracted. Both db4 and sym8 works equally well at level-2 (details shown in appendix-3). This horizontal crystal shows a strong repetivity of features at 5m distance horizontally with the break of 15m distance vertically. These features are the ploughing lines for new tea seedlings plantation.

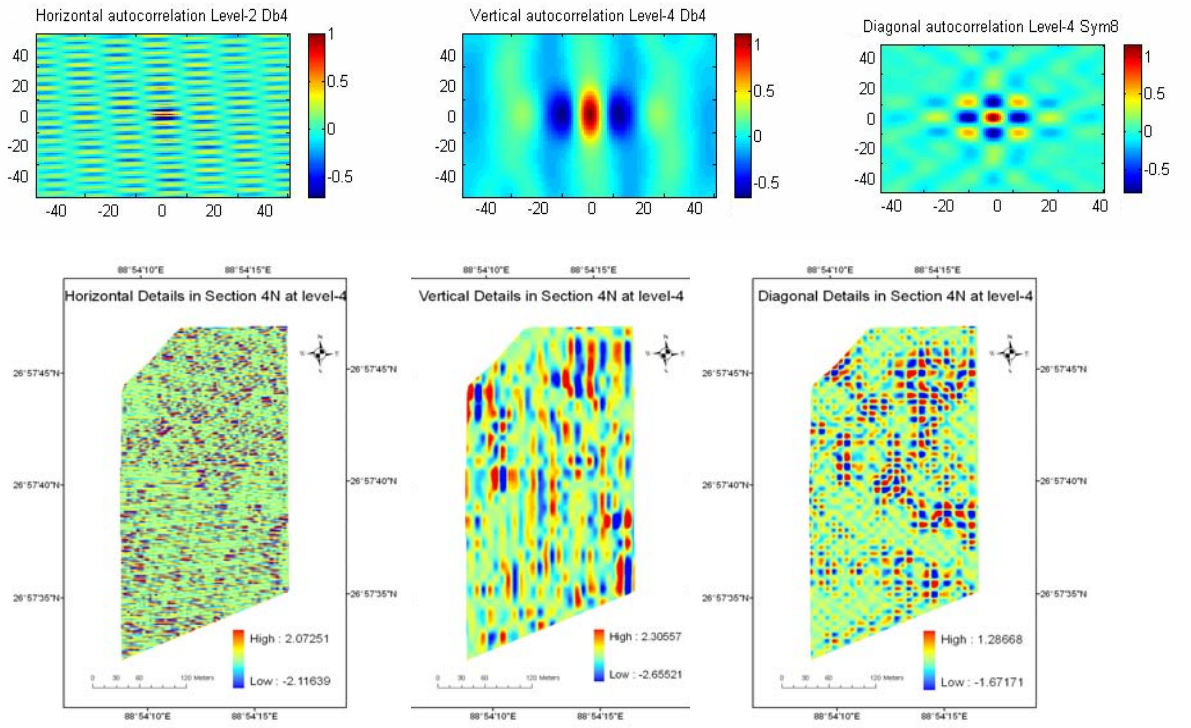

Figure 6-38: Horizontal, Vertical and diagonal details of the section 4N at ready to replant stage with their respective anisotropic autocorrelation.

Proper planting programme, including decision on spacing and planting time is undertaken during this stage. Wavelet analysis extracts the detail features present in the field, which can be of great help to assess and improve the implementation of planting programme. Soil moisture is very essential during planting of new seedlings so this section was replanted in autumn while rains moisture is still in the soil and is preserved by mulching. Cattle manure was mixed thoroughly with the excavated soil at the rate of 2kgs/hectare and was supplied four rounds of NPK (2:1:3) / Year during replantation. In the section tea clone or Jat TV-1, TV-20, TEENALI was planted.

6.4.2. Impact of climatic parameters on the yield

Before uprooting section 18 and 4N were very poor in production (less than 1400 unit) the figure 6-39 shows the last 5-6 years of production chart of both the section just before their uprooting. In the plot the impact of rainfall and rainy days on yield was also shown. 2003 was comparatively more wet year than 1999 but the yield in both the sections were not corresponding it, may be due to that section was in its minimal production stage in well managed situation so fails to react significantly with very low fluctuation in rainfall.

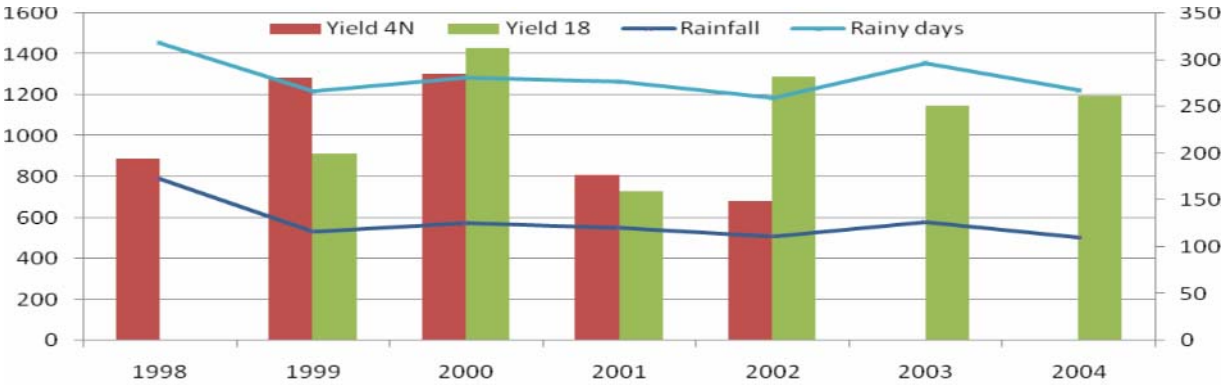

Figure 6-39: Yield variation in last 5 years in section 18 and 4N with rainfall

6.4.3. Impact of soil parameters on the yield

As discussed in the previous parts of the thesis, soil can be the second most significant factor, after management activities which were responsible for variation in the tea field, soil analysis was done. In this analysis, only those sections of the Hope Tea garden were considered, for which yield and soil samples were of the same year from the existing datasets provided by TRA (soil samples of year 2002-2007). Below table 6-6 gives a descriptive statistics and correlation plot of the average pH (Top), pH (sub), Organic carbon, Nitrogen percentage and Potassium in part per million of 30 different sections of Hope Tea Garden, with their respective yield.

Table 6.6: Descriptive Statistics and Pearson Correlations of soil properties with yield of different sections of Hope tea garden

	Mean	STD		Yield	pH-top	pH-Sub	OC	N%	K(ppm)
Yield	2363.31	629.951	Pearson Correlation						
			Sig. (2-tailed)						
pH(top)	4.3526	.24115	Pearson Correlation	-.096					
			Sig. (2-tailed)	.621					
pH(sub)	4.4314	.26525	Pearson Correlation	-.048	.812				
			Sig. (2-tailed)	.806	.000				
OC	2.10730	0.69593	Pearson Correlation	-.112	-.609	-.489			
			Sig. (2-tailed)	.562	.000	.007			
N%	.17932	.056320	Pearson Correlation	-.093	-.617	-.500	.956		
			Sig. (2-tailed)	.630	.000	.006	.000		
K(ppm)	160.28	49.142	Pearson Correlation	.041	-.028	.056	-.311	-.367	
			Sig. (2-tailed)	.834	.885	.772	.101	.050	
Age	41.17	36.517	Pearson Correlation	-.619	.29	.113	-.317	-.349	-.099

*Correlation is significant at the 0.01 level (2-tailed).

Standard deviation of the yield shows that there was huge variation among different sections, which can be accounted by the age of tea plantation, disease and other contamination along with the terrain conditions. It was found that age of the section had strong negative correlation with the yield. The soil parameters were also mutually correlated, like strong correlation was found between organic carbon and Nitrogen (more than 95%), which was expected. There was also good correlation between pH, organic carbon and nitrogen and top soil pH plays more role compare to sub soil pH. This implies that places which were more acidic were expected to be richer in organic carbon and nitrogen. pH plays very important role in availability of secondary and micro nutrients like potash, manganese, etc. Top and sub soil pH composition were also correlated, sub soil was found to be a bit more acidic than top soil in general

There was no significant one to one correlation coming out of the yield and the soil parameters but age of the tea plant was strongly inversely related to the yield. To model the variation in yield of different sections, different soil parameters and age were analysed by multiple linear regression. The problem aroused by high correlation amongst the predictor variables was during the drawing of the inferences about the relative contribution of each predictor variable to the success of the model.

Table 6.7: Multiple Linear Regression Model Summary

Model	R	R Square	Adjusted R Square	Std. Error of the Estimate
1	.772(a)	.596	.485	451.950

a Predictors: (Constant), pH(top), K(ppm), Age, OC, pH(sub), N%

The adjusted R square shows model accounts for 48.5% of variance, which was a good model for yield prediction based on soil properties, as many external factors also plays the important role in production capability of the field.

Table 6.8: ANOVA Test

Model		Sum of Squares	Df	Mean Square	F	Sig.
1	Regression	6617800.080	6	1102966.680	5.400	.001(a)
	Residual	4493686.127	22	204258.460		
	Total	11111486.207	28			

a Predictors: (Constant), pH(top), K(ppm), Age, OC, pH(sub), N%

b Dependent Variable: yield

Anova table shows high significance (0.01) of the model, which should be less than 0.05. This shows that 99% probability is that by manipulating the soil parameters, we can measure the resulting change in the yield.

Table 6.9 : Contribution of parameters in model

Model		Unstandardized Coefficients		Standardized Coefficients	T	Sig.
		B	Std. Error	Beta	B	Std. Error
1	(Constant)	4961.942	2530.448		1.961	.063
	OC	20.820	427.657	.023	.049	.962
	Age	-15.959	2.965	-.925	-5.383	.000
	pH(sub)	-1195.229	621.368	-.503	-1.924	.067
	K(ppm)	-2.466	2.054	-.192	-1.200	.243
	N%	-5727.554	5613.449	-.512	-1.020	.319
	pH(top)	1050.797	807.398	.402	1.301	.207

a Dependent Variable: yield

Standardized Beta coefficients give the measure of contribution of each variable to the model i.e. how strongly each predictor variable influences the criteria variable. For example 0.023 beta value indicates that change of 1 standard deviation in the organic carbon will result in a change of 0.023 standard deviation in the yield. Lower the beta value lesser the impact of predictor variable on the criteria variable.

Using enter method adjusted R square was 48.5. Age is the most significant predictor variable, though beta value for pH and N% also indicates some impact on the criteria variable yield. To know exact impact of each soil variable experiments needs to be conducted in the controlled environment and with sufficient number of cases.

6.4.4. Soil properties of Section 4N

By the above discussion we found that soil had significant impact on crop variability. To analyse the variation within a section due to soil fifty samples were collected by TRA from the section. The descriptive statistics of the collected samples for pH (Top), pH (Sub), percentage of organic carbon, nitrogen and potash percentage were shown in table 6-8.

Table 6.10: : Descriptive Statistics of the Soil Samples of section 4N.

	pH (Top)	pH(Sub)	Organic Carbon %	Nitrogen%	Available Potash %
Mean	4.719592	4.490204	2.518633	0.216612	0.010600
Std Dev.	0.280943	0.253208	0.072187	0.002379	0.000186
Variance	0.078929	0.064115	0.005211	0.000006	0.000000
Kurtosis	2.234108	-0.626122	8.333885	1.150374	-0.453254
Skewness	-1.86813	-0.41720	-2.61705	-1.15224	-0.40526

The table shows that section was highly acidic with significant variation. In general soil was well suited for healthy tea growth having good organic carbon, high nitrogen and fairly high

potash content and highly acidic field. Variations in soil properties were not alarming and were generally within the acceptable range.

The quantile-quantile plot of nitrogen, organic carbon, pH and potash percentage were drawn (figure 6-40) to see the distribution pattern.

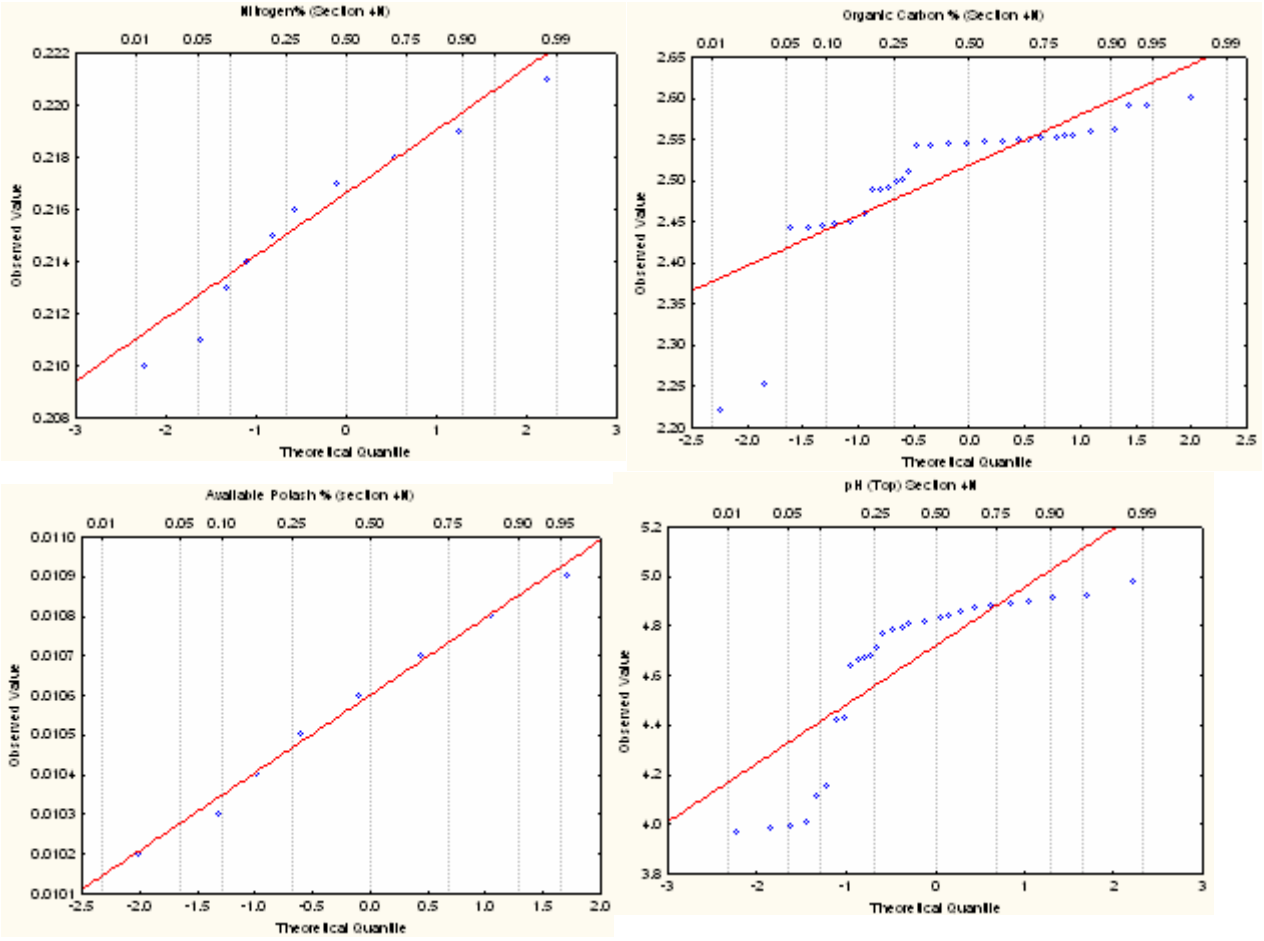

Figure 6-40: Quantile-Quantile plot of nitrogen, organic carbon, pH and potash percentage.

The plot shows that organic carbon and pH of the soil had skewed distribution but nitrogen was almost normal in distribution while potash was almost on the line, i.e. perfectly normal. In the multispectral satellite images the reflection of the land in case of soil, is mainly due to organic carbon and Fe_2O_3 present in the soil. This variation of organic carbon with the section can be responsible upto some extend for the variations captured by image. To analyse the frequency distribution of soil pH both at top and sub level and organic carbon, histogram plot was drawn (figure 6-41).

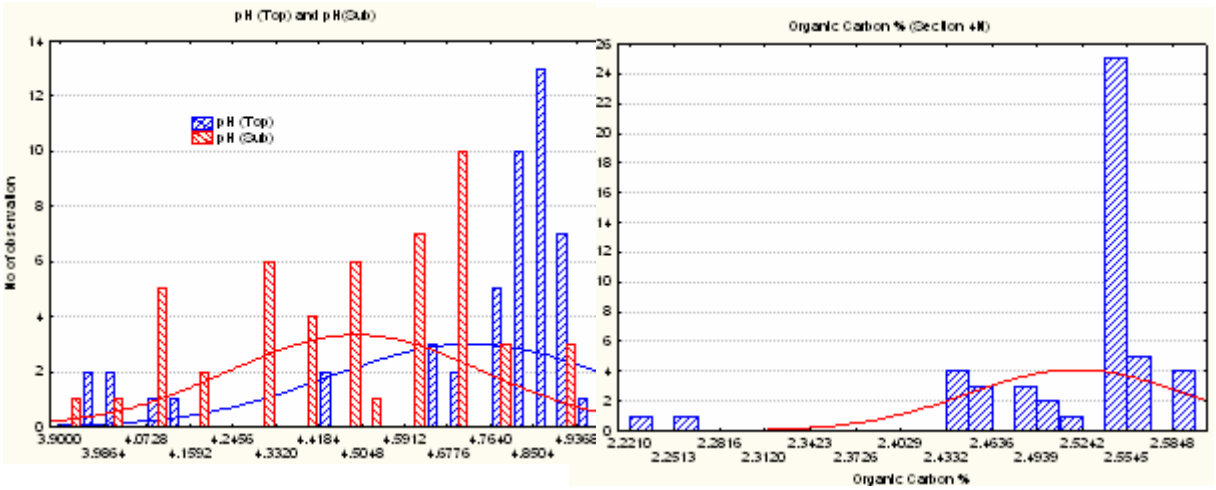

Figure 6-41: Histogram of soil pH at top and sub level and organic carbon.

fected by different parameters had more variation and a bit less acidic in nature. On the other hand organic carbon had also huge variation in the section, reflecting variation in vegetative condition of soil. If these samples were collected with there geographic locations than they could of very high importance for analysing the patterns of the section.

7. Discussion

In order to discern the underlying pattern in the section during different phases of replantation multiscale and multidirectional data mining was done by using wavelets. Wavelets after decimation of the image of section, gives different levels of information. The approximation crystal has the identity of that level contains highest amount of information. Multiresolution capability of wavelets enables the user to analyze the different information existing at different scale. In this study, the approximation crystal at decimation level 3 and 4 had reasonable amount of information, after deducting the unnecessary details (high frequency information) from it and gives general pattern of the section. Further going down the decimation level, no significant features was found to be analyzed. To get best level out of them a trade off was done based on extend of information required. The study was done on two different resolution images. The google earth images were at 1m resolution and were generalized well by level-4 i.e. at 16m ground scale. Liss III fused image was at 2.5m resolution and was generalised at level-3 i.e. at 20 m scale. The impact of replantation stage was also observed on section 4N (for which two time period data was available), when the field was covered by Guatemala the level of generalization was at higher scale, i.e. coarser resolution (20m), because variation became smoother with the vegetation coverage and when it was a bare land most suitable generalization was observed at 16m resolution. Pattern of the field was also changed upto much extent, because of the human induced features in the last stage

For fine scale information, wavelets were found to be very effective in revealing the unobservable pattern with the help of anisotropic autocorrelation. In the first stage of replantation no strong details were observed in any particular direction, because the image was acquired after 5-10 days of levelling of the field and was left open at that time. But repetivity of features were found at 20 m and 30m distance in horizontal and vertical direction, which can be management lines. In the section covered by young Guatemala strong horizontal features at 10m distance were found, at 10m scale. These features were not visible in the input image. Similarly during mature Guatemala stage diagonal features were found stronger at 10m scale. Last two stages were of same section, so the temporal change was also observed. These diagonal features were broken in 'ready to replant stage'; while clear horizontal features at 5m distance in 4m ground resolution was observed. These extracted details needs to be analysed on field. The reason for these directional features can be diseases in soil or plant, effect of the presence of shade trees (now uprooted), soil nutrient deficiency or management activities. Hence, wavelets were found very efficient in extracting fine information, but for proper replantation impact analysis, multi temporal datasets needs to be taken from the same section and then field survey needs to be done.

Among the analysed wavelets for approximation, Haar wavelet was found unsuitable for replantation process studies because of its blocky pattern. Db4 and Sym8 behaved more or less same because of their compactness at upper scale, as dilation increases, shape of wavelet come into play and became more prominent at lower levels. But for detail crystals sym8 and db4 has different results.Symmlets-8 was more symmetric wavelet and had long compact support having 16 coefficients compared to daubechies-4 which was asymmetric wavelet with 8 coefficients. Sym8 gives more generic pattern because of its longer support size, as more will be the number of pixels covered in one translation than db4. Db4 with eight coefficients and four vanishing moment was more suitable wavelet for the crystals

having some prominent fine pattern at very less separation. Sym8 gives more regular and smooth pattern, hence more suitable for low frequency detail information extraction.

At different levels of approximation results, a range of complexity and details were removed and at this scale the hydrological influence of vegetation can be modelled. In many landscapes, pedogenesis occurs in response to the way water moves through it therefore the spatial distribution of topographic attributes that characterize these flow paths inherently and capture the soil and vegetation variability (Moore et.al. 1991). Following information was derived from Digital Elevation Model, obtained from cartosat stereo pairs to get a better understanding of how the relationship between vegetation greenness and topography and hydrology can be analyzed using wavelets.

- Elevation (meter)
- Slope (degrees)
- Flow accumulation (number of pixels)
- Sedimentation index (unitless)
- CTI (unitless)

The Pearson correlation coefficient was calculated to measure the linear relation between these parameters and the selected approximation of each stage. Maximum correlation coefficient was found with elevation, other parameters have very weak correlation (less than 12%) with their selected generalization (table 6-5). The expected relation between soil wetness, slope and vegetation is not found in the sections. This may be due to the sections were well managed and had no moisture scarcity in it, so the impact of wetness on vegetation cannot seen explicitly and the relief variation was so low that it will not cause any significant structure on land. Though very weak quantitative relationship was observed for each stage of replantation with the topography, but for the sections having difference in elevation 10-12m (section 4N and section 16) extent of spatial dependence was significant. The cross correlation plot shows 75-100m long range of spatial relation exists for section 16 and 4n (under Guatemala). That means strong and comparatively stable spatial structure exists in the field, which can be modelled with the help of these parameters (though weakly). In the study there was no pixel to pixel correlation was found among the vegetation pattern coming out of wavelet decimated image and different topographical and hydrological parameters. The cause for a relation is always elsewhere, usually in the system (field - observation - data). To analyse these relation, 3x3 pixel window was used to draw a correlation map and cross correlation plot was drawn between the above stated topographic properties and the selected landscape structure.

Cross correlation plot as well as detail features extracted by wavelets, both show very significant change in field with the change in replantation stage in section 4N. The features and relationships were altered by management interference and the weak topographical relationship was broken.

Positive impact of climate (rainfall) was observed when fluctuation was high (figure 6-14) but for the sections under study, the yield were already far below the mark and with limited change in rainfall (occurred just five year before their uprooting), no significant trend was observed (figure 6-39).

The selected landscape structure can potentially be analyzed and characterized on the basis of soil cover analysis. For the sections under study, soil organic carbon and pH had significant variation among the collected samples, which could be a responsible factor for upcoming patterns. Soil organic carbon plays one of the major role in the spectral variation of remote sensing data among the soil properties These soil properties could have better analysed if the collected samples had their geographical locations with them.

Vegetation was generally observed to follow the drainage lines, ploughing and management lines. Thus, detail management activity needs to be asses along with soil information to analyse the extracted pattern.

8. Conclusion and Recommendation

8.1. Conclusions

The main objective of the research was the assessment of wavelet technology for the use of pattern analysis in the different stages of tea replantation and then to find the natural or human induced cause for upcoming pattern.

Which level/levels best represents the image during the different stages of replantation?

In general different stages of replantation were found to be better represented at 16-20m of ground resolution. The sections which were open had more clear features, so been most revealing at comparatively higher resolution (4 to 16m). Sections under Guatemala were generally well represented at 20m resolution level. As the images under analysis were from two different spatial resolutions due to non availability of data, so level-3 and level-4 was observed as most suitable, for approximation. 1m resolution data was generalised well at level-4 (16m on ground) and 2.5m resolution data at level-4 (20m on ground). Wavelets were found as a very efficient data mining tool in detail information extraction. The horizontal features extracted at 5m interval in the field covered by young Guatemala (at 10m resolution) were even not visible in the input image. The table 8.1 gives most suitable levels found for best representation of each crystal in the four stages of replantation.

8.1: Most suitable levels for each stage with their respective details.

Stage of Replantation	Approximation	Horizontal	Vertical	Diagonal
Just after uprooting	Level-4 (16m)	Level-3(8m)	Level-3(8m)	Level-3 (8m)
Young Guatemala	Level-3 (20m)	Level-2(10m)	Level-3(20m)	Level-3(20m)
Mature Guatemala	Level-3(20m)	Level-3(20m)	Level-2(10m)	Level-2 (10m)
Ready to replant tea seedlings	Level-4(16m)	Level-2(4m)	Level-4(16m)	Level-4 (16m)

Which particular wavelet is best during each stages of replantation?

In this study both db4 and sym8 was found suitable for general pattern extraction of different stages of replantation. Haar wavelet because of its blocky pattern (which is not natural for the agricultural field) was rejected throughout all the stages. Difference between sym8 and db4 emerged more clearly in detail crystals. Where features were not very strong, both of them were found equally good. In general, it was observed that sym8 being longer in support size and nearly symmetrical wavelet better reveals smooth details while db4 can better isolate fine details and signal discontinuities.

The difference among them (db4 and sym8) increases while going down the levels because in upper level crystals, comparatively higher frequency information presents. Wavelet basis of both of them are very compact at upper levels and basic shape are nearly same (as symmlets is derived from Daubechies). By going down the level, wavelet gets more and more flatten and hence at lower levels impact of shape of each wavelet became more pronounced. The table 8.1 gives most suitable wavelets found for each crystal in each stage.

8.2: Most suitable wavelets for each stage with their respective details.

Stage of Replantation	Approximation	Horizontal	Vertical	Diagonal
Just after uprooting	Db4/ Sym8	Sym8	Sym8	Sym8
Young Guatemala	Db4/ Sym8	Db4	Sym8	Db4
Mature Guatemala	Db4/ Sym8	Db4/sym8	Sym8	Db4
Ready to replant tea seedlings	Db4/ Sym8	Db4	Db4	Db4

How to analyze for finding the causes of the observed pattern extracted from wavelets?

The derived landscape structure of the fields were mainly guided by the management activities, in which drainage lines were one of the most effective driving force. The replantation phase had most active human inference over the natural processes, to improve the field quality at the best possible level. Continuous nutrient supply, ploughing, levelling and other field management activities had disturbed the natural characteristics of the sections, observed most strongly in the case of section 4N, where two time period data was available for the same section.

In the study it was found that the selected pattern of the field was very weakly correlated with the wetness index, flow accumulation, sedimentation index and slope. A bit better (10-30%) correlation was found with elevation as well as its range of association observed from cross correlation was also strong (40m), which means the relationship can be modelled easily. Though quantitative linear relationship between the extracted pattern and topographic parameters was not strong, but in general it was found that flat and elevated part of field respond better for vegetation.

Physical and chemical properties of soil including soil moisture jointly cause maximum within field variation. The variation in tone of satellite images of the sections under study, upto some extent, can also be accounted to variation found in organic carbon and pH. Generally nutrients were supplied equally over a section, so natural variably though get smother but still exist. Hence for proper management of uprooted field undergoing replantation, each part of the section needs to be treated differently, based on its local requirement. Wavelets can help to delineate these site specific management zones and to decide the areas which require more intensive soil sampling to obtain a complete picture of the soils and vegetation in the section.

8.2. Summary and limitations of the study

Wavelet provides more affluent warehouse for spatial analysis, as it operate locally and characterizes both low and high frequency resolution information simultaneously. Hence enables better filtering of structures compare to Fourier and other frequency domain function. Along with the multiresolution capability of wavelets boundary pixel problem is one of the short coming of wavelets. During the study irregular shape of the field arouse as a trouble, which was treated by replacing the 'no-data' outside the study area by the image mean, to decrease the biasness due to abrupt change in frequency. Then images were decimated to filter variation at several spatial scales. Most suitable patters were selected for each section by autocorrelation, which filters out constant values. Thereby combination of both provides a richer repertoire for spatial analysis.

The low vegetation variability was generally associated with areas that have either steep surface or low flow accumulation. Evaluation of the influence of the various hydrological processes that are related to vegetation, accurate DEM (Digital elevation model) and field drainage information as well as soil

properties (like pH, organic carbon) with the help of cross correlation. No strong relation emerged among them, as the possible hydrological effects on changes in the vegetation were not only guided by the relief and weather but also by the management strategies. The patterns of soil development and its properties vary laterally with topography, this gives a relationship that allows for prediction of soil attributes from landscape position but at large scale. While the sections under analysis were of nearly 10-13 hectares size and elevation variation was even less than 4 meters as well as the sections were well drained and no water logging or sink was found. So the variation in vegetation was difficult to analyse only on the topographic basis. To do better analysis human-influenced landscape at the section level, micro level information of soil properties along with their spatial location, needs to be bring together with these topographic parameters.

8.3. Recommendations

- This study requires very high resolution multispectral data having NIR band information.
- Multi-temporal data set of the same section could be much better for analysis of different stages of replantation.
- Soil samples needs to collect with their geospatial information, which can help for correlating soil properties with other spatial dataset.
- A thorough check on the drainage layout and design of different management activities are recommended.
- After extraction of pattern through wavelets, extensive field check is recommended to observe the local cause of the generated features on the image which may be diseases, water logging and other problems.

References

- Amgaa T., Stein A., Bakker W. H. (2003), Wavelet based analysisfor object separation fromlaser altimeter data. M.Sc. Geoinformatics ITC.

- Abbate A, DeCusatis C. M., Das P.K.(2002). Wavelets and Subbands, Fundamentals and Applications. *Birkhauser.*

- Banerjee B. (1992a). Botanical classification of tea. K.C. Willson, M.N. Clifford (Eds), Tea: Cultivation to consumption. *Chapman and Hall, London*, pp.25-51.

- Bosch E. h., Oliver M. A. and Webster R.(2004). Wavelets and the Generalization of the Variogram. *Mathematical Geology*, 36, 2, 147-186.

- Bruce A., Gao H.Y. (1996) Applied Wavelet Analysis with S-PLUS. *Springer.*

- Chen G.Y., Xie W.F. (2007). Pattern recognition with SVM and dual tree complex wavelets. *Image and Vision Computing*, 25, 960-966.

- Colombo R., Bellingeri D., Fasolini D. and Marino C. M. (2003). Retrieval of leaf area index in different vegetation types using high resolution satellite data. *Remote Sensing of Environment,* 86 120-131.

- Dutta R., Patel N.R., Stein A. (2006). Assessment of Tea Bush Health and Yield Using Geospatial Techniques. *M.Sc. Geoinformatics Thesis IIRS-ITC*

- Dutta R. (2008). Image Mining for Monitoring Tea Replantation and Assessing G x M x E Interaction Inuencing Tea Quality. *PhD proposal ITC The Netherlands*

- Epinat V., Stein A., Jong S.M. and Bouma J. (2001). A wavelet characterization of high-resolution NDVI patterns for precision agriculture. *JAG*, 3, 2, 121-132.

- Evans J.P. and Geerken R.(2006). Classifying rangeland vegetation type and coverage using a Fourier component based similarity measure. *Remote Sensing of Environment* 105 (2006) 1-8.

- Frazier Michale W. (2000). An Introduction to Wavelets through Linear Algebra. *Springer*.

- Freeman S., West J., James C., Lea V. and Mayes S. (2004). Isolation and characterization of highly polymorphic microsatellites in tea (*Camellia sinensis*). *Molecular Ecology Notes* (2004) 4, 324–326

- Gandah M., Stein A., Brouwer J. and Bouma J. (2000). Dynamics of spatial variability of millet growth and yield at three sites in Niger, West Africa and implications for precision agriculture research. *Agriculture Systems* 63 123-140.

- Geerken R., Zaitchik B. and Evans J.P. (2005). Classifying rangeland vegetation type and coverage from NDVI time series using Fourier Filtered Cycle Similarity. *International Journal of Remote Sensing*. 26, 24, 20, 5535-5554.

- Gonzalez R. C., Woods R.E., Eddins S.L. (2004).Digital image processing using MATLAB. *Pearson Education in South Asia.*

- Green. M.J. (1971). An evaluation of some criteria used in selecting large yielding tea clones. *Journal of Agricultural Science (Cambridge)* 76, 143-156.

- Immerzeel W.W.,Quiroz R.A. and Jong S.M.De (2005). Understanding Precipitation Pattern and Land Use Interaction in Tibet using Harmonic analysis of SPOT VGT-S10 NDVI time series. *International Journal of Remote Sensing,*00,00,2005,1-15.

- Jensen A., Harbo L.C. (2001).Ripples in Mathematics The Discrete Wavelet Transform. *Springer.*

- Jensen John R (1996). Introductory Digital Image Processing, A Remote Sensing Perspective. Prentice Hall Series.

- Kamau D.M. (2008). Productivity and resource use in ageing tea plantation. *PhD thesis Wageningen University, Wagheningen, The Netherlands.*

- Kravchenko A. N., and Bullock D. G. 2002a. Spatial variability of soybean quality data as a function of field topography: I Spatial data analysis. *Crop Science*. 42: 804-815

- Kravchenko A. N., Thelen K.D., Bullock D.G., and Miller N. R. 2003. Relationship among Crop Grain Yield, Topography, and Soil Electrical Conductivity Studied with Cross-Correlograms. *Agron. Journal*. 95:1132-1139.

- Lark R.M. (2006). The representation of complex soil variation on wavelet packet bases. *European Journal of Soil Science*, December 57,868-882.

- Luo Daisheng (1998). Pattern recognition and image processing. *Horwood Publishing Chichester*.

- Mondal, T.K.,Bhattacharya, A., LaxmiKumaran, M. and Ahuja,P.S., 2004. Recent advances of tea (Camellia sinensis) biotechnology. *Plant Cell, Tissue and Organ Culture* 76, 195-254.

- Moore, I.D, Gesseler, P.E., Nielsen, G.A. and Peterson, G.A.,1993. Soil attribute prediction using terrain analysis. *Soil Science Society of American Journal*. 57(2) : 443-452.

- Ogden R.T. (1997). Essential Wavelets for Statistical Applications and Data Analysis. *Birkhauser Boston.*

- Paul C. and Genderen J. L. V (1998). Multisensor image fusion in remote sensing: concepts methods and applications. *International Journal of Remote Sensing*, 19, 5, 823-854.

- Resnikoff Howord L. and Wells Raymond O. (2000). Wavelet Analysis, The Scalable Structure of Information. *Springer.*

- Ruan J. and Hardter R. (2001). Productivity and quality response of tea to balanced nutrient management – Examples from China tea gardens. *Plant Nutrition – Food security and susceptibility of agroecosystems*, 324-325.

- Schowengerdt, R. A. (1997). Remote Sensing, Models and Methods for Image Processing. Academic Press, Second Edition.

- Starck J.K., Murtagh F. and Bijaoui A. (1998). Image Processing and Data Analysis, The multiscale approach. *Cambridge University Press.*

- Stein A., J. Broumer and J. Bouma, 1997 Methods for comparing spatial variability patterns of Millet yield and soil data. *Soil Science Society of American Journal.* 61: 861-870.

- Stein A., Meer F.V., Gorte B. (1999). Spatial Statistics for Remote Sensing. *Kluwer Academic Publication.*

- Verhagen A. J, Stein A., Epinat V. (2000). Use of Wavelets to Compare Simulated Yield Patterns for Precision Agriculture at the Field Scale. *Precision Agriculture*, 2, 333-346.

- Xu X.L., Ma K.M., Fu B.J., Song C.J. and Liu W. (2008). Relationships between vegetation and soil and topography in a dry warm river valley, SW China. *Catena* 75 (2008) 138-145.

- Zhu C. and Yang X (1998). Study of remote sensing texture analysis and classification using wavelet. *International Journal of Remote Sensing,* 19, 16, 3197-3203.

Annexures:

Appendix-1: Results of Detail crystals autocorrelations at different levels by Haar, db4 and sym8.

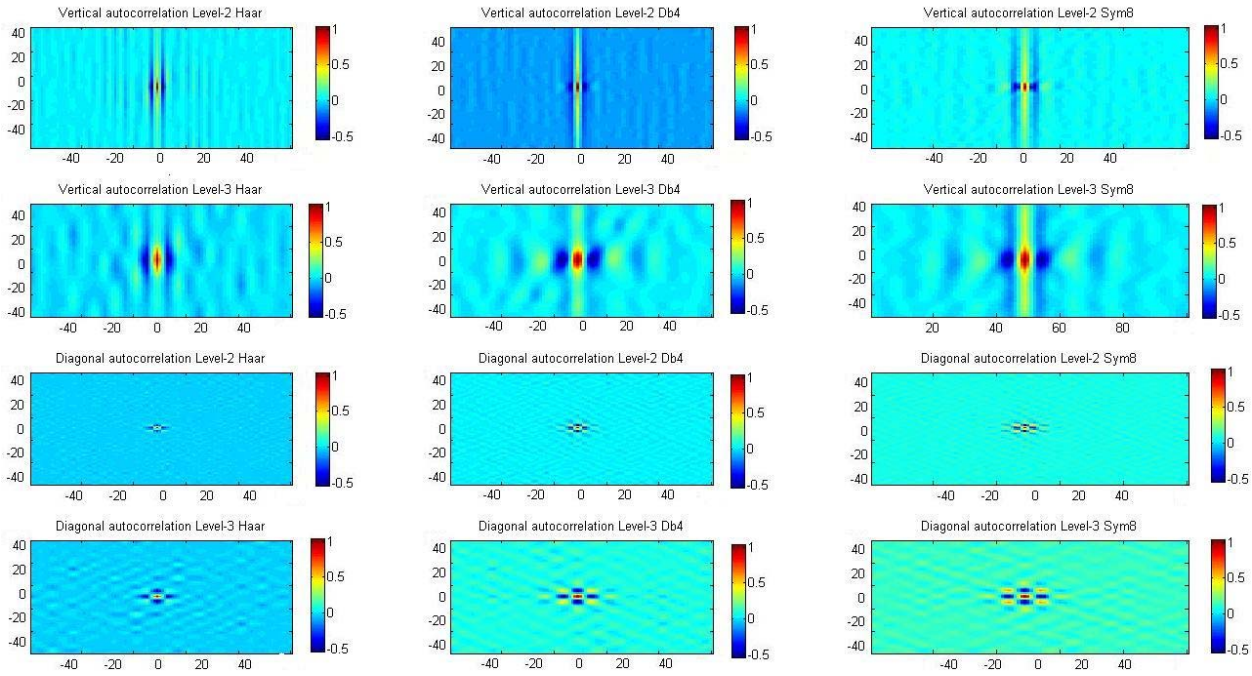

Figure 0-1 Autocorrelation of Section 18 vertical and Diagonal Details

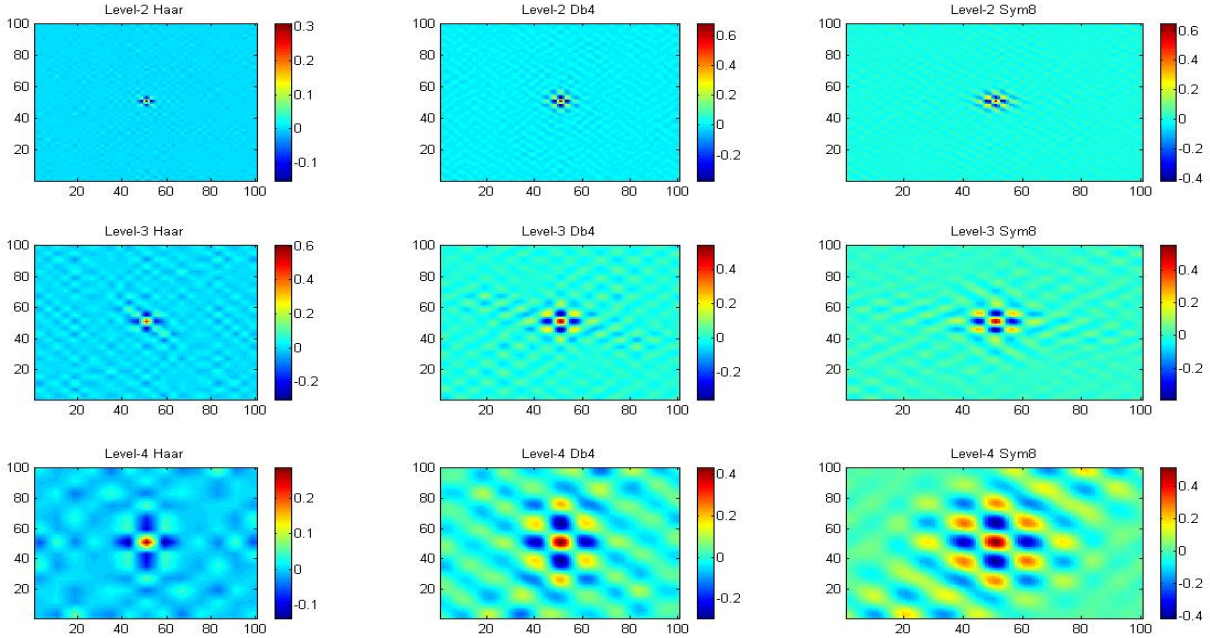

Figure 9-0-2: Autocorrelation of Section 4N under Guatemala in diagonal direction.

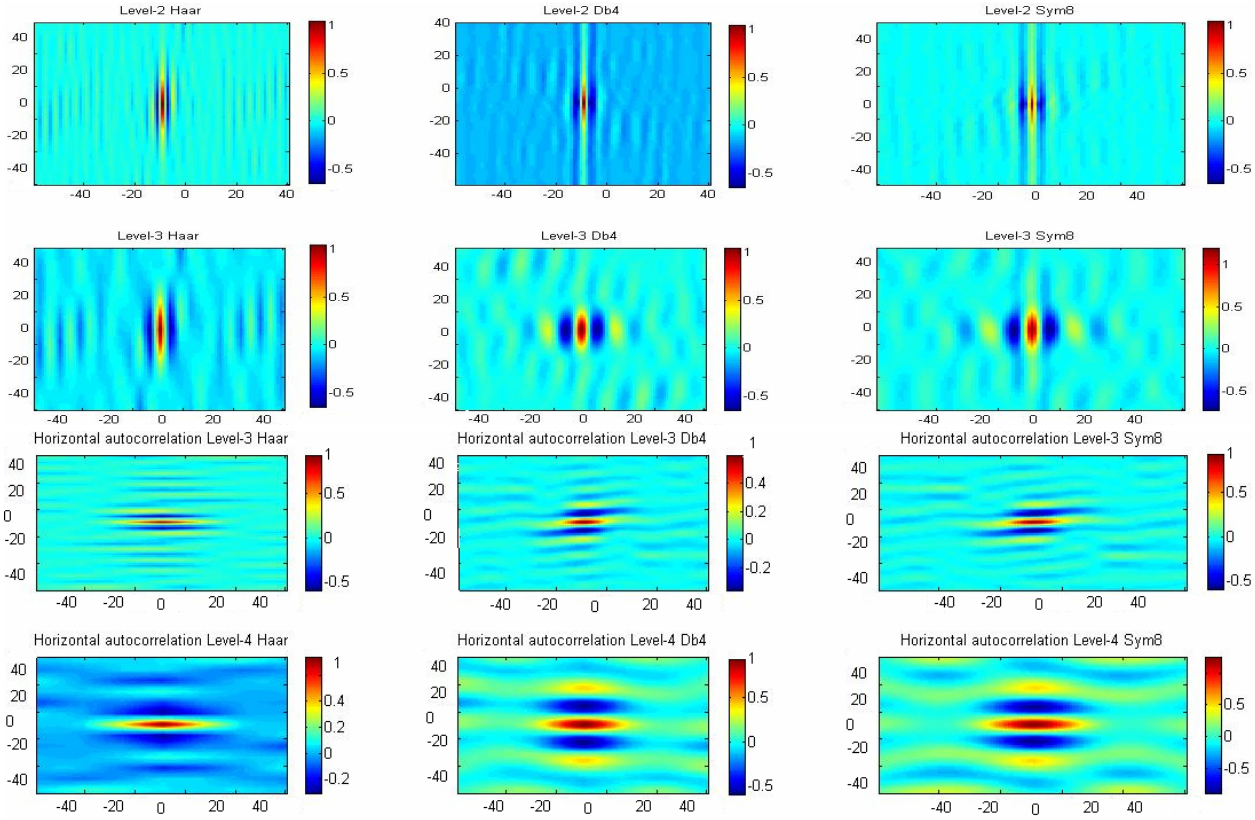

Figure 0-3 Autocorrelation of Vertical and Horizontal Details of Section 4N (with Guatemala)

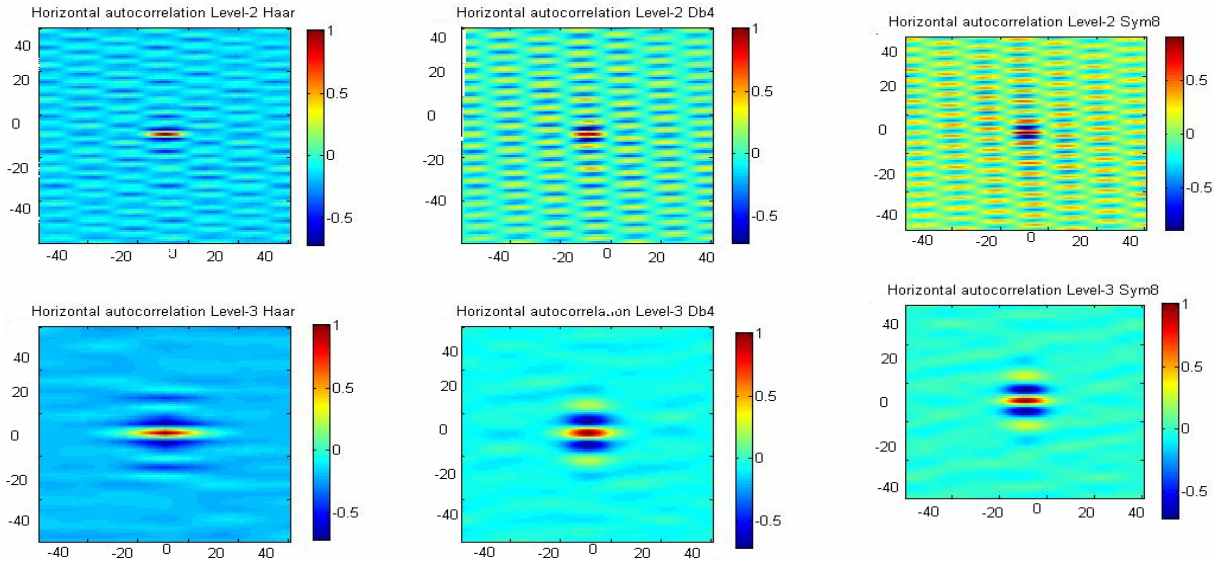

Figure 0-4: Horizontal direction autocorrelation of Section 4N (Ready to replant)

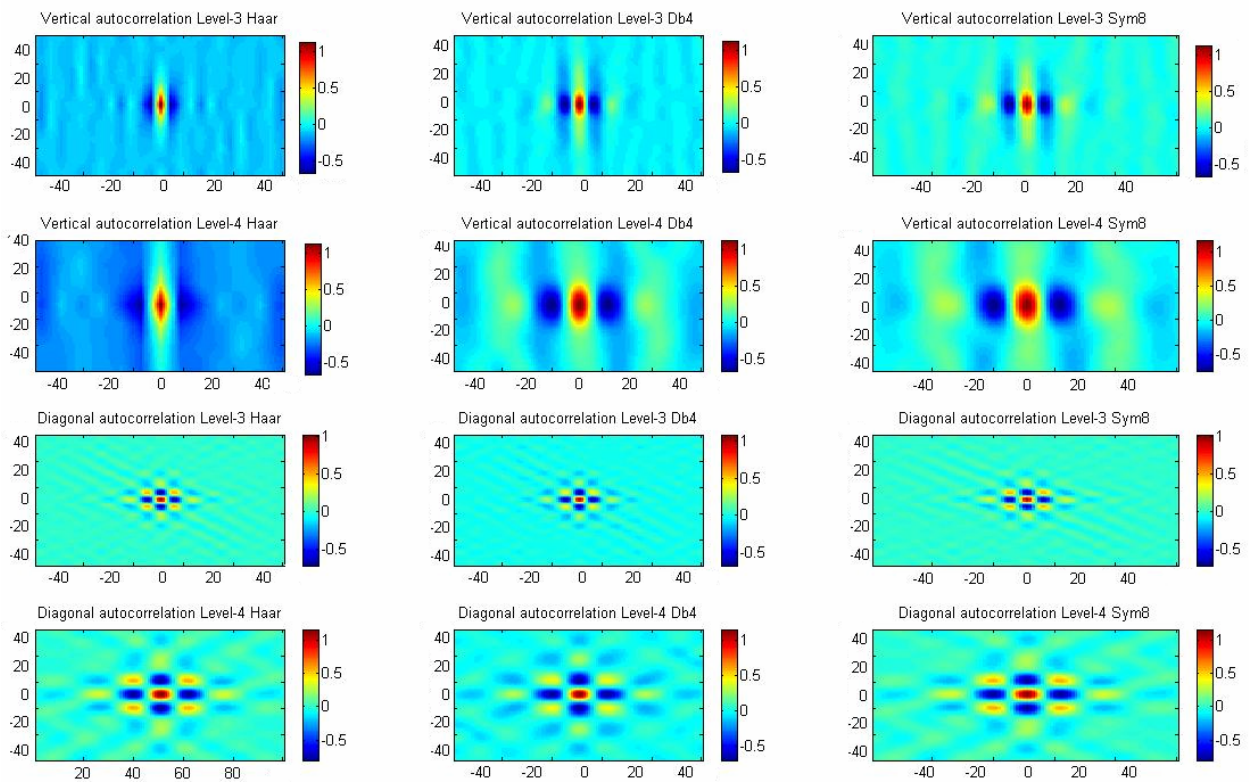

Figure 0-5: Vertical and Diagonal autocorrelation of Section 4N (Ready to replant)

Appendix - 2

Codes in MATLAB

```
%%%% Read image%%%%%
X = load('8b.txt');
%%%% Wavelet decimation
[c1,s1] = wavedec2(X,6,'db4');
A1 = wrcoef2('a',c1,s1,'db4',1);
A2 = wrcoef2('a',c1,s1,'db4',2);
A3 = wrcoef2('a',c1,s1,'db4',3);
A4 = wrcoef2('a',c1,s1,'db4',4);
A5 = wrcoef2('a',c1,s1,'db4',5);
A6 = wrcoef2('a',c1,s1,'db4',6);

%%%%% Plot approximation%%%%%%
subplot(2,3,1);imagesc(A1),colorbar();
title('Approximation A1')
subplot(2,3,2);imagesc(A2),colorbar();
title('Approximation A2')
subplot(2,3,3);imagesc(A3),colorbar();
title('Approximation A3')
subplot(2,3,4);imagesc(A4),colorbar();
```

```
title('Approximation A4')
subplot(2,3,5);imagesc(A5),colorbar();
title('Approximation A5')
subplot(2,3,6);imagesc(A6),colorbar();
title('Approximation A6')
%%%%% Save approximation to bring it to ArcGIS %%%%%
save A1_db4.txt A1 -ascii;
save A2_db4.txt A2 -ascii;
save A3_db4.txt A3 -ascii;
save A4_db4.txt A4 -ascii;
save A5_db4.txt A5 -ascii;
save A6_db4.txt A6 -ascii;

%%%%%%% Energy contribution of each crystal %%%%%%%
[Ea,Eh,Ev,Ed] = wenergy2(c1,s1)

%%% Horizontal Details %%%%%%
H1 = wrcoef2('h',c1,s1,'db4',1);
H2 = wrcoef2('h',c1,s1,'db4',2);
H3 = wrcoef2('h',c1,s1,'db4',3);
H4 = wrcoef2('h',c1,s1,'db4',4);
H5 = wrcoef2('h',c1,s1,'db4',5);
H6 = wrcoef2('h',c1,s1,'db4',6);
subplot(2,3,1);imagesc(H1),colorbar();
title('Horizontal Details H1')
subplot(2,3,2);imagesc(H2),colorbar();
title('Horizontal Details H2')
subplot(2,3,3);imagesc(H3),colorbar();
title('Horizontal Details H3')
subplot(2,3,4);imagesc(H4),colorbar();
title('Horizontal Details H4')
subplot(2,3,5);imagesc(H5),colorbar();
title('Horizontal Details H5')
subplot(2,3,6);imagesc(H6),colorbar();
title('Horizontal Details H6')
save H1_db4.txt H1 -ascii;
save H2_db4.txt H2 -ascii;
save H3_db4.txt H3 -ascii;
save H4_db4.txt H4 -ascii;
save H5_db4.txt H5 -ascii;
save H6_db4.txt H6 -ascii;

%%%%% VERTICAL%%%%%
V1 = wrcoef2('v',c1,s1,'db4',1);
V2 = wrcoef2('v',c1,s1,'db4',2);
V3 = wrcoef2('v',c1,s1,'db4',3);
```

```
V4 = wrcoef2('v',c1,s1,'db4',4);
V5 = wrcoef2('v',c1,s1,'db4',5);
V6 = wrcoef2('v',c1,s1,'db4',6);

subplot(2,3,1);imagesc(V1),colorbar();
title('Vertical Details V1')
subplot(2,3,2);imagesc(V2),colorbar();
title('Vertical Details V2')
subplot(2,3,3);imagesc(V3),colorbar();
title('Vertical Details V3')
subplot(2,3,4);imagesc(V4),colorbar();
title('Vertical Details V4')
subplot(2,3,5);imagesc(V5),colorbar();
title('Vertical Details V5')
subplot(2,3,6);imagesc(V6),colorbar();
title('Vertical Details V6')
save V1_db4.txt V1 -ascii;
save V2_db4.txt V2 -ascii;
save V3_db4.txt V3 -ascii;
save V4_db4.txt V4 -ascii;

%%%%%DIAGONAL %%%%%%%
D1 = wrcoef2('d',c1,s1,'db4',1);
D2 = wrcoef2('d',c1,s1,'db4',2);
D3 = wrcoef2('d',c1,s1,'db4',3);
D4 = wrcoef2('d',c1,s1,'db4',4);
D5 = wrcoef2('d',c1,s1,'db4',5);
D6 = wrcoef2('d',c1,s1,'db4',6);
subplot(2,3,1);imagesc(D1),colorbar();
title('Horizontal Details D1')
subplot(2,3,2);imagesc(D2),colorbar();
title('Horizontal Details D2')
subplot(2,3,3);imagesc(D3),colorbar();
title('Horizontal Details D3')
subplot(2,3,4);imagesc(D4),colorbar();
title('Horizontal Details D4')
subplot(2,3,5);imagesc(D5),colorbar();
title('Horizontal Details D5')
subplot(2,3,6);imagesc(D6),colorbar();
title('Horizontal Details D6')
save D1_db4.txt D1 -ascii;
save D2_db4.txt D2 -ascii;
save D3_db4.txt D3 -ascii;
save D4_db4.txt D4 -ascii;
```

Codes in R

```
# load the necessary packages in R
library (sp)
library (gstat)
library (lattice)
library (rgdal)
library (foreign)

#############################################################
##### Program to calculate the local correlation map
#############################################################
nb <- 2
Path <- 'E:\\88888\\corr\\'
i<-1
input <- paste(Path, 'A3sym',i,'.txt', sep='')
temp <- read.table(input, skip = 6)
d <- dim(temp)
nri <- d[1]
nci <- d[2]
img <- array(0, c(nri,nci,nb))
img[,,i] <- as.matrix(temp)
for(i in 1:nb)
{
 input <- paste(Path, 'A3sym',i,'.txt', sep='')
 temp <- read.table(input, skip = 6)
 img[,,i] <- as.matrix(temp)
}
#############################################################################################
############ setting window size and assigning rows and columns of output aggregated image
#############################################################################################
ws <- 3
n1 <- (ws-1)/2
n2 <- (ws+1)/2
g1 <- array(0, (ws*ws))
g2 <- array(0, (ws*ws))
y <-  array(0, (ws*ws))
#############################################################################################
### initialization of vector that holds the output of each block after processing
#############################################################################################
out <- array(0,c(nri,nci))
x1 <- 0
   for(i in n2:(nri-n1))
   {
   for(j in n2:(nci-n1))
     {
      sr <- seq(from = i-n1,to = i+n1,by = 1)
      sc <- seq(from = j-n1,to = j+n1, by = 1)
```

```
        for(k in sr)
          {
          for(l in sc)
            {
            x1 <- x1+1
             g1[x1] <- img[k,l,1]
             g2[x1] <- img[k,l,2]
            }
          }
          x1 <- 0
          s1 <- sd(g1)
          s2 <- sd(g2)
          m1 <- mean(g1)
          m2 <- mean(g2)
          for(m in 1:(ws*ws))
               {
               y[m] <- ((g1[m]-m1)/s1)*((g2[m]-m2)/s2)
               }
                ysum <- sum(y)
                yav  <- ysum/((ws*ws)-1)
                 out[i,j] <- round(yav, digits = 5)
          g1 <- array(0, (ws*ws))
          g2 <- array(0, (ws*ws))
          y <-  array(0, (ws*ws))
      }
    }
write.table(out[,], file = paste(Path,'cor','.txt',sep=''),append=FALSE,quote=TRUE,sep ="
",eol="\n",na="NA",dec=".",row.names=FALSE,col.names=FALSE,qmethod=c("escape","double"))
image(out)
##############################################################################################
############ Cross correlation calculation
##############################################################################################
cross_corr = readGDAL("dem.mpr")
cross_corr$slope = readGDAL("slope.mpr")$band1
cross_corr$acc = readGDAL("acc.mpr")$band1
cross_corr$App = readGDAL("a3sym1.mpr")$band1
cross_corr$wet = readGDAL("wetness_index.mpr")$band1
cross_corr$sed = readGDAL("sediment_index.mpr")$band1
str(cross_corr)
object.size(cross_corr)
write.table(cross_corr[], "all.txt")
cross_corr <- read.csv("all.csv")
a= ccf(cross_corr$sym,cross_corr$dem)
b= ccf(cross_corr$sym,cross_corr$slope)
c= ccf(cross_corr$sym,cross_corr$sed)
d= ccf(cross_corr$sym,cross_corr$wet)
```

```
e= ccf(cross_corr$sym,cross_corr$acc)
###### # PLOT: 2 cross_corr 2 pictures on one plot #############
op <- par(mfrow = c(2, 2),pty = "s")
plot(a, ci = 0.95, type = "p",col = "red",  xlab = "Lag", ylab = "Cross Correlation",
    ylim = NULL, main ="A4 Sym8 with Elevation",
    ci.col = "blue", ci.type = c("white", "ma"))

plot(b, ci = 0.95, type = "p",col = "red",  xlab = "Lag", ylab = "Cross Correlation",
    ylim = NULL, main ="A4 Sym8 with Slope",
    ci.col = "blue", ci.type = c("white", "ma"))

plot(c, ci = 0.95, type = "p",col = "red",  xlab = "Lag", ylab = "Cross Correlation",
    ylim = NULL, main ="A4 Sym8 with Sedimentation",
    ci.col = "blue", ci.type = c("white", "ma"))

plot(d, ci = 0.95, type = "p",col = "red",  xlab = "Lag", ylab = "Cross Correlation",
    ylim = NULL, main ="A4 Sym8 with Wetness",
    ci.col = "blue", ci.type = c("white", "ma"))

plot(e, ci = 0.95, type = "p",col = "red",  xlab = "Lag", ylab = "Cross Correlation",
    ylim = NULL, main ="A4 Sym8 with Flow Accumulation",
    ci.col = "blue", ci.type = c("white", "ma"))
```